

# A MODEL-INDEPENDENT APPROACH TO DARK ENERGY COSMOLOGIES: CURRENT AND FUTURE CONSTRAINTS

$$S = \int_{\mathcal{V}} d^4x \sqrt{-g} \left[ \sum_{i=1}^5 \mathcal{L}_i + \mathcal{L}_m[g_{\alpha\beta}] \right]$$

Alejandro Guarnizo Trilleras

Alejandro Guarnizo Trilleras

$$\frac{3P_2(1+z)^3}{2E^2 \left( P_3 + 2 + \frac{E'}{E} \right)} - 1 = \eta = h_2 \left( \frac{1 + k^2 h_4}{1 + k^2 h_5} \right)$$

RUPRECHT-KARLS-UNIVERSITÄT HEIDELBERG  
FAKULTÄT FÜR PHYSIK UND ASTRONOMIE  
INSTITUT FÜR THEORETISCHE PHYSIK  
2015



---

# Dissertation

*submitted to the*

Combined Faculties of the Natural Sciences and Mathematics  
of the Ruperto-Carola-University of Heidelberg, Germany

*for the degree of*

Doctor of Natural Sciences

---

Put forward by

M.Sc. Alejandro Guarnizo Trilleras

Born in Bogotá, Colombia

*Oral examination:* 16 December 2015



---

**A MODEL-INDEPENDENT APPROACH TO  
DARK ENERGY COSMOLOGIES:  
CURRENT AND FUTURE CONSTRAINTS**

---

Referees: Prof. Dr. Luca Amendola  
Prof. Dr. Matthias Bartelmann



## **Eine modelunabhängige Beschreibung kosmologischer Modelle mit Dunkler Energie: Derzeitige und zukünftige Einschränkungen**

Die effektive anisotropische Spannung  $\eta = -\Phi/\Psi$  ist eine Schlüsselvariable bei der Erforschung des physikalischen Ursprungs der Dunkler Energie. Um eine Theorie bedingte Systematik, bei der Charakterisierung kosmologischer Modelle durch die Messung von  $\eta$  zu vermeiden, ist eine modellunabhängige Herangehensweise von großer Bedeutung. Mittels der Kombination von Beobachtungen von Galaxienhaufen, der Messung des schwachen Gravitationslinseneffekt und der Beobachtung von Supernovae machen wir Vorhersagen, mit denen zukünftige Missionen  $\eta$  lediglich auf der Basis direkt beobachtbarer Größen bestimmen können. Neben diesen Ergebnissen finden wir, dass falls  $\eta$  unabhängig von  $k$  ist, zukünftige Beobachtungen auf großen Skalen  $\eta$  auf bis zu 10% genau bestimmen können und mit mehr als 60% Genauigkeit, falls es die Form aus Horndeskimodellen hat. Um den momentan erlaubten Bereich für  $\eta$  zu finden, werden die Daten der Wachstumsrate  $f\sigma_8$  aus Messungen der „Redshift Space Distortion“ (RSD), der Hubbleexpansion  $H(z)$  und des erlaubten Bereichs der Größe  $P_2$ , die durch den Erwartungswert des Verhältnisses zwischen der Galaxie-Galaxie Korrelation und der Galaxie-Geschwindigkeit Kreuzkorrelation definiert ist, genutzt. Mit den aktuellen Datensätzen erhalten wir  $\eta = 0.646 \pm 0.678$  bei einer Rotverschiebung von  $z = 0.32$ , welches in Übereinstimmung mit den Vorhersagen des  $\Lambda$ CDM Modelles ist. Schließlich erstellen wir ein kosmologisches Ausschlussdiagramm für modifizierte Gravitationstheorien in Analogie zu den Ausschlussdiagrammen, die in Laborexperimenten ermittelt werden.

## **A Model-Independent Approach to Dark Energy Cosmologies: Current and Future Constraints**

The effective anisotropic stress  $\eta = -\Phi/\Psi$  is a key variable in the characterisation of the physical origin of the dark energy. It is however important to use a fully model-independent approach when measuring  $\eta$  to avoid introducing a theoretical bias into the results. We forecast the precision with which future large surveys can determine  $\eta$  in a way that only relies on directly observable quantities, using the joint combination of Galaxy Clustering, Weak Lensing and Supernovae probes. Among the results, we find that a future large scale survey can constrain  $\eta$  to within 10% if  $k$ -independent, and to within 60% if it is restricted to follow the Horndeski model. In order to find current constraints on  $\eta$  data for the growth rate  $f\sigma_8$  coming from Redshift Space Distortion measurements, observations of the Hubble expansion  $H(z)$ , and a constraint for the quantity  $P_2$  defined as the expectation value of the ratio between galaxy-galaxy and galaxy-velocity cross correlations, have been used. We find a value at  $z = 0.32$  of  $\eta = 0.646 \pm 0.678$ , in agreement with the predicted value for the  $\Lambda$ CDM model. Finally, we produce a cosmological exclusion plot for modified gravity in analogy with the exclusion plots produced in laboratory experiments.



*No! No one can control Dark Energon! It **dominates** and destroys **everything** it touches!*

STARSCREAM, TRANSFORMERS: WAR FOR CYBERTRON.



*A mi madre Maria Eva y mis hermanos Cristian y Miguel*



# CONTENTS

<b>Acknowledgements</b>	<b>xxiii</b>
<b>Contributions</b>	<b>xxvi</b>
<b>Notation and Conventions</b>	<b>xxviii</b>
<b>Preface</b>	<b>xxxi</b>
<b>I Preliminaries</b>	<b>1</b>
<b>1 Introduction</b>	<b>2</b>
1.1 General Relativity in a Nutshell . . . . .	2
1.1.1 Postulates and Mathematical Foundations of General Relativity . . .	3
1.1.2 The Gravitational Action . . . . .	6
1.1.3 Cosmological Constant Act I: Bianchi Identities . . . . .	7
1.2 The Cosmological Arena . . . . .	8
1.2.1 Cosmological Constant Act II: Einstein's Static Universe . . . . .	9
1.2.2 Cosmic Inventory . . . . .	11
1.2.3 Cosmological Distances and Redshift . . . . .	13
1.2.3.1 Redshift . . . . .	13
1.2.3.2 Comoving distance $\chi(z)$ . . . . .	14
1.2.3.3 Angular diameter distance $d_A(z)$ . . . . .	15

1.2.3.4	Luminosity distance $d_L(z)$ . . . . .	15
1.2.4	Cosmological Constant Act III: Vacuum Energy . . . . .	16
1.3	Cosmological Perturbation Theory . . . . .	18
1.3.1	Statistical <i>Intermezzo</i> : Correlation Function and Power Spectrum . . . . .	22
1.3.2	The Initial Matter Power Spectrum . . . . .	24
1.4	Observing Dark Energy . . . . .	26
1.4.1	Supernovae . . . . .	26
1.4.2	Large-scale Structure . . . . .	29
1.4.3	Future Observations: The Euclid Survey . . . . .	31
<b>2</b>	<b>Dark Energy Cosmologies</b> . . . . .	<b>34</b>
2.1	Beyond Einstein - A Journey Through Modified Gravity . . . . .	34
2.1.1	Higher Derivatives . . . . .	37
2.1.2	New Degrees of Freedom . . . . .	39
2.1.3	Extra Dimensions . . . . .	42
2.2	The Horndeski Lagrangian . . . . .	43
2.3	Modifying Linear Perturbation Equations . . . . .	47
2.4	Model-Independent Observables In Dark Energy Cosmologies . . . . .	49
2.4.1	Assumptions . . . . .	50
2.4.2	Background and Linear Perturbation Observables . . . . .	51
2.4.3	The Horndeski Lagrangian: The Quasi-Static Regime . . . . .	54
<b>II</b>	<b>Results</b> . . . . .	<b>59</b>
<b>3</b>	<b>Current Constraints on the Anisotropic Stress</b> . . . . .	<b>60</b>
3.1	Initial Setup . . . . .	60
3.2	Current Constraints on $\eta$ . . . . .	62
3.2.1	Constraints on $P_2 = 2E_G$ . . . . .	62
3.2.2	Constraints on $R = f\sigma_8$ and $P_3$ . . . . .	63
3.2.3	Constraints on $E$ and $E'$ . . . . .	67
3.2.4	Constraints on $\eta$ . . . . .	69
3.3	Summary and Conclusions . . . . .	70
<b>4</b>	<b>Future Constraints on the Anisotropic Stress</b> . . . . .	<b>73</b>
4.1	Fisher Forecast for the Anisotropic Stress . . . . .	73

4.1.1	Galaxy Clustering . . . . .	75
4.1.1.1	$z$ binning . . . . .	76
4.1.1.2	$k$ binning . . . . .	77
4.1.2	Weak Lensing . . . . .	81
4.1.2.1	$k$ binning . . . . .	86
4.1.3	Supernovae . . . . .	87
4.1.4	Combining the Matrices . . . . .	89
4.2	Summary and Conclusions . . . . .	94
<b>5</b>	<b>A Cosmological Exclusion Plot</b>	<b>97</b>
5.1	Exclusion plot in the plane $(\lambda, \Delta Q)$ . . . . .	98
5.2	Exclusion plot in the planes $(h_4, h_2)$ and $(h_5, h_2)$ . . . . .	100
<b>6</b>	<b>Conclusions and Outlook</b>	<b>103</b>
<b>A</b>	<b>Properties of the Fisher Matrix</b>	<b>108</b>
A.1	Properties . . . . .	109
A.2	Fisher Matrix for the Power Spectrum . . . . .	111
<b>B</b>	<b>Relations in the Horndeski Lagrangian</b>	<b>114</b>
<b>C</b>	<b>Semi-analytical Study on the Degeneracy for <math>\bar{A}</math> and <math>\bar{R}</math></b>	<b>118</b>
	<b>Bibliography</b>	<b>122</b>

## LIST OF TABLES

3.1	Data for the growth rate $f\sigma_8$ from RSD [1]. . . . .	65
3.2	Values of $\tilde{R}$ and $\tilde{R}'$ from $\chi^2$ minimization with marginalization over $\sigma_8$ . . . . .	66
3.3	Constraints on $\eta$ and $\bar{\eta}$ . . . . .	69
4.1	(a) Fiducial values and errors for $\bar{A}$ , $\bar{R}$ and $E$ using six redshift bins. Units of galaxy number densities are $(h/\text{Mpc})^3$ . (b) Fiducial values and errors for $\bar{A}$ , $\bar{R}$ and $E$ using six bins, considering a redshift dependent bias. . . . .	78
4.2	Values of $k_1$ , $k_2$ and $k_{\text{max}}$ for every redshift bin, in units of $(h/\text{Mpc})$ . . . . .	78
4.3	Relative errors for $\bar{A}$ , $\bar{R}$ and $E$ at every redshift and every $k$ -bin (labeled with the index $i$ ). Since fiducial values for $\bar{A}$ , $\bar{R}$ and $E$ are independent of $k$ , these are the same for the three $k$ -bins. . . . .	82
4.4	Errors on $E$ and $\bar{L}$ from weak lensing only (with six redshift bins) and a list of the value $\ell_{\text{max}}$ used at each redshift together with the corresponding $z_{\text{med}}$ value. . . . .	84
4.5	Borders of the $\ell$ -bins for each redshift bin converted from the $k$ -bins according to (4.26). . . . .	84
4.6	Redshift uncertainties, number of supernovae, fiducial value of $E$ and errors for each bin. . . . .	88
4.7	Errors on $E$ from the three probes. . . . .	89
4.8	Fiducial values and errors for the parameters $P_1$ , $P_2$ , $P_3$ , $E'/E$ and $\bar{\eta}$ for every bin. The last bin has been omitted since $R'$ is not defined there. . . . .	92
4.9	Same as table 4.8, but with four redshift bins. The last bin has again been omitted. . . . .	92

4.10	Here, the errors on $P_1, P_2, P_3$ and $\eta$ are listed for the $z, k$ -varying case with a similar structure as table 4.3. . . . .	93
4.11	Absolute errors on $h_2$ and $h_4$ . Because of the degeneracy between $h_5$ and $h_4, h_5$ has been fixed. The fiducial values are $h_2 = 1$ and $h_4 = 0$ . . . . .	94



## LIST OF FIGURES

1.1	Spatial geometry of the Universe: Flat Universe ( $K = 0$ ), Open Universe ( $K = -1$ ) and Closed universe ( $K = 1$ ). Credit: NASA/WMAP Science Team. . . . .	9
1.2	Planck cosmic recipe. Values for the matter-energy content of the Universe before and after Planck [2]. Figure taken from <a href="http://sci.esa.int/planck/">http://sci.esa.int/planck/</a> . . . . .	12
1.3	The galaxy power spectrum calculated with CAMB (red dotted line) and using the analytical approximation for the transfer function $T_{BBKS}$ (black dashed line). . . . .	26
1.4	Top: Modulus distance for the Union 2.1 compilation [3]. The black line represents the best-fit for a flat $\Lambda$ CDM cosmology. Bottom: Confidence regions in the $(\Omega_m, \Omega_\Lambda)$ plane. Considering only SN observations, the constraints suggest a model with non-negligible vacuum energy (or cosmological constant) with $\Omega_\Lambda \sim 0.7$ and $\Omega_m \sim 0.3$ . Figures obtained from the Supernova Cosmology Project webpage <a href="http://supernova.lbl.gov/Union/">http://supernova.lbl.gov/Union/</a> . . . . .	27
1.5	An artist view of the Euclid Satellite. Credit ESA, Image obtained from the Euclid Consortium webpage. . . . .	31
2.1	<i>Islands</i> of modified gravity. Adapted from [4]. Theories are classified according to the way in which they avoid Lovelock's restrictions. . . . .	38
2.2	Marginalized posterior distributions at 68% and 95% confidence level for the two parameters $\alpha_{M0}$ and $\beta$ of the exponential evolution, $\Omega(a) = \exp(\Omega_0 a^\beta) - 1$ . $\alpha_{M0}$ is defined as $\Omega_0 \beta$ and the background is fixed to $\Lambda$ CDM. The value $\Omega_{M0} = 0$ corresponds to the $\Lambda$ CDM model also at perturbation level. Figure obtained from [5]. . . . .	46

2.3	Planck constraints on modified gravity. 68% and 95% confidence regions for the two parameters $\Sigma_0$ and $\mu_0$ ( $Y_0$ ) obtained from Planck CMB measurements in combination with WL, BAO and RSD [5]. . . . .	48
3.1	Constraint on $P_2 = 2E_G$ at $z = 0.32$ , from large-scale gravitational lensing, galaxy clustering and structure growth rate [6, 7]. The black line represents the fiducial $\Lambda$ CDM for $P_2$ . . . . .	63
3.2	Observations of $\bar{R} = f\sigma_8$ from RSD in the redshift range 0.067–0.8 [1]. The black line represents the fiducial $\Lambda$ CDM for $\bar{R}$ . Data with open markers correspond to the original data corrected by the Alcock-Paczynski effect $F_{AP}(z)$ . . . . .	64
3.3	Third order fit for $\bar{R}$ ; shadow regions represent the $1\sigma$ (light) and $2\sigma$ (dark) level for the fit. The black line represents the fiducial $\Lambda$ CDM for $\bar{R}$ . . . . .	66
3.4	(Top): Observational data for $H(z)$ [8], coming from spectroscopic study of luminous red galaxies [9, 10], and early-type galaxies [11], (Bottom): Third order fit to $H$ , shadow regions represent the $1\sigma$ (light) and $2\sigma$ (dark) level for the fit. The black line represent the fiducial $\Lambda$ CDM for $H(z)$ . . . . .	67
3.5	Observational constraints on $\bar{\eta}$ . For visualization, we slightly shift the values around $z = 0.32$ . . . . .	69
3.6	Contour plots for $\eta$ and $\bar{\eta}$ evaluated at the mean of $P_2$ and $P_3$ at $z = 0.32$ . $E$ and $E'$ are allowed to vary along their observational bounds (in the case of direct observations of the Hubble expansion $H(z)$ ). Models like $f(R)$ gravity who predict an scale-independent value of $\eta = 1/2$ are inside our constraints. . . . .	70
4.1	Errors on $\bar{A}$ , $\bar{R}$ and $E$ from Galaxy Clustering in the $z$ -binning case. The black line represents the fiducial $\Lambda$ CDM model. . . . .	79
4.2	Redshift-dependent bias $b(z)$ from Euclid specifications [12, 13]. . . . .	80
4.3	Graphical representation of the errors on $\bar{A}$ and $\bar{R}$ in the $k$ binning case. The bins are labeled as $z_a$ $a \in \{1, 6\}$ and $k_i$ with $i \in \{1, 3\}$ . . . . .	81
4.4	Errors on $E(\bar{z}_a)$ and $\bar{L}(\bar{z}_a)$ from weak lensing. The black line represents the fiducial $\Lambda$ CDM model. Plots made by Adrian Vollmer. . . . .	85
4.5	Graphical representation of the errors on $\bar{L}$ in the $k$ binning case, same as fig. 4.5. . . . .	86
4.6	Errors on $E$ from Supernovae. The black line represents the fiducial $\Lambda$ CDM model. Plot made by Simone Fogli. . . . .	88
4.7	Errors on $P_1$ , $P_2$ and $P_3$ in the $z$ -varying case. The black line represents the fiducial $\Lambda$ CDM model. . . . .	91

4.8	Constraints on $\eta(k)$ in the Horndeski case for $z = 0.6$ (light) and $z = 1.4$ (dark). The black line represents the fiducial $\Lambda$ CDM model. Plot made by Adrian Vollmer. . . . .	94
5.1	Fisher analysis scheme for the anisotropic stress. . . . .	98
5.2	$\Delta\bar{Q}$ as a function of $\lambda$ . The colored region can be excluded by a Euclid-like survey at the $1\sigma$ level. The curve approaches $\Delta\bar{Q} \approx 0.021$ for large $\lambda$ . Plot made by Adrian Vollmer. . . . .	99
5.3	Testing the equivalence principle with a torsion balance. The plot shows the upper limits for the Yukawa interactions coupled to baryon number with 95% confidence. The shaded region is experimentally excluded. Figure taken from [14] . . . . .	100
5.4	Exclusion plots for the set of functions $\{h_2, h_4, h_5\}$ . $h_2$ as a function of $h_4$ (top), $h_4$ as a function of $h_5$ (mid), and $h_2$ as a function of $h_5$ (bottom). The colored region can be excluded by a Euclid-like survey at the $1\sigma$ level. Plots made by Adrian Vollmer. . . . .	101
C.1	Confidence contours for $\bar{A}$ and $\bar{R}$ in the three cases: orange line $V_{\text{eff}}$ , blue line $V_{\text{eff}} \approx V_{\text{survey}}$ , and green line $V_{\text{eff}} \approx P(k, \mu)^2$ . . . . .	120



## ACKNOWLEDGEMENTS

My first and biggest thanks go to my advisor Luca Amendola, for giving me the excellent opportunity to pursue my doctoral studies in the mecca of Dark Energy, he truly joined to the dark side!. I acknowledge all his support, patience and his offer of an interesting project. I would like to acknowledge the Heidelberg Graduate School of Fundamental Physics (HGSFP) for holding an excellent graduate program, to all the staff at the Institute for Theoretical Physics (ITP) who were really kind and also very patient with my fantastic German skills, and to the University of Heidelberg for providing me all the benefits achieved in being part of this prestigious University. I spent my whole doctoral studies in a charming place: the Westzimmer at Philosophenweg 16, a dark (fix properly) old and mistique room, where all this thesis was researched and written. Big thanks for the financial support from the Deutsche Akademische Austauschdienst (DAAD) through the program “*Forschungsstipendium für Doktoranden und Nachwuchswissenschaftler*”, and also to the Deutsche Forschungsgemeinschaft (DFG) through the project TRR33 “*The Dark Universe*”.

I would also like to thank all the members of the Cosmology Group and visitors during my stay, namely, Yashar Akrami, Guillermo Ballesteros, Emilio Bellini, Alicia Bueno, Santiago Casas, Simone Fogli, Florian Führer, Adalto Gomes, Caroline Heneka, Luisa Jaime, Rocky Kolb, Frank König, Martin Lüben, Valerio Marra, Matteo Martinelli, Eloisa Menegoni, Mariele Motta, Henrik Nersisyan, Io Odderskov, Suttituk Othatawong, Valeria Pettorino, Gerasimos Rigopoulos, Ignacy Sawicki, Martina Schwind, Elena Sellentin, Adam Solomon, Laura Taddei, Valeri Vardanyan, Wessel Valkenburg, Adrian Vollmer, Christof Wetterich and Miguel Zumalacárregui for their friendship, stimulating discussions, soccer time, BBQ’s, lunches, laughs, and incredible support. Special thanks to Florian and Frank for the boring task of translating the abstract in German.

Germany is an awesome country, my second home, a place with open doors to all the world. Bad and good weather, schnitzel, thousands of potatoes (and beers), terrific chocolates, Wacken Open Air (2012, 2013, 2014), Chinese food, beautiful landscapes, *bitte* and soccer everywhere (thanks to *Die Mannschaft* for the fourth world cup 4×☆). Heidelberg, the city where I lived... I simply said: I fall in love with it!, its like an entity acting always in favor of your happiness. A small world, too many countries, languages, cultures and a non-enumerable set of incredible people. My stay in Heidelberg would not be as awesome as it was, if I had not met all the people I have met. Specially, I would like to thank José Alonso, Fabrizio Arrigoni, Eduardo Bañados, Anahi Caldu, Mauricio Carrasco, Esteban Durango, Agnese Fabris, Nohora Galán, Oscar Garcia, Juan Camilo Ibañez, Pablo Klinkisch, Lucy Maxton, Sindy Mojica, Elena Manjavacas, Gustavo Morales, Marta Muga, Mauricio Ortiz, Fabian Olivares, Katherinne Soza, and Viviana Torres for their friendship, soccer time, Neckarwiese moments, dancing nights (yes, dancing), movies, advice during the hard times, and tunel blacks in Sonderbar. Honorary mention to Lucy for her kind proofreading support. I have not been leaving Germany yet (becoming 50% chilean), but I already miss you all!. Thanks as well to all my friends in Colombia, who virtually give me support and loyal advice, I had felt them close.

I would also like to thank Matthias Bartelmann for agreeing to be my second referee, and also to Eva K. Grebel and Markus Oberthaler who will take part in the oral examination. Special thanks to Leonardo Castañeda for all his support, advices and scolding; a friendship which is strongly coupled with time. Finally, I want to thank the support given by my family, to my mother located at a distance of  $2.94 \times 10^{-10}$ pc from Heidelberg, to my brother Miguel located at  $1.90 \times 10^{-10}$ pc, and to my brother Cristian spreading across the whole Universe!. This thesis is dedicated with all my love to you!

*It was a real journey through the dark...thanks to all for these random events that were in some way connected with me!.*



## CONTRIBUTIONS

### DECLARATION BY AUTHOR

This thesis is composed of my original work, and contains no material previously published or written by another person except where due reference has been made in the text. I have clearly stated the contribution by other authors to jointly-authored works that I have included in my thesis. The content of my thesis is the result of work I have carried out since the commencement of my graduate studies at the Institut für Theoretische Physik, Ruprecht-Karls-Universität Heidelberg and does not include material that has been submitted by myself to qualify for the award of any other degree or diploma in any university or other tertiary institution. Part of this thesis was based on the following contributions:

- [1] Luca Amendola, Simone Fogli, **Alejandro Guarnizo**, Martin Kunz & Adrian Vollmer, “Model-independent Constraints on the Cosmological Anisotropic Stress”. *Phys. Rev. D* **89**, 063538 (2014). **Chapter 4** is based entirely on this publication; my contribution corresponds to the “*Galaxy Clustering*” part (**Subsection 4.1.1**), “*Weak Lensing*” part (**Subsection 4.1.2**) was made by Adrian Vollmer, and “*Supernovae*” made by Simone Fogli (**Subsection 4.1.3**). **Subsection 4.1.4** was made jointly with all the authors.
- [2] **Alejandro Guarnizo**, Luisa Jaime, Adrian Vollmer & Luca Amendola, “A Cosmological Exclusion Plot for Modified Gravity”. **Chapter 3** & **Chapter 5**. To be submitted. My contribution corresponds to **Chapter 3**, and plots presented in **Chapter 5** (fig. 5.2 and fig. 5.4) (with some slightly changes), were made by Adrian Vollmer.
- [3] **Alejandro Guarnizo**, Luca Amendola, Martin Kunz & Adrian Vollmer “Semi-analytical Study on the Generic Degeneracy for Galaxy Clustering Measurements”. *Proceedings of the International Astronomical Union*, **10**, pp 347-350. **Appendix C**. This contribution was entirely made by my own.



## NOTATION AND CONVENTIONS

The sign convention used for the metric tensor is  $(-, +, +, +)$ , the speed of light is taken in geometrized units  $\hbar = c = 1$ . Greek indices  $\alpha, \beta, \dots$  are used for space-time coordinates and runs from 0 to 3, latin indices  $a, b, \dots$  are used only for spatial coordinates and runs from 1 to 3. Bold symbols  $\mathbf{A}, \mathbf{B}, \mathbf{C}, \dots$  denote vectorial quantities. Tensorial quantities are denoted with calligraphic fonts  $\mathfrak{A}, \mathfrak{B}, \mathfrak{C}$ .

Symbol	Definition
$G$	Gravitational Constant ( $6.67 \times 10^{-11} \text{ m}^2/\text{kg s}^2$ )
$\kappa$	$8\pi G$
$a$	Scale factor (with present value $a_0 = 1$ )
$t$	Cosmic time
$\tau$	Conformal time $\tau = \int a^{-1} dt$
$N$	Number of $e$ -foldings $N = \ln a$
$z$	Redshift: $z = a_0/a - 1$
$\cdot$	Time derivative
$'$	Derivative with respect to $\tau$
$d_L, d_A$	Luminosity distance, angular diametral distance
$H$	Hubble parameter: $H = \dot{a}/a$
$\mathcal{H}$	Conformal Hubble parameter $\mathcal{H} = aH$
$H_0, h$	Present Hubble parameter: $H_0 = 100h \text{ km sec}^{-1} \text{ Mpc}^{-1}$
$E(z)$	Hubble parameter normalized by $H_0$ : $E(z) = H(z)/H_0$
$\rho$	Energy density
$p$	Pressure

Symbol	Definition
$w$	Equation of state (EoS) $w = p/\rho$
$K$	Spatial curvature of the Universe
$\Lambda$	Cosmological constant
$c_s$	Sound speed
$k$	Comoving wavenumber
$P(k)$	Power spectrum
$G$	Growth function
$f$	Growth rate
$\ell$	Spherical harmonics multipoles
$C_\ell$	Multipole power spectrum
$\Psi, \Phi$	Gravitational Potentials
$\delta$	Density contrast
$\eta$	Anisotropic stress
$S$	Action
$g_{\alpha\beta}$	Metric tensor components
$g$	Metric determinant
$R_{\alpha\beta\gamma\delta}$	Riemann tensor
$R_{\alpha\beta}$	Ricci tensor
$R$	Ricci scalar
$G_{\alpha\beta}$	Einstein tensor
$T_{\alpha\beta}$	Energy-Momentum tensor
$\partial_\alpha$	Partial derivative with respect to $x^\alpha$
$\nabla_\alpha$	Covariant derivative
$A_{,B}$	Derivative of $A$ with respect to $B$
$A_{(\alpha\beta)}$	Symmetrization $A_{\alpha\beta} \equiv (1/2)(A_{\alpha\beta} + A_{\beta\alpha})$
$A_{[\alpha\beta]}$	Antisymmetrization $A_{\alpha\beta} \equiv (1/2)(A_{\alpha\beta} - A_{\beta\alpha})$
$\square$	d'Alembertian $\square = \nabla^\gamma \nabla_\gamma$
$\phi$	Scalar field
$X$	Kinetic energy: $X = -(1/2)g^{\alpha\beta}\partial_\alpha\phi\partial_\beta\phi$



## PREFACE

The current accelerated expansion of the Universe was, without doubt, the most surprising discovery at the end of the last century. A static model, proposed by Einstein with the *ad-hoc* inclusion of the cosmological constant  $\Lambda$ , was ruled out by Hubble's observations of galaxies recession in 1931, and instabilities coming from perturbations in the energy density. Thus,  $\Lambda$  was forgotten at that time. Cosmology became an exact science, with more accurate data, which implies a better way to falsify models of the Universe. From the genesis of the so-called *standard cosmological model* some ideas have survived until today, such as the Big Bang model supported by observations of the Cosmic Microwave Background (CMB), the inflationary paradigm, and dark matter, which is still an open issue. In 1998, two independent groups studying the distance-luminosity relation of Supernovae, discovered that something strange had happened: the Universe was not only expanding, but doing it so in an accelerated way.  $\Lambda$  was back from the dead to play a key rule in explaining this speed-up. Recent data of the Planck satellite [15] also confirm that observations of the CMB are well described by the flat  $\Lambda$ CDM model ( $\Lambda$  and Cold Dark Matter), whose parameters are determined to percent-level accuracy [2]. The cosmological model that arises from these data is such that only 5% of today's energy density consists of baryonic matter described by the standard model of particle physics. Another 27% appears to be matter that is only interacting gravitationally with the visible world (dark matter), and the remaining 68% is made up of a cosmological constant.

Present models associate the cosmological constant with contributions of vacuum fluctuations at the quantum level. The problem comes when comparing the expected value to the observed one using cosmological data: they differ by around 121 orders of magnitude, which is the so-called fine tuning problem of  $\Lambda$ , the worst prediction so far in the history of physics. Another problem it suffers is why the energy density associated is comparable with today's matter content (the coincidence problem) [16]. One attempt to solve this

inconsistency is to consider general dark energy models beyond the cosmological constant, including modifications of Einstein's theory of General Relativity (GR), and modifications in the matter sector. Generically, such an alternative is called *dark energy*.

The most abundant and accurate source of cosmological information comes from the CMB [17, 18]. It basically consists of photons coming from the last scattering surface, which marks the era in which they were released from their tight coupling to baryons, and were left to travel through space. The fluctuations in the temperature of these photons carry imprints of primordial perturbations when the universe was about a thousand times smaller than at the present time. Projects as WMAP [19] and recently Planck [15] have measured these angular fluctuations in temperature with remarkable accuracy, confirming the predictions of the standard cosmological model. CMB also provides an interesting arena to test dark energy models, since matter perturbations and fluctuations of these fields can introduce variations in the redshifts of photons traveling through overdense regions. The so called Integrated Sachs-Wolfe (ISW) effect links the evolution of the gravitational potentials with the matter distribution via the Poisson equation, which depends on the gravitational theory used.

But, how can we modify gravity? one approach comes from the action principle: due to its elegance, it is believed that all physical theories should be completely specified by an associated action, and asserts that the evolution of physical fields involved in the theory is determined by a variational principle of an action  $S$ . Usually, this action is an integral of some function of the fields (which in GR corresponds to the metric tensor), taken over the space-time with an appropriate weight. The resulting variation of the action gives the equations of motion for the fields. In the case of GR, the action is constructed with the Ricci scalar  $R$  and a function of the matter fields, which leads to the so-called Einstein-Hilbert action. This seems a plausible way to modify gravity: instead of adding exotic kinds of matter, one can modify the geometric part of the action, including additional degrees of freedom or higher powers of the scalar. Motivations come from two sides: first, even if GR has been tested in the solar system regime, it has not been tested (accurately) on cosmological scales, and thus the actual speed-up of the Universe should be produced by extensions of GR. Secondly, Einstein's theory is not held as a fundamental theory, since so far a quantum description of gravity is incomplete; other issues related to singularities arise, for instance black holes and the Big Bang.

Other modifications include extra degrees of freedom (scalar, vector and tensor fields), higher dimensions, higher derivatives in the field equations, and theories in which the Lorentz invariance is violated. However, higher order theories have several theoretical and practical problems. Generally, the field equations involve derivatives of at least fourth order, which results in ghost (states of negative kinetic energy) and other kinds of instabilities. When studying these modifications of gravity, a model-independent approach is always desirable. It allows us to classify large families of theories with parameters which

deviate from the standard approximation (i.e. the  $\Lambda$ CDM model). At the background level, the modifications of gravity are encoded in the equation of state of dark energy (which should be close to  $-1$  to generate the current acceleration), Quintessence models and natural extensions of GR via generalizations of the Einstein-Hilbert action (for instance  $f(R)$  gravity), could be studied within this. In a linear perturbation framework the effective gravitational constant (or the clustering of dark energy) and the anisotropic stress (or gravitational slip), encompass the deviations from the standard Poisson equation, and thus a possible scenario to test modified gravity models. Recently Amendola et. al. [20] showed, assuming a *perfect* knowledge of background and perturbations quantities, and assuming a family of modifications of gravity with a single scalar field, the Horndeski Lagrangian, that the only model-independent observable is the anisotropic stress  $\eta$ . When assuming these specific lagrangian in the quasi-static approximation, a simple expression which beautifully links truly observables, and theory, could be obtained. In this way, we can rule out dark energy models if, for instance, the scale behaviour is not satisfied.

Fortunately, there is an increasing amount of data to test various models. Besides higher precision measurements of the CMB, galaxy surveys such as the Sloan Digital Sky Survey (SDSS) [21] and the 2dF Galaxy Redshift Survey (2dFGRS) [22] have been achieving high accuracy. The observed matter distribution alone is sufficient information to exclude several ideas accounting for the present cosmic acceleration or, to tightly constrain their parameters. The study of supernovae still provides the most precise constraints so far. Future galaxy surveys, such as Euclid, an ESA selected medium-class mission that will be launched in 2020, would provide new opportunities to verify the current standard cosmological model, and also to constrain modified gravity theories. By combining galaxy clustering and weak lensing information, the accuracy of the Euclid survey makes it possible to distinguish between GR and other modifications of gravity. Statistical tools like for instance the Fisher matrix provide an elegant way, constraints on cosmological parameters and/or additional quantities which characterize the theoretical dark energy model; in this way we can make an educated guess as to how well surveys will measure them. We will then reach a new era of high accuracy measurements, an ultimate opportunity to unscramble the dark energy paradigm: *(High)-precision cosmology is coming!*

## OUTLINE OF THE THESIS

The outline of this thesis is as follows: In [Chapter 1](#) we summarize the main ingredients of the standard cosmological model, from a brief overview of the mathematics behind it (Einstein Field equations), to a description of cosmological perturbations. The problems of the cosmological constants are also addressed, in addition to a short explanation of the current observations of dark energy.

[Chapter 2](#) is devoted to discussing (in some detail) the modified gravity models invoked to explain the actual accelerated expansion of the universe: we focus, however, on a subclass of modifications with a single scalar field, namely the Horndeski Lagrangian. Model-independent parameterizations for those dark energy cosmologies are also explained.

In [Chapter 3](#) we start showing the results of this thesis. Using the main result of [\[20\]](#), and current data of the growth rate  $f\sigma_8$ , the Hubble parameter  $H(z)$  and data derived from galaxy-galaxy and galaxy-velocity correlations, we find bounds on the anisotropic stress at some specific redshift.

[Chapter 4](#) is devoted to finding the future constraints on the anisotropic stress by performing a Fisher analysis. Adopting the specifications from the Euclid survey, we use the combination of Galaxy Clustering (GC), Weak Lensing (WL) and Supernovae (SN), to obtain constraints on the cosmological anisotropic stress  $\eta$  in a model-independent way.

Using the strategy of the previous chapter, in [Chapter 5](#) we use our forecast to create a cosmological exclusion plot, with the aim of ruling out modified gravity models. For that purpose we use the theoretical form of the anisotropic stress, coming from the quasi-static regime of the Horndeski Lagrangian.

Finally, we draw the conclusions in [Chapter 6](#)



Part I

**Preliminaries**

## INTRODUCTION

*“Most of the fundamental ideas of science are essentially simple, and may, as a rule, be expressed in a language comprehensible to everyone.”*  
Albert Einstein

General relativity is the most accepted gravitational theory so far. Proposed by Albert Einstein in 1916, general relativity explains gravitational phenomena as a consequence of space-time curvature due to the content of matter and energy. In this way, a transition between the classical description of gravity as a long-interacting force (Newton) to a purely geometric property of the space-time (Einstein) was made [23]. Even if General Relativity (hereafter GR) has a solid observational evidence (at least at a percent level in the solar system regime [24, 25]), and for its simplicity and beauty is almost a *perfect theory* [26], gravity is still mysterious, and confrontation with observational data at large (cosmological) scales suggest that possible modifications of Einstein’s theory could in principle be made.

## 1.1 General Relativity in a Nutshell

As we all know gravity was first described by Newton as a long-distance force, which, when considering two objects of masses  $m_1$  and  $m_2$ , depends on the numerical product of them and the distance of separation. This simple phenomenological description allowed scientist in centuries XVII to XIX to make amazing scientific developments (in Astronomy indeed). Although, Newtonian gravity explained for instance the motion of the planets in the solar system, and the free-fall of objects, it was inherently unable to take into account *why* the force should take that particular form.

The Newtonian description, based on the existence of inertial reference systems (even if that idealistic description is still debated), was incompatible with the electromagnetic interaction beautifully synthesized by Maxwell in late XIX century. The main problem was a long-range interaction with an infinite speed of propagation. This is the seed for the relativistic theory of motion introduced by Einstein in 1905, theory who relies on two “simple” postulates

1. (*Relativity principle*) *The laws of physics are the same in all inertial frames of reference.*
2. (*Constancy of the speed of light*) *The speed of light  $c$  in vacuum is the same in all inertial frames.*

Notice that this relativistic description was in direct conflict with the Newtonian description of gravity, due to the constancy of the speed of light. The fundamental issue was reconciling the Newtonian description with the constancy of the speed of light in all inertial frames, which was the work of Einstein between 1905 and 1916: the gestation of (GR). The key ingredient, the *Einstein’s equivalence principle* which generalizes the weak equivalence principle <sup>1</sup> and could be written as :

*Einstein’s equivalence principle:* Experiments cannot distinguish if an object experiences a free-fall in a uniform gravitational field  $g$ , (with  $g$  the magnitude of the acceleration in the gravitational field) or if it is accelerating with  $a = g$ .

Einstein’s magnificent idea was to consider the trajectories of particles in free-fall and argue that they are moving *freely* in a curved space-time. Thus, a particle in a curved space-time does not experience acceleration, it is simply following a geodesic on it. But, which entity curves this space-time? The answer could not be more surprising: any kind of matter or energy. The link between matter content and curvature (as we will see later) is given by the Einstein field equations, a set of 10 differential equations which describes entirely the motion of particles given the energy content. Thus summarizing, according to Jon Archibald Wheeler [27]: “*Space-time tells matter how to move; matter tells space-time how to curve.*”.

### 1.1.1 Postulates and Mathematical Foundations of General Relativity

The literature on GR is impressively large. There are however milestones books as e.g. [27–32]. We will try here to define as concisely as possible the mathematical foundations -in a 3 + 1 form (3 postulates, 1 theorem)-, keeping however a bit of formality. The first definition concerns the mathematical space in which GR lives:

<sup>1</sup>The equivalence between inertial mass and gravitational mass of a body.

**Postulate 1.1.** *The space-time is described by a pair  $(\mathcal{M}, \mathbf{g})$  being  $\mathcal{M}$  a four dimensional connected Hausdorff  $C^\infty$  manifold and  $\mathbf{g}$  a Lorentzian metric on  $\mathcal{M}$ .*

The curvature of the manifold is well described by the Riemann curvature tensor  $\mathfrak{R}$ , whose components could be written as

$$R_{\beta\gamma\delta}^\alpha = \partial_\gamma \Gamma_{\delta\beta}^\alpha - \partial_\delta \Gamma_{\gamma\beta}^\alpha + \Gamma_{\gamma\sigma}^\alpha \Gamma_{\delta\beta}^\sigma - \Gamma_{\sigma\delta}^\alpha \Gamma_{\gamma\beta}^\sigma, \quad (1.1)$$

being  $\Gamma_{\beta\gamma}^\alpha$  the connections (or Christoffel symbols)

$$\Gamma_{\beta\gamma}^\alpha = \frac{1}{2} g^{\alpha\sigma} [\partial_\gamma g_{\sigma\beta} + \partial_\beta g_{\sigma\gamma} - \partial_\sigma g_{\beta\gamma}], \quad (1.2)$$

with  $g_{\alpha\beta}$  the components of the metric tensor  $\mathbf{g}$ . A fundamental restriction imposed on the manifold  $\mathcal{M}$  in GR is that it should be torsion-free, formally [33]:

**Theorem 1.2** (Fundamental Theorem of Riemannian Geometry). *In a Riemannian manifold  $(\mathcal{M}, \mathbf{g})$ , there is a unique symmetric connection  $\Gamma_{\beta\gamma}^\alpha$  which is compatible with the metric  $\mathbf{g}$ . This connection is called **Levi-Civita connection**.*

The condition of torsion-free manifold is satisfied imposing that the torsion, represented here by the Cartan torsion tensor  $S_{\beta\gamma}^\alpha$  vanish:

$$S_{\beta\gamma}^\alpha \equiv \Gamma_{[\beta\gamma]}^\alpha = 0, \quad (1.3)$$

and the relation between the connection and the metric comes from the metric compatibility

$$\nabla_\gamma g_{\alpha\beta} = 0. \quad (1.4)$$

This postulate however could be relaxed, allowing the manifold to have a non-vanishing torsion. From the particle physics point of view, this requirement seems reasonable, since spinor fields could in principle coupled spin, with the torsion tensor. Strictly speaking, the role of the Poincaré group in quantum theory (from which unitary and irreducible representations are labeled as mass and spin), is restored in GR, since without this, the only structure group acting on  $\mathcal{M}$  is the Lorentz one. The theory that emerges from this condition is known as the *Einstein-Cartan-Sciama-Kibble* (ECSK) formulation, firstly described by Cartan in 1922 [34], and extended by Sciama [35] and Kibble [36] in the late 1950s.

Let us move forward to the energy-momentum side. As we will see later, the energy-momentum tensor plays an important role in the geometrical description of the space-time, since it gives the link between the matter content and the curvature, via the Einstein field equations.

**Postulate 1.3.** *Local conservation: There exist a symmetric tensor  $T_{\alpha\beta} = T_{\alpha\beta}(\psi) = T_{\beta\alpha}$  which is a function of the matter fields  $\psi$  and their derivatives which satisfies:*

- i.  $T_{\alpha\beta} = 0$  on  $\mathcal{U} \subset \mathcal{M}$  if and only if  $\psi_i = 0$  for all  $i$  on  $\mathcal{U}$ .*
- ii.  $\nabla_\beta T^{\alpha\beta} = 0$ . (Local energy conservation)*

Finally, we have the postulate of the Einstein field equations:

**Postulate 1.4.** *The metric on the manifold  $(\mathcal{M}, \mathbf{g})$  is entirely determined by Einstein field equations:*

$$R_{\alpha\beta} - \frac{1}{2}Rg_{\alpha\beta} = \kappa T_{\alpha\beta}, \quad (1.5)$$

with  $R_{\alpha\beta}$  the Ricci tensor ( $R_{\alpha\beta} = R_{\alpha\eta\eta\beta}^\eta$ ),  $R$  the Ricci scalar ( $R = g^{\alpha\beta}R_{\alpha\beta}$ ),  $T_{\alpha\beta}$  the energy-momentum tensor and  $\kappa = 8\pi G$ ,  $G$  the gravitational constant and we set units of  $c = 1$ .

If we define the Einstein tensor  $G_{\alpha\beta}$  as:

$$G_{\alpha\beta} \equiv R_{\alpha\beta} - \frac{1}{2}Rg_{\alpha\beta}, \quad (1.6)$$

then we have a geometrical restriction (coming also from the local conservation of the energy-momentum tensor)

$$\nabla_\beta G^{\alpha\beta} = 0, \quad (1.7)$$

which is known as the Bianchi identity. Notice that we can add a constant term, for instance  $\Lambda g_{\alpha\beta}$ , in the geometric side of the Einstein field equations (hereafter EFE's), which still satisfies the Bianchi condition. As we will discuss later, this introduction is now considered as standard for cosmology, since it reproduces current observations; further details will be shown in [Section 1.2](#).

The motion of a particle is dictated by its trajectory on the space-time,  $x^\alpha(\lambda)$ , where  $\lambda$  is a parameter. A free particle, i.e., a particle without external forces acting on it (different from gravity), satisfies the geodesic equation:

$$V^\mu \nabla_\mu V^\nu = 0, \quad (1.8)$$

with  $V^\mu = \frac{dx^\mu}{d\lambda}$  the tangent vector to the trajectory. An equivalent well-know form of this equation is:

$$\frac{d^2 x^\gamma}{d\lambda^2} + \Gamma_{\alpha\beta}^\gamma \frac{dx^\alpha}{d\lambda} \frac{dx^\beta}{d\lambda} = 0. \quad (1.9)$$

This expression applies to the following cases:

- Massive particles, in which the parameter  $\lambda$  matches with the proper time and then the corresponding tangent vector  $V^\alpha$  is normalized:  $g_{\alpha\beta}V^\alpha V^\beta = -1$ .
- Massless particles, like the photon, in which the tangent vector, denoted by  $k^\alpha$  is null, i.e.,  $g_{\alpha\beta}k^\alpha k^\beta = 0$ .

The Newtonian limit (Poisson equation) is recovered as the weak field limit of the EFE's, in which a Minkowski space-time is slightly perturbed by a gravitational potential; special relativity is, as we expected, a particular case of GR in which the manifold  $\mathcal{M}$  is conformally flat and  $\mathbf{g} = \mathbf{n}$ , with  $\mathbf{n}$  the Minkowski tensor.

### 1.1.2 The Gravitational Action

A problem that Einstein faced just after the development of GR was to find a Lagrangian from which his equations could be obtained, after a variational principle  $\delta S = 0$ , being  $S$  the total action. Independently, Einstein and Hilbert found the action associated with the gravitational field, commonly known as the Einstein-Hilbert action  $S_{EH}$ . As we all know, the Lagrangian should be constructed from a scalar quantity, and the natural choice was to use the simplest scalar coming from the geometrical side: the Ricci scalar  $R$ . The total action, including the Gibbons-York-Hawking boundary term  $S_{GYH}$  [37, 38] which relaxed the conditions imposed when varying the action <sup>2</sup>, and the action associated with all matter fields  $S_M(\psi, g_{\alpha\beta})$ , could be written as [32]:

$$S = \frac{1}{2\kappa} (S_{EH} + S_{GYH}) + S_M(\psi, g_{\alpha\beta}), \quad (1.10)$$

$$= \frac{1}{2\kappa} \left( \int_{\mathcal{V}} d^4x \sqrt{-g} R + 2 \oint_{\partial\mathcal{V}} d^3y \varepsilon \sqrt{|h|} K \right) + S_M(\psi, g_{\alpha\beta}), \quad (1.11)$$

here  $\mathcal{V}$  is a hypervolume in  $\mathcal{M}$ ,  $\partial\mathcal{V}$  its boundary,  $h$  the determinant of the induced metric,  $K$  the trace of the extrinsic curvature over  $\partial\mathcal{V}$ , and  $\varepsilon$  is equal to  $+1$  if  $\partial\mathcal{V}$  is time-like and  $-1$  if  $\partial\mathcal{V}$  is space-like; coordinates  $x^\alpha$  labeled the finite region  $\mathcal{V}$  and  $y^\alpha$  for the boundary  $\partial\mathcal{V}$ . After varying the action w.r.t. the metric  $g^{\alpha\beta}$  we find the standard form of EFE's

$$\frac{1}{\sqrt{-g}} \frac{\delta S}{\delta g^{\alpha\beta}} = 0 \quad \Longrightarrow \quad R_{\alpha\beta} - \frac{1}{2} R g_{\alpha\beta} = \kappa T_{\alpha\beta}, \quad (1.12)$$

where the energy-momentum tensor is defined as

$$T_{\alpha\beta} \equiv - \frac{2}{\sqrt{-g}} \frac{\delta S_M(\psi, g_{\alpha\beta})}{\delta g^{\alpha\beta}}. \quad (1.13)$$

Another very interesting variational approach comes when consider *non-metricity*, that means, the connection  $\Gamma_{\beta\gamma}^\alpha$  and the metric  $g_{\alpha\beta}$  are treated as independent quantities. Thus,

<sup>2</sup>The usual procedure to obtain the Einstein's equations from the action fixing  $\delta g_{\alpha\beta}$  and  $\delta \partial g_{\alpha\beta}$  to vanish at the boundary, making the variational principle overconstrained.

in addition to the variation w.r.t. the metric, an additional constraint comes after varying the action w.r.t. to the connection<sup>3</sup>. This method is known as the *Palatini variation* [39]. Notice that here we also assume a torsionless manifold, and just non-metricity. In general, if we consider also non-vanishing torsion (as the case of the ECSK formalism), the field equations are not uniquely determined. As we will see in [Subsection 2.1.2](#) with a specific example of an extended gravity theory, this approach will give completely different field equations, and thus, different interpretation of the additional degrees of freedom introduced.

### 1.1.3 Cosmological Constant Act I: Bianchi Identities

From the postulate of the energy conservation dictated by the relation

$$\nabla_\alpha T^{\alpha\beta} = 0, \quad (1.14)$$

it follows from the EFE's a geometrical restriction on the Einstein tensor  $G_{\alpha\beta}$

$$\nabla_\alpha G^{\alpha\beta} = 0, \quad (1.15)$$

which is known as the Bianchi identity. We can now guess a first kind of modification in the geometrical sector, which still satisfies this condition. For instance, a constant term  $\Lambda g_{\alpha\beta}$  still fulfills the condition due to metric compatibility,

$$\nabla_\alpha (\Lambda g_{\alpha\beta}) = \Lambda \nabla_\alpha g_{\alpha\beta} = 0. \quad (1.16)$$

The EFE's with a cosmological constant are simply obtained adding the term  $-2\Lambda$  in the Einstein-Hilbert action, which reads:

$$R_{\alpha\beta} - \frac{1}{2} R g_{\alpha\beta} + \Lambda g_{\alpha\beta} = \kappa T_{\alpha\beta}. \quad (1.17)$$

We will back on that in the next section when considering the cosmic content of the Universe. Last but not least, the Einstein-Hilbert action somehow works as a template for other gravitational theories, since apart from issues of instability and higher derivatives, extended gravity theories could be constructed with a geometrical scalar, or powers of the Ricci scalar. We will focus on this in [Chapter 2](#).

---

<sup>3</sup>This constraint in the case of GR its simply the metric compatibility written as  $\nabla_\gamma(\sqrt{-g}g^{\alpha\beta}) = 0$ .

## 1.2 The Cosmological Arena

GR is the main ingredient to construct models that can describe the evolution of the Universe. After being tested experimentally, at solar system level, cosmological models were constructed based on EFE's. We can say that Modern cosmology born in 1917, when Einstein applied his equations to describe a static Universe, with an *ad-hoc* introduction of the *cosmological constant* term, which acts against gravity. Between 1920 and 1930, Alexander Friedmann, Georges Lemaître, Howard P. Robertson and Arthur Geoffrey Walker, using the well known cosmological principle, based on statistical properties of the Universe at large scales (around 100 Mpc), *independently* found a solution to the EFE's, describing and expanding (or contracting Universe). We will come back to the history behind the static proposal by Einstein in a subsequent section. This postulate of isotropy and homogeneity, allow us to write the metric of a maximally symmetric universe given by the Robertson-Walker metric<sup>4</sup> [17, 40, 41]

$$ds^2 = -dt^2 + a^2(t) \left[ \frac{dr^2}{1 - Kr^2} + r^2 d\theta^2 + r^2 \sin^2 \theta d\varphi^2 \right], \quad (1.18)$$

being  $a(t)$  the scale factor, and  $K$  a parameter describing the spatial geometry of the Universe ( $K = 0$  for a flat Universe,  $K = 1$  for a closed one, and  $K = -1$  for an open), fig. 1.1. This manifold is represented by a foliation  $\mathcal{M} = \Sigma \times \mathbb{R}$  in which  $\Sigma$  is a maximally symmetric 3-manifold and  $\mathbb{R}$  the temporal coordinate of space-time. The metric on  $\Sigma$  corresponds to the spatial part of eq. (1.18)

$$d\tilde{s}^2 = \tilde{g}_{ij} dx^i dx^j = \frac{dr^2}{1 - Kr^2} + r^2 d\theta^2 + r^2 \sin^2 \theta d\varphi^2. \quad (1.19)$$

The cosmological principle yields a perfect fluid form for the energy-momentum tensor

$$T_{\alpha\beta} = (\rho + p)u_\alpha u_\beta + pg_{\alpha\beta}, \quad (1.20)$$

with  $p$  the pressure,  $\rho$  the energy density, and  $u^\alpha$  the four-velocity of fundamental observers. Einstein field equations for the metric eq. (1.18) and energy-momentum content given by eq. (1.20) are

$$H^2 = \left( \frac{\dot{a}}{a} \right)^2 = \frac{\kappa}{3} \rho - \frac{K}{a^2}, \quad \text{Temporal component} \quad (1.21)$$

and

$$\frac{\ddot{a}}{a} = -\frac{\kappa}{6} (\rho + 3p), \quad \text{Spatial components} \quad (1.22)$$

---

<sup>4</sup>For historical reasons, the name of the metric is given just by Robertson and Walker (RW), nevertheless is usual to find it as FLRW, or just FL.

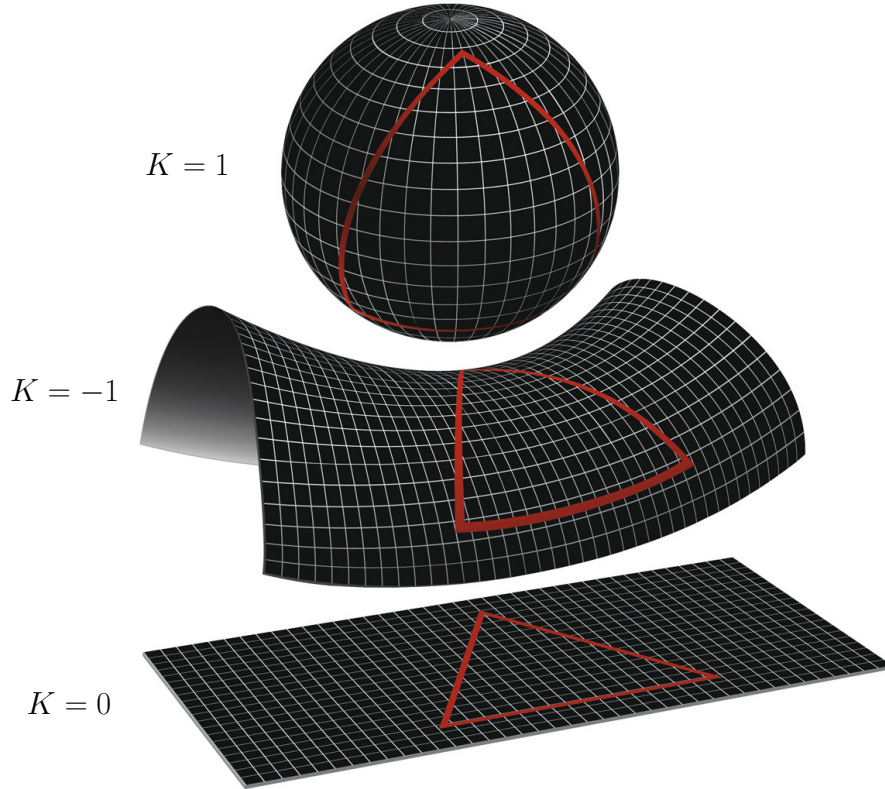


**Figure 1.1:** Spatial geometry of the Universe: Flat Universe ( $K = 0$ ), Open Universe ( $K = -1$ ) and Closed universe ( $K = 1$ ). Credit: NASA/WMAP Science Team.

in which we define the Hubble parameter as  $H \equiv \frac{\dot{a}}{a}$ . Energy conservation, coming from  $\nabla_{\beta} T^{0\beta} = 0$  reduces to

$$\frac{d}{dt}(\rho a^3) + p \frac{d}{dt}(a^3) = 0. \quad (1.23)$$

We can now get some conclusions from the form of the equations eq. (1.21) and eq. (1.22). For example, a static solution, demanding  $\dot{a} = 0$  is consistent with eq. (1.21) if  $\rho > 0$  and the Universe is open ( $K = +1$ ). The problem however comes when contrasting this kind of Universe with eq. (1.22), since  $\ddot{a}$  never goes to zero if the pressure is also positive. This is the reason why this set of equations, commonly known as *Friedmann-Lemaître equations*, does not admit a static solution.

### 1.2.1 Cosmological Constant Act II: Einstein's Static Universe

In [Subsection 1.1.3](#) we announced the cosmological constant term in the EFE's as the most simple modification on the gravitational sector which still satisfies the Bianchi identity.

However, the history of Einstein's motivation for the introduction of  $\Lambda$  is really interesting, and deserves a few words here. As anticipated, just after the genesis of GR, in 1917 Einstein proposed a model to describe the evolution of the universe, which from his common sense should be immutable, and thus, static [42]. In the case of the presence of matter, gravity will make this universe collapse. In order to prevent this, Einstein presented a constant term in his field equations, which acts as a repulsive force against gravity. That was then the physical origin of the cosmological constant.

From the EFE's with cosmological constant, eq. (1.17), the Friedmann-Lemaître equations becomes

$$H^2 = \frac{\kappa}{3}\rho - \frac{K}{a^2} + \frac{\Lambda}{3}, \quad (1.24)$$

and,

$$\frac{\ddot{a}}{a} = -\frac{\kappa}{6}(\rho + 3p) + \frac{\Lambda}{3}, \quad (1.25)$$

This set of equations admits a static solution for  $\rho > 0$ ,  $p > 0$  in an open universe, and of course, with the restriction  $\Lambda > 0$ . Besides this, alternative cosmologies were built admitting dynamical solutions, for instance the models of Friedmann in 1922, and Lemaître in 1927 (this in addition gives a simple form the distance-redshift relation  $v = H \cdot d$ , verified two years later by Hubble's observations [43]), which influenced theoretical developments towards a fully description of the universe.

Einstein himself considered the Friedmann model as “*abominable*”; even the mathematics behind were totally correct, the status of a dynamical universe was completely unacceptable. His conversion wait until 1931, the year in which he published a three-page paper (with not significantly new contribution) in favor of the dynamical solution [44]. One can think that Hubble's observations were the deepest reason in Einstein's conversion from a static to a dynamical universe. However, as was explained in detail on [45], the main cause might be the works by Eddington in 1930, showing that the static solution was in fact, unstable. Their biographical notes suggest that even Einstein was conscious about the current observations of the expansion by Hubble, the unsatisfactory explanation of them (mainly the measured redshift on galaxies and the age of the Universe inferred from it), were enough to consider them as secondary proof. After his change, Einstein jointly with de Sitter built the cosmological paradigm (the so called Einstein-de Sitter model) valid until mid of the 1990's, which consist in a flat universe ( $K = 0$ ) and zero cosmological constant ( $\Lambda = 0$ ). As pointed by Gamow in 1970 [46], Einstein regret the introduction of  $\Lambda$ : “*he remarked that the introduction of the cosmological constant term was the biggest blunder he ever made in his life*”. At the end it seems Einstein was not totally wrong.

### 1.2.2 Cosmic Inventory

The set of equations previously mentioned are not enough to describe the whole dynamical system of the expansion history. In order to solve this, is necessary to introduce a relation between the pressure  $p$  and the energy density  $\rho$ , which is usually taken as a equation of state (hereafter e.o.s.) in the form [17, 40]

$$p = w\rho, \quad (1.26)$$

being  $w$  a parameter, which could depend on time  $w = w(t)$ . The e.o.s., in addition with the Friedmann-Lemaître equations, and the conservation equation, determine entirely the cosmological model at background level. If we consider a constant e.o.s. the solution of eq. (1.23) becomes

$$\rho \propto a^{-3(1+w)}, \quad (1.27)$$

For relativistic species  $w = 1/3$ , leading to  $\rho \propto a^{-4}$  (radiation dominated epoch), and for non-relativistic species, when pressure is negligible ( $w = 0$ ),  $\rho \propto a^{-3}$  (matter dominated epoch). The condition on the scale factor to have acceleration is  $\ddot{a} > 0$ , thus from eq. (1.22), we find a condition over the e.o.s.  $w < -1/3$ . The particular case  $w = -1$  is obtained assuming a constant energy density in (1.23) which gives

$$p = -\rho, \quad (1.28)$$

This case is the so-called cosmological constant. We can associate an energy density, (the vacuum energy density) by the relation [47]

$$\rho_\Lambda = \frac{\Lambda}{\kappa}. \quad (1.29)$$

If we define the cosmological parameters as

$$\Omega_m \equiv \frac{\kappa\rho_m}{3H^2}, \quad \Omega_K = -\frac{K}{H^2a^2}, \quad \Omega_\Lambda \equiv \frac{\Lambda}{3H^2}. \quad (1.30)$$

it becomes

$$\Omega_m + \Omega_\Lambda + \Omega_K = 1, \quad (1.31)$$

known as the *cosmic sum rule*. We can also consider the values of the  $\Omega$ 's at the present time considering as well contributions from matter ( $\rho_m$ ) and radiation ( $\rho_r$ ) in the energy density  $\rho$ :

$$\Omega_m^{(0)} \equiv \frac{\kappa\rho_m^{(0)}}{3H_0^2}, \quad \Omega_r^{(0)} \equiv \frac{\kappa\rho_r^{(0)}}{3H_0^2}, \quad \Omega_K^{(0)} = -\frac{K}{(H_0a_0)^2}, \quad \Omega_\Lambda \equiv \frac{\Lambda}{3H_0^2}. \quad (1.32)$$

which gives the standard formula for the Hubble expansion

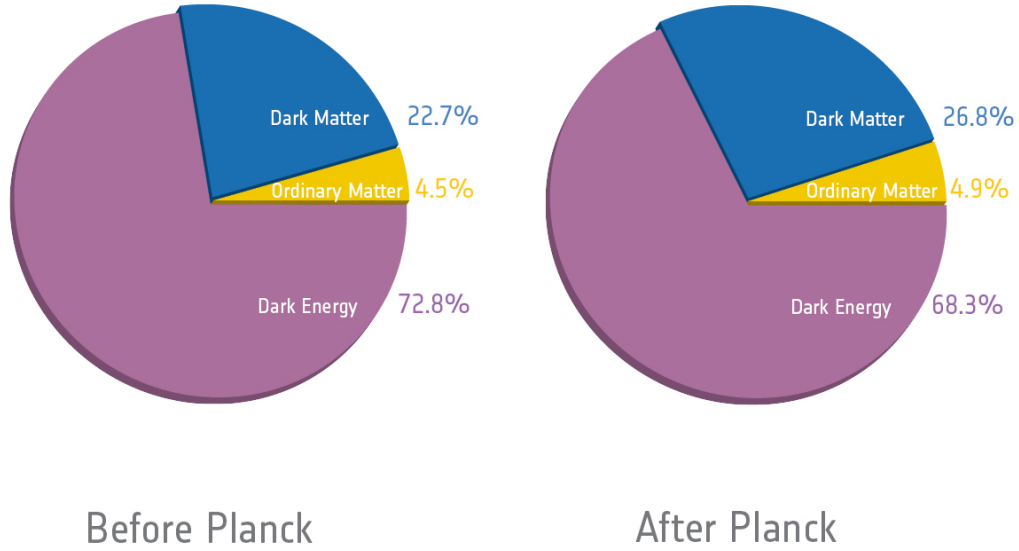


**Figure 1.2:** Planck cosmic recipe. Values for the matter-energy content of the Universe before and after Planck [2]. Figure taken from <http://sci.esa.int/planck/>.

$$H^2(a) = H_0^2(\Omega_m^{(0)}a^{-3} + \Omega_r^{(0)}a^{-4} + \Omega_K^{(0)}a^{-2} + \Omega_\Lambda). \quad (1.33)$$

being  $H_0$  the Hubble parameter today, which is usually written as

$$H_0 = 100 h \text{ km sec}^{-1} \text{ Mpc}^{-1} = 2.133h \times 10^{-42} \text{ Gev}, \quad (1.34)$$

where  $h$  denote the uncertainty in the measure of  $H_0$ .

We can infer from these numbers a observational bound on the cosmological constant term. Notice that from eq. (1.24), the cosmological constant should be at the same order of the square of  $H_0$

$$\Lambda \approx H_0^2 = (2.133 h \times 10^{-42} \text{ Gev})^2, \quad (1.35)$$

this could be interpreted this as an energy density:

$$\rho_{\Lambda}^{(\text{Obs})} \approx \frac{\Lambda m_{\text{pl}}^2}{8\pi} \approx 10^{-48} \text{GeV}^4, \quad (1.36)$$

where  $m_{\text{pl}} \approx 10^{19}$  GeV have been used. We will discuss in some detail the impact of these value on [Subsection 1.2.4](#).

Observations from Supernovae and Cosmic Microwave Background (CMB) put constraints on the cosmological parameters. For instance, recent data from the Planck satellite [2] show that our Universe is dominated by an unknown component called *Dark Energy* which is responsible of the actual cosmic acceleration, see fig. 1.2. The conclusion could not be more intriguing: we are now experiencing an era of cosmic acceleration with a fluid of negative equation of state! Even if many observations support the standard cosmological model + cosmological constant, namely the  $\Lambda$ CDM model, the introduction of this vacuum energy has implicit some theoretical issues that we will discuss in detail in [Subsection 1.2.4](#). This is why commonly we talk about dark energy as the *most mysterious problems in physics* so far, and of course, the reason why we look for alternative explanations for the cosmic speed-up.

### 1.2.3 Cosmological Distances and Redshift

In 1998 the first evidence of an accelerated universe came from measurements of Supernovae IA [48, 49] when two independent groups studying the supernovae brightness determined a non-zero cosmological constant contribution to the cosmic content <sup>5</sup>. The main ingredient of this observations were cosmological distances, and the reason is that they depend directly on cosmological parameters. To see that clearly, we will first define the redshift.

#### 1.2.3.1 Redshift

We introduce the concept of cosmological redshift considering a light pulse emitted at the point  $E$  that reaches the point  $O$ . We define  $1+z$ , being  $z$  the cosmological redshift, as the ratio between the wavelength measured by the observer  $O$ ,  $\lambda_O$  and the emitted wavelength on  $E$ ,  $\lambda_E$ . Since the wavelength is inversely proportional to the period we have

$$(1+z) = \frac{\lambda_O}{\lambda_E} = \frac{\Delta T_O}{\Delta T_E}. \quad (1.37)$$

---

<sup>5</sup>We will focus more on Supernovae observations in [Subsection 1.4.1](#)

Now, the periods  $\Delta T_0$  and  $\Delta T_E$  are related to the scale factor by

$$\frac{\Delta T_0}{a(t_0)} = \frac{\Delta T_E}{a(t_E)}, \quad (1.38)$$

thus

$$(1+z) = \frac{\lambda_0}{\lambda_E} = \frac{a(t_0)}{a(t_E)}, \quad (1.39)$$

being  $a(t_0)$  the *size of the Universe* at the time in which the light from an object is observed, and  $a(t_e)$  is the size at the time in which light was emitted. Fixing  $a(t_0) = 1$  (measured today) and with  $a(t)$  the redshift at some cosmic time  $t$  we arrive to the known expression:

$$a(t) = \frac{1}{1+z}. \quad (1.40)$$

### 1.2.3.2 Comoving distance $\chi(z)$

First, we want to choose a better choice of coordinates in the Robertson-Walker metric. Setting  $r = \sin \chi$  ( $K = +1$ ),  $r = \chi$  ( $K = 0$ ), and  $r = \sinh \chi$  ( $K = -1$ ), the line-element of  $\Sigma$  could be written as

$$d\tilde{s}^2 = d\chi^2 + (f_K(\chi))^2 [d\theta^2 + \sin^2 \theta d\varphi^2], \quad (1.41)$$

with

$$f_K(\chi) = \begin{cases} \sin \chi, & K = +1, \\ \chi, & K = 0, \\ \sinh \chi, & K = -1, \end{cases} \quad (1.42)$$

Since observations are based on radiation traveling through the space-time in null geodesics, in the case of an FLRW is possible to choose radial geodesics, in which we have  $ds^2 = 0 = -dt^2 + a^2(t)d\chi^2$ . Thus we have that radiation emitted at the point  $E$  and received at  $O$  satisfies

$$d_c \equiv \chi = \int_E^O d\chi = \int_{t_E}^{t_O} \frac{dt}{a(t)}, \quad (1.43)$$

using  $t_0 = 0$  and writing this expression in terms of redshift using eq. (1.40) we define the comoving distance as

$$d_c = \frac{1}{a_0 H_0} \int_0^z \frac{d\tilde{z}}{E(\tilde{z})}, \quad (1.44)$$

where

$$E(z) \equiv \frac{H(z)}{H_0}, \quad (1.45)$$

is the dimensionless Hubble parameter.

### 1.2.3.3 Angular diameter distance $d_A(z)$

The angular diameter distance  $d_A$  is defined as the ratio between the proper diameter of an object  $D$  to its apparent angular diameter (in radians)  $\delta$

$$d_A = \frac{D}{\delta}. \quad (1.46)$$

Again, from the metric assuming the source laying in a sphere of radius  $\chi$ , the proper diameter becomes

$$D = a(t_1)f_K(\chi_1)\delta, \quad (1.47)$$

and

$$d_A = a(t_1)f_K(\chi_1), \quad (1.48)$$

thus using the expression for the comoving distance eq. (1.44) we have

$$d_A(z) = \frac{1}{1+z} \begin{cases} \frac{1}{H_0\sqrt{|\Omega_k|}} \sinh[\sqrt{\Omega_k}H_0d_c(z)], & \Omega_k > 0, \\ d_c(z), & \Omega_k = 0, \\ \frac{1}{H_0\sqrt{|\Omega_k|}} \sin[\sqrt{-\Omega_k}H_0d_c(z)], & \Omega_k < 0, \end{cases} \quad (1.49)$$

This distance is useful for instance in CMB observations.

### 1.2.3.4 Luminosity distance $d_L(z)$

Finally, we will define the luminosity distance  $d_L$  as the relation between the flux of a source  $\mathcal{F}$  and its luminosity  $L$

$$d_L = \sqrt{\frac{L}{4\pi\mathcal{F}}}. \quad (1.50)$$

Instead of making a formal derivation, a small trick will be used here: The Etherington Theorem, a geometrical property of null geodesics in Riemannian space-times [50]. This theorem provides a simple relation between the angular diameter distance and the luminosity one:

$$d_L = (1+z)^2 d_A, \quad (1.51)$$

explicitly

$$d_L(z) = (1+z) \begin{cases} \frac{1}{H_0\sqrt{|\Omega_k|}} \sinh[\sqrt{\Omega_k}d_c(z)], & \Omega_k > 0, \\ d_c(z), & \Omega_k = 0, \\ \frac{1}{H_0\sqrt{|\Omega_k|}} \sin[\sqrt{-\Omega_k}H_0d_c(z)], & \Omega_k < 0, \end{cases} \quad (1.52)$$

Having these tools in hands, we are able to move to a different topic, related to the inconsistencies of the cosmological constant, and why modified gravity theories and other scenarios have been brought to our attention.

### 1.2.4 Cosmological Constant Act III: Vacuum Energy

We assert, from the mathematical point of view, that Einstein's gravitational description allows the introduction of the cosmological constant and also briefly discuss the physical purpose behind. But, there is any way to connect the introduction of  $\Lambda$  with "well-known" processes at the particle physics level? The answer is *yes* and the *vacuum* will start playing a key role. Here we want to briefly summarize the results from Carroll's review [47], which also encodes the main "120-number" issue between the quantum description and the current observation of  $\Lambda$ .

In order to understand the identification of  $\Lambda$  as vacuum energy, we will consider the consequences of the energy-momentum tensor associated with a single scalar field  $\phi$  with potential  $V(\phi)$  described by the action

$$S = \int_{\mathcal{V}} d^4x \sqrt{-g} \left[ \frac{1}{2} g^{\alpha\beta} \partial_\alpha \phi \partial_\beta \phi - V(\phi) \right]. \quad (1.53)$$

Thus, the associated energy-momentum tensor of this action, eq. (1.13), is

$$T_{\alpha\beta} = \frac{1}{2} \partial_\alpha \phi \partial_\beta \phi + \frac{1}{2} (g^{\gamma\delta} \partial_\gamma \phi \partial_\delta \phi) g_{\alpha\beta} - V(\phi) g_{\alpha\beta}, \quad (1.54)$$

The lowest energy state is such that the kinetic term vanishes, i.e.  $\partial_\alpha \phi$ , thus the energy-momentum tensor reduces to

$$T_{\alpha\beta} = -V(\phi_0) g_{\alpha\beta}, \quad (1.55)$$

being  $\phi_0$  the value of the scalar field which makes the potential  $V$  minimum. Now, we can just simply rename this potential as  $\rho_{\text{vac}}$ , so the energy-momentum tensor could be finally written as

$$T_{\alpha\beta} = -\rho_{\text{vac}} g_{\alpha\beta}. \quad (1.56)$$

A simple and elegant link arises when compared this vacuum energy description with the perfect fluid one, described by eq. (1.20). We can see that this energy-momentum corresponds to a perfect fluid if we set  $p_{\text{vac}} = -\rho_{\text{vac}}$ . As final step, we can just simply move the geometric term  $\Lambda g_{\alpha\beta}$  to the right side of EFE's, and then make the identification of the cosmological constant as vacuum energy.

There is another contribution coming from quantum mechanics, associated with the lowest energy level of vacuum fluctuations. As almost every elementary example, when learning quantum mechanics, is associated with harmonic oscillators. Let us then consider a system composed by oscillators of frequency  $\omega$  with a potential  $V(x) = \frac{1}{2}\omega x^2$ . In classical mechanics, the lowest energy corresponds to the case in which the oscillators are in rest, which is equivalent to have  $x = 0$ . However, due to the Heisenberg uncertainty principle, there exists a minimum energy, since we cannot have the particle with zero position and momentum at the same time, equals to<sup>6</sup>  $E = \frac{1}{2}\omega$ . In the field theory scheme, the lowest energy can be written as an infinite sum of harmonic oscillators, which however diverges. We can put an upper bound on this sum until a cutoff scale  $k_{\text{max}}$ , and thus the vacuum energy density could be written as

$$\rho_{\text{vac}} = \int_0^{k_{\text{max}}} \frac{4\pi k^2 dk}{(2\pi)^3} \frac{1}{2} \sqrt{k^2 + m^2} \propto k_{\text{max}}^4. \quad (1.57)$$

In order to have some guess about this number, we can assume that GR should be valid until the Planck scale, thus, we can use the Planck mass  $m_{\text{pl}} \simeq 10^{18}$  GeV in this cutoff to obtain:

$$\rho_{\text{vac}} \simeq 10^{72} \text{ GeV}^4. \quad (1.58)$$

Hence, if we make the ratio between this vacuum energy, and the observed value coming from cosmological data, eq. (1.36), we find

$$\frac{\rho_{\text{vac}}}{\rho_{\Lambda}^{(\text{Obs})}} \approx \frac{10^{72} \text{ GeV}^4}{10^{-48} \text{ GeV}^4} \sim 10^{120}. \quad (1.59)$$

This problem, well know as the fine-tuning problem, has been described as “*the worst theoretical prediction in the history of physics*” [51]. Other contributions coming from the scale of broken symmetry in the electroweak model, and in the QCD scale, does not improve the situation [52, 53]. This problem was present before the confirmation in 1998 of the accelerated expansion of the Universe, and so far, no satisfactory explanation exists. Nevertheless, we pray to the *santo*  $\Lambda$ CDM model as the most accurate description of our Universe.

We will finish this  $\Lambda$  play in the arena with another issue, known as the coincidence problem. The main idea behind is *why?* today's present values of the energy density for

<sup>6</sup>Recall that in our units convention  $\hbar = 1$ .

matter and dark energy are of the same order:

$$\rho_{\text{m}}^{(0)} \sim \rho_{\Lambda}^{(0)}, \quad (1.60)$$

indicating that we are living a very special period in the cosmic history, requiring also very special initial conditions in the early Universe. The redshift at which this coincidence occurs can be computed from the redshift dependence of the matter density (which scale as  $z^3$ ) and matching this with the constant energy density of dark energy (cosmological constant), which gives  $z_{\text{coinc}} \approx 0.55$  [54]. This issue has motivated explanations which relies for instance on interacting dark energy, or coupled quintessence [55], or also scenarios of quintessence with non-standard behavior, see [56]. Another very interesting approach consists in *anthropic considerations*, which basically means that some of the values of the parameters used to describe the universe cannot be determined by fundamental ideas, but quoting explicitly Carroll’s paper “*the truism that intelligent observers will only ever experience conditions which allow for the existence of intelligent observers*”. In simple words, this could be rephrased saying that the physical theories need to take into account the existence of life on Earth. This enlightened discussion is however far from our purposes (lamentably). Further details should be found in [57–59].

The lesson at the end of this cosmological constant performance is that even if  $\Lambda$  “should” be zero, when compared with its quantum field theory „*Doppelgänger*“, amazingly it fits all current cosmological observations. Due to this lack of consistency, alternative approaches as modified gravity are playing nowadays on the stage as potential candidates to explain the current acceleration of the Universe.

### 1.3 Cosmological Perturbation Theory

In the previous sections we described cosmology based on the Robertson-Walker metric, plus additional assumptions regarding the e.o.s. However, that description is far from the *real* universe, which is not exactly homogeneous, neither isotropic. Cosmological perturbation theory offers a powerful tool to investigate the effects of deviations from the FLRW background. There exists a vast literature about cosmological perturbation theory [60–67]. Here we try to make a minimalist description of it. In linear cosmological perturbation theory the main assumption is that we can describe the perturbed real universe  $(\mathcal{M}, \mathbf{g})$  by a metric tensor  $\mathbf{g}$  which is a small deviation from the background  $(\mathcal{M}^{(0)}, \mathbf{g}^{(0)})$ , being  $\mathbf{g}^{(0)}$  the metric given by eq. (1.18). This sentence has a deep physical meaning and the mathematical effort to formulate the problem properly has a long history in cosmology. In one of the most influential works on the topic, Bardeen found the method to formulate the problem of linear perturbation in a new language known as *gauge invariant variables* [60].

In general, the metric on this perturbed manifold could be written as [61, 62]

$$ds^2 = a^2(\tau) \left[ -(1 + 2\psi)d\tau^2 + 2\omega_i d\tau dx^i + ((1 + 2\phi)\gamma_{ij} + 2h_{ij}) dx^i dx^j \right], \quad (1.61)$$

with  $\psi(\mathbf{x}, \tau)$  and  $\phi(\mathbf{x}, \tau)$  scalar perturbations<sup>7</sup>,  $\gamma_{ij}$   $\omega_i(\mathbf{x}, \tau)$  a 3-vector and  $h_{ij}(\mathbf{x}, \tau)$  a symmetric, traceless second-rank 3-tensor. In this general case, there are 10 degrees of freedom  $\{1 + 1 + 3 + 5\}$ , corresponding to  $\{\psi, \phi, \omega_i, h_{ij}\}$ . However, the decomposition theorem [63] shows that at linear level, vector and tensor perturbations are decoupled. In addition, vector perturbations decay in an expanding universe, while tensor perturbations are relevant only for the description of gravitational waves. Just scalar perturbations are enough to describe formation of large-scale structure in the universe, thus we focus on them. In what follows we will use mainly [16, Ch. 4], [17, Ch. 5] and [68, Ch. 8].

We can simplify the perturbed metric with a suitable choice of gauge invariant quantities [69–71]. For instance, if we choose them to be  $\omega_i = 0$ ,  $\psi = \Psi$ ,  $\phi = \Phi$  we can write eq. (1.61) in the so-called *Newtonian* or *longitudinal* or *shear-free* gauge

$$ds^2 = a^2(\tau) \left[ -(1 + 2\Psi)d\tau^2 + (1 + 2\Phi) \delta_{ij} dx^i dx^j \right]. \quad (1.62)$$

In the other hand, the most general form for the energy-momentum tensor could be written as [72]

$$T_{\alpha\beta} = (\rho + p)u_\alpha u_\beta + pg_{\alpha\beta} + [2q_{(\alpha}u_{\beta)} + \pi_{\alpha\beta}], \quad (1.63)$$

$q_\alpha$  representing heat fluxes and  $\pi_{\alpha\beta}$  is the anisotropic pressure tensor. We consider the case of perfect fluids ( $q_\alpha = 0, \pi_{\alpha\beta} = 0$ ), and assume that the perturbed fluid *remains* a perfect fluid. Let us define the perturbed quantities

$$\delta \equiv \frac{\delta\rho}{\rho}, \quad \theta \equiv \nabla_i v^i, \quad (1.64)$$

where

$$\frac{\delta\rho}{\rho} \equiv \frac{\rho(x) - \langle\rho\rangle}{\langle\rho\rangle}, \quad (1.65)$$

is the *density contrast*, with  $\langle\rho\rangle$  denoting the spatial average, and  $\theta$  is the velocity divergence. The perturbation of the four-velocity reads

$$u^\alpha = \frac{1}{a} \left[ (1 - \Psi), v^i \right], \quad (1.66)$$

$$u_\alpha = a \left[ -(1 + \Psi), v_i \right], \quad (1.67)$$

<sup>7</sup>Beware of signs: some authors use other signature for the metric and/or opposite signs for the scalars, we use the notation of [17].

Thus, the perturbed components of the energy-momentum tensor are [17, 68]

$$\delta T_0^0 = -\delta\rho, \quad (1.68a)$$

$$\delta T_i^0 = -\delta T_0^i = (1+w)\rho v^i, \quad (1.68b)$$

$$\delta T_i^j = c_s^2 \delta\rho, \quad (1.68c)$$

where we have defined the sound speed

$$c_s^2 \equiv \frac{\delta p}{\delta\rho} = \frac{\dot{p}}{\dot{\rho}}, \quad (1.69)$$

being  $w$  is the e.o.s. In order to derive first-order equations, we decompose the Einstein tensor and the energy-momentum tensor into background and perturbed parts:  $G_\alpha^\beta = G_\alpha^{\beta(0)} + \delta G_\alpha^\beta$  and  $T_\alpha^\beta = T_\alpha^{\beta(0)} + \delta T_\alpha^\beta$ . The first order Einstein equations are given by

$$\delta G_\alpha^\beta = 8\pi G \delta T_\alpha^\beta. \quad (1.70)$$

When using the expressions for the perturbed energy-momentum tensor eq. (1.68), the perturbed Einstein equations becomes [16, p. 48]

$$3\mathcal{H}(\mathcal{H}\Psi - \Phi') + \nabla^2\Phi = -4\pi G a^2 \delta\rho, \quad (1.71a)$$

$$\nabla^2(\Phi' - \mathcal{H}\Psi) = 4\pi G a^2 (1+w)\rho\theta, \quad (1.71b)$$

$$\Psi = -\Phi, \quad (1.71c)$$

$$\Phi'' + 2\mathcal{H}\Phi' - \mathcal{H}\Psi' - (\mathcal{H}^2 + \mathcal{H}')\Psi = -4\pi G a^2 c_s^2 \delta\rho, \quad (1.71d)$$

begin  $\mathcal{H} = aH$  the comoving Hubble parameter, and prime denotes derivatives w.r.t. the conformal time  $\tau$ . Another important relation comes from the continuity equation of the perturbed energy-momentum tensor  $\delta T_{\alpha;\beta}^\beta$ . In the case  $\alpha = 0$  we have

$$\delta' + 3\mathcal{H}(c_s^2 - w)\delta = -(1+w)(\theta + 3\Phi'), \quad (1.72)$$

where the continuity equation eq. (1.23) for the background has been used. In the case of non-relativistic matter ( $c_s^2 = 0$ ,  $w = 0$ ) this expression reduces to

$$\delta' = -\theta - 3\Phi'. \quad (1.73)$$

This equation describes how the density at position  $x$  increases if there is a velocity divergence at the same point; the term  $\Phi'$  is negligible at small scales. The equation for

$\alpha = i$  could be written as

$$\theta' + \left[ \mathcal{H}(1 - 3w) + \frac{w'}{1 + w} \right] \theta = -\nabla^2 \left( \frac{c_s^2}{1 + w} \delta + \Psi \right), \quad (1.74)$$

and for non-relativistic matter reduces to

$$\theta' + \mathcal{H}\theta = -\nabla^2 \Psi - \nabla^2 (c_s^2 \delta), \quad (1.75)$$

which is nothing but the *Euler equation* in the Newtonian context.

A useful way to study the above equations is going to the *Fourier space*, that means all the perturbation quantities  $\{\delta, \theta, \Psi, \Phi, \dots\}$ , that we summarize here as  $\mathcal{A}$ , are the sum of plane waves  $\delta_k e^{i\mathbf{k}\cdot\mathbf{r}}$ ,  $k$  being the wavenumber:

$$\mathcal{A} = \int e^{i\mathbf{k}\cdot\mathbf{r}} \mathcal{A}_k d^3k, \quad (1.76)$$

It is convenient to introduce all the perturbations as Fourier modes, e.g.,  $\delta(\mathbf{r}, t) = \delta_k(t) e^{i\mathbf{k}\cdot\mathbf{r}}$ . With this in mind, the perturbation variables and its derivatives can be substituted as

$$\mathcal{A}(x, \tau) \rightarrow e^{i\mathbf{k}\cdot\mathbf{r}} \mathcal{A}(\tau), \quad (1.77a)$$

$$\nabla \mathcal{A}(x, \tau) \rightarrow e^{i\mathbf{k}\cdot\mathbf{r}} \mathbf{k} \mathcal{A}(\tau), \quad (1.77b)$$

$$\nabla^2 \mathcal{A}(x, \tau) \equiv \nabla_i \nabla^i \mathcal{A}(x, \tau) \rightarrow -e^{i\mathbf{k}\cdot\mathbf{r}} k^2 \mathcal{A}(\tau), \quad (1.77c)$$

Futhermore, the modes  $e^{i\mathbf{k}\cdot\mathbf{r}}$  can be simply dropped out, since the equations are linear, and decoupled between different modes. The perturbation equations (1.71), (1.72) and (1.74) becomes

$$k^2 \Phi + 3\mathcal{H} (\Phi' - \mathcal{H}\Psi) = 4\pi G a^2 \rho \delta, \quad (1.78)$$

$$k^2 (\Phi' - \mathcal{H}\Psi) = -4\pi G a^2 (1 + w) \rho \theta, \quad (1.79)$$

$$\Psi = -\Phi, \quad (1.80)$$

$$\Phi'' + 2\mathcal{H}\Phi' - \mathcal{H}\Psi' - (\mathcal{H}^2 + 2\mathcal{H}') \Psi = -4\pi G a^2 c_s^2 \rho \delta, \quad (1.81)$$

$$\delta' + 3\mathcal{H}(c_s^2 - w)\delta = -(1 + w)(\theta + 3\Phi'), \quad (1.82)$$

$$\theta' + \left[ \mathcal{H}(1 - 3w) + \frac{w'}{1 + w} \right] \theta = k^2 \left( \frac{c_s^2}{1 + w} \delta + \Psi \right). \quad (1.83)$$

Combining eq. (1.78) and eq. (1.79) we get the relativistic Poisson equation

$$k^2\Phi = 4\pi Ga^2\rho[\delta + 3\mathcal{H}(1+w)\theta/k^2] = 4\pi Ga^2\rho\Delta, \quad (1.84)$$

where we define the gauge-invariant density perturbation

$$\Delta \equiv \delta + 3\frac{\mathcal{H}(1+w)\theta}{k^2}. \quad (1.85)$$

### 1.3.1 Statistical *Intermezzo*: Correlation Function and Power Spectrum

So far we set the basic formalism of perturbations which is the most useful tool to describe the large scale structure of the Universe. A little of statistics is necessary now to quantify the observables we measure with cosmological observations, following [16, Ch. 3] and [73]. A basic assumption, given at the beginning of this discussion about the pillars of modern cosmology, is the cosmological principle, based on statistical properties of structures at larges scales. We will now consider an estimator which allow us to measure the *inhomogeneities* in the distribution of matter. Let us define the *two-point correlation function*  $\zeta$  as the “average of the relative excess number of pairs found at a given distance  $r$ ”. That means, if  $n_i$  with  $i$  1 or 2, denotes the number of objects in certain volume  $dV_i$  at position  $r_i$ , with an average given by  $\langle n_i \rangle = n_0 dV_i$ , we can write the average number of pairs found in  $dV_1$  and  $dV_2$  as

$$\langle n_1 n_2 \rangle = n_0^2 dV_1 dV_2 [1 + \zeta(\mathbf{r}_1, \mathbf{r}_1)], \quad (1.86)$$

being  $n_0 = N/V$  the mean number density. Furthermore, If we consider that matter is strictly random distributed, then any two volume elements would be uncorrelated, and  $\zeta$  would vanish. In addition, if  $\zeta$  is positive (negative), then we say those two volume elements are correlated (anti-correlated). Assuming a statistically homogeneous Universe,  $\zeta$  can only depend on the difference vector  $\mathbf{r}_{12} = \mathbf{r}_2 - \mathbf{r}_1$ , and due to statistical isotropy,  $\zeta$  only depend on the modulus distance  $r$  between  $\mathbf{r}_1$  and  $\mathbf{r}_2$ . Henceforth, we denote the two-point correlation function as  $\zeta(r)$ , inverting eq. (1.86):

$$\zeta(|\mathbf{r}_2 - \mathbf{r}_1|) = \frac{\langle n_1 n_2 \rangle}{n_0^2 dV_1 dV_2} - 1 \equiv \langle \delta(\mathbf{r}_2) \delta(\mathbf{r}_2) \rangle. \quad (1.87)$$

Thus, the correlation function is also written as the average over all possible positions

$$\zeta(\mathbf{r}) = \frac{1}{V} \int_V \delta_m(\mathbf{x}) \delta_m(\mathbf{x} + \mathbf{r}) d^3x. \quad (1.88)$$

In the previous section we described variables that encode perturbations, for instance, the density contrast  $\delta$  or the gravitation potential  $\Phi$ . Now, since by definition the average of some of these perturbations is identically zero, we need to construct estimators based on

quadratic terms. The *power spectrum* could be defined as:

$$P_\delta = A|\delta_k|^2, \quad (1.89)$$

being  $\delta_k$  the Fourier coefficients of  $\delta$ , and  $A$  some constant. If instead two different variables enters into the quadratic form as for example  $\delta_k\Phi_k$  we called this the *cross-correlation* power spectrum. We are interested now in one importante relation, known as the Wiener-Khinchin theorem, which relates the two-point correlation function with the power spectrum via a Fourier transform. Let us now formally define the matter power spectrum as

$$P(\mathbf{k}) \equiv V\delta_{\mathbf{k}}\delta_{\mathbf{k}}^* = \frac{1}{V} \int \delta(\mathbf{x})\delta(\mathbf{y})e^{-i\mathbf{k}\cdot(\mathbf{x}-\mathbf{y})}d^3x d^3y, \quad (1.90)$$

if we use now  $\mathbf{r} = \mathbf{x} - \mathbf{y}$ , and using the definition of the two-point correlation function eq. (1.88) we can write

$$P(\mathbf{k}) = \frac{1}{V} \int_V \delta(\mathbf{x})\delta(\mathbf{x} - \mathbf{r})e^{-i\mathbf{k}\cdot\mathbf{r}}d^3x d^3r = \int \zeta(\mathbf{r})e^{-i\mathbf{k}\cdot\mathbf{r}}d^3r, \quad (1.91)$$

Thus we summarize with an important conclusion, which is amongst the whole theoretical construction, the main result one should have clear when learning cosmology:

*“The power spectrum is the Fourier transform of the two-point correlation function”*

Another definition which is also standard in cosmology comes when consider *ensamble averages* instead of volume average. For instance for the ensemble  $V\delta_{\mathbf{k}}\delta_{\mathbf{k}'}^*$ , we can write

$$V\langle\delta_{\mathbf{k}}\delta_{\mathbf{k}'}^*\rangle = \frac{1}{V} \int \langle\delta(\mathbf{x})\delta(\mathbf{y})\rangle e^{-i\mathbf{k}\cdot\mathbf{x}+i\mathbf{k}'\cdot\mathbf{y}}d^3x d^3y, \quad (1.92)$$

$$= \frac{1}{V} \int \langle\delta(\mathbf{x})\delta(\mathbf{y} + \mathbf{r})\rangle e^{-i(\mathbf{k}-\mathbf{k}')\cdot\mathbf{y}-i\mathbf{k}\cdot\mathbf{r}}d^3r d^3y, \quad (1.93)$$

If we fix the position and then take the average of the ensambles, it can be enter in the integration acting only over  $\delta$ . Hence, we have

$$V\langle\delta_{\mathbf{k}}\delta_{\mathbf{k}'}^*\rangle = \frac{1}{V} \int \zeta(\mathbf{r})e^{-i(\mathbf{k}-\mathbf{k}')\cdot\mathbf{y}-i\mathbf{k}\cdot\mathbf{r}}d^3r d^3y, \quad (1.94)$$

$$= \frac{1}{V} \int e^{-i(\mathbf{k}-\mathbf{k}')\cdot\mathbf{y}}d^3y \int \zeta(\mathbf{r})e^{-i\mathbf{k}\cdot\mathbf{r}}d^3r, \quad (1.95)$$

$$= \frac{(2\pi)^3}{V} P(\mathbf{k})\delta_D(\mathbf{k} - \mathbf{k}'), \quad (1.96)$$

where the definition of the Dirac delta  $\delta_D$  had been used, and also we include the Fourier volume term  $(2\pi)^3$ . Another piece of statistic is necessary for our further purposes related with estimation of parameters and its errors, namely the *Fisher matrix* formalism. This

discussion however is left for [Appendix A](#).

### 1.3.2 The Initial Matter Power Spectrum

Having this tools in hands, is time now to ask in which way we can measure the properties or large scale structure today (i.e. the matter power spectrum). The answer for this seems to be *simple*, and the gravitational potential  $\Phi(k, t)$  plays an important role: the power spectrum today can be constructed from the initial power spectrum generated at the *inflationary epoch*, evolved with suitable functions of scale  $k$  and time  $a$ . In a very minimalistic description, inflation is a process occurring at very early times in the universe, in which quantum fluctuations evolved with time to generate the large scale structures we see now. These fluctuations then generate overdense regions, and due to gravitational instabilities<sup>8</sup>, matter collapses and generate structures. Inflation itself has a long and interesting history, developed by Guth early 1980's [74], inflation born as a candidate to solve classical problems of cosmology, such as the flatness and horizon problem. A complete review however is far from our purposes, and we just need here a basic ingredient: the power spectrum generated at that epoch. We can associate the anisotropies generated as fluctuations of a scalar field commonly denoted as the *inflaton*. The power spectrum generated by this field could be written as [17]

$$P_{\Phi}(k) = \frac{50\pi^2}{9k^3} \left( \frac{k}{H_0} \right)^{n_s-1} \delta_H^2, \quad (1.97)$$

being  $n_s$  the spectral index and  $\delta_H^2$  ( $\sim 4.6 \times 10^{-5}$  for the  $\Lambda$ CDM model) represents the amplitude of the gravitational potential; from current Planck constraints, the value of the spectral index is  $n_s = 0.9603 \pm 0.0073$  [75]. As anticipated, the gravitational potential today can be written in terms of the primordial one. Neglecting anisotropic stresses, it reads

$$\Phi(k, a_0) = \frac{9}{10} \Phi(k, a_i) T(k) G(a_0), \quad (1.98)$$

with  $T(k)$  is the *transfer function*, which relates the primordial potential to its value after horizon-crossing and matter-radiation equality

$$T(k) \equiv \frac{\Phi(k, a_{\text{Late}})}{\Phi_{\text{LS}}(k, a_{\text{Late}})}, \quad (1.99)$$

---

<sup>8</sup>Classically, we can understand a gravitational instability as the *war* between gravity and pressure. Matter is attracted to the center of an overdense region, but repelled by pressure. When the region is overdense enough, gravity wins. This process is similar as the gravitational instabilities inside stars, when the pressure generated by nuclear fusion and photons trying to scape, is not enough to stop gravity and the star finally collapse.

( $a_{\text{Late}}$  is the transfer epoch from the radiation era), and  $G(a)$  the *growth function* describing the evolution of potentials at late times [16]:

$$\frac{\Phi(a)}{\Phi(a_{\text{Late}})} \equiv \frac{G(a)}{a}. \quad (1.100)$$

Although the formal derivation of the transfer function implies the solution of the perturbation equations into the matter era, some approximate forms had been obtained so far. For instance, a popular fit given by Bardeen, Bond, Kaiser and Szalay (BBKS) [76] reads

$$T_{BBKS} = \frac{\ln(1 + 0.171x)}{0.171x} \left[ 1 + 0.284x + (1.18x)^2 + (0.399x)^3 + (0.490x)^4 \right]^{-1/4}, \quad (1.101)$$

with  $x \equiv k/k_{\text{eq}}$ , and we define the scale of radiation-matter equality as

$$k_{\text{eq}} = H_0 \sqrt{\frac{2\Omega_m^{(0)}}{a_{\text{eq}}}}. \quad (1.102)$$

Our final ingredient is to relate the matter overdensity with the potential at late times via the Poisson equation, eq. (1.84), in the sub-horizon approximation ( $k \gg \mathcal{H}$ ):

$$k^2 \Phi = 4\pi G a^2 \rho \delta, \quad (1.103)$$

and then

$$\delta_m(k, a) = \frac{2k^2 a}{3\Omega_m^{(0)} H_0^2} \Phi(k, a), \quad (1.104)$$

when we make explicit the contribution of matter with the subscript m. Thus, using eq. (1.97) and eq. (1.98), the power spectrum of matter perturbations at the present epoch reads [16, p. 75]

$$P_{\delta_m}(k, a) \equiv \langle |\delta_m(k, a_0)|^2 \rangle = \frac{2\pi^2 \delta_H^2}{(\Omega_m^{(0)})^2} \left( \frac{k}{H_0} \right)^{n_s} T^2(k) G^2(a_0) H_0^{-3}, \quad (1.105)$$

In fig. 1.3 we show the initial matter power spectrum calculated numerically (using the numerical integrator CAMB [77]), and the approximation given by  $T_{BBKS}$  transfer function. The linear regime, in which this solution is valid is given by scales of the order  $k \sim 0.05h \text{ Mpc}^{-1}$ , and intermediate range, which could be still solved using for instance the Zel'dovich approximation [78] lies in the range,  $0.05h \text{ Mpc}^{-1} \gtrsim k \gtrsim 0.15h \text{ Mpc}^{-1}$ . Finally, small scales characterized by  $k \lesssim 0.15h \text{ Mpc}^{-1}$ , enters into the non-linear regime, and thus numerical techniques such as  $N$ -body simulations should be taken into account.

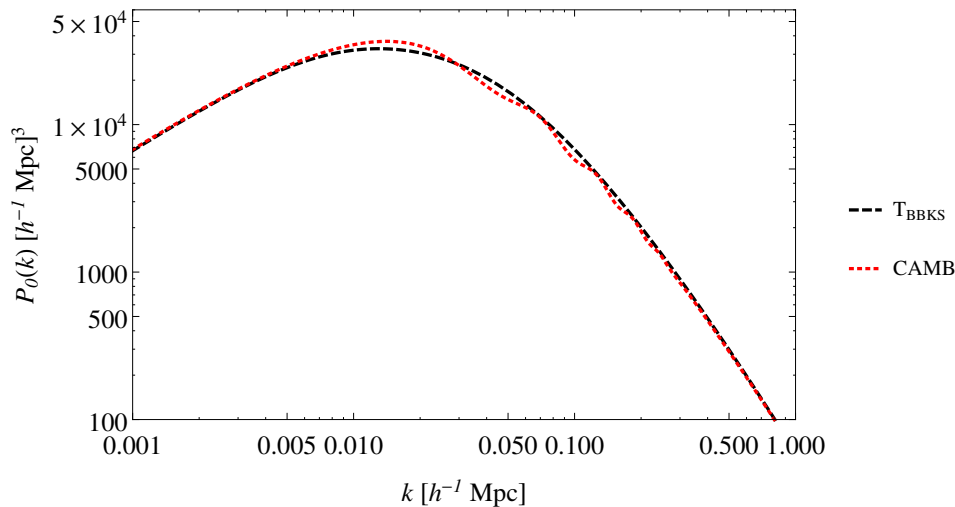


**Figure 1.3:** The galaxy power spectrum calculated with **CAMB** (red dotted line) and using the analytical approximation for the transfer function  $T_{BBKS}$  (black dashed line).

## 1.4 Observing Dark Energy

There are many probes supporting the existence of dark energy than can be classified mainly in two groups. The first group corresponds to geometrical probes, such as Supernovae observations, measurements of the Hubble expansion, and the Baryon Acoustic Oscillation (BAO) scale. In the second one, dynamical tests are considered, for instance information from the CMB spectrum and large-scale structure (LSS) observations. The age of the universe, when compared with the age of stars, provide also information. For our future forecasts we need information from LSS (which includes weak lensing) and SN, here we want to emphasize in Supernovae and LSS only; observations related with CMB, even powerful and so far give the best constraints on cosmological parameters, are far beyond our purposes, and then, will not be considered here.

### 1.4.1 Supernovae

We anticipate in [Subsection 1.2.1](#) that the model that had been conquering cosmology (besides the issues related to dark matter in rotation curves of galaxies) was the Einstein-de Sitter, consisting of the set of parameters  $(\Omega_m, \Omega_\Lambda) = (1, 0)$  and zero curvature  $K = 0$ . This picture significantly changed in the 90's when two independent groups studying the light curves of some particular objects (known as supernovae type IA or simply SNIa), brought the cosmological constant back. We will here briefly discuss this important astrophysical observation which changed totally our understanding of the Universe, and put

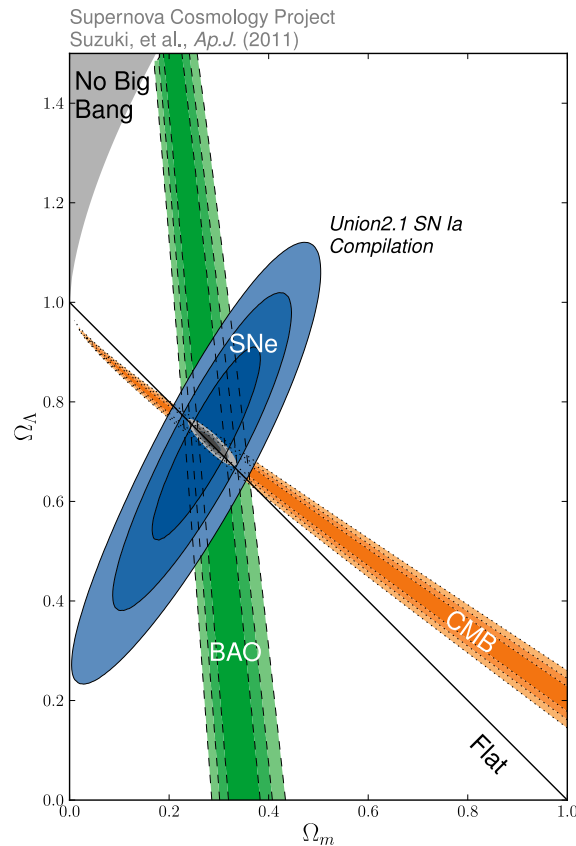
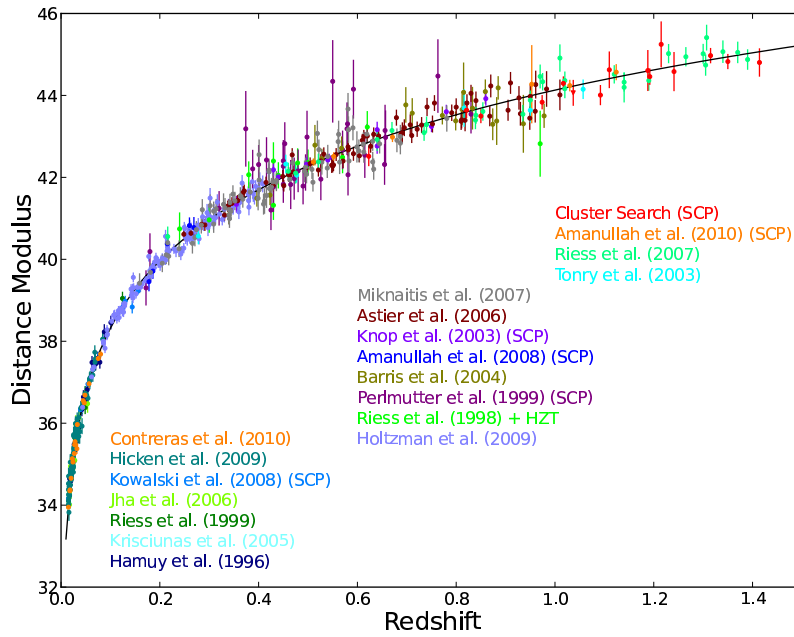


**Figure 1.4:** Top: Modulus distance for the Union 2.1 compilation [3]. The black line represents the best-fit for a flat  $\Lambda$ CDM cosmology. Bottom: Confidence regions in the  $(\Omega_m, \Omega_\Lambda)$  plane. Considering only SN observations, the constraints suggest a model with non-negligible vacuum energy (or cosmological constant) with  $\Omega_\Lambda \sim 0.7$  and  $\Omega_m \sim 0.3$ . Figures obtained from the Supernova Cosmology Project webpage <http://supernova.lbl.gov/Union/>.

the laws of physics walking in a tightrope.

Supernovae are basically explosions, occurring when, for instance, a white dwarf starts stealing mass from a companion star, and exceeds the Chandrasekhar limit. When this limit is crossed, the hydrostatic equilibrium between pressure and gravity does not hold anymore and, as a consequence, the white-dwarf collapse and eventually dies. These events are extremely luminous, almost comparable with the luminosity of the host galaxy. Supernovae then are classified in terms of the lines we observed in the light-curve of the explosion. An interesting phenomenon occur in this event, which is that they have an almost constant absolute luminosity at the peak of brightness (around  $M \sim -19.5$ ) [79]. But, how we can relate this astrophysical objects with cosmological observations? As similar as the beautiful link between geometry and matter dictated by EFE's, an interesting equation, known as the *Pogson equation*, relates the magnitude of an object with its flux by:

$$m_1 - m_2 = -\frac{5}{2} \log_{10} \left( \frac{\mathcal{F}_1}{\mathcal{F}_2} \right), \quad (1.106)$$

in which  $m_1$  and  $m_2$  are luminosities of two objects with fluxes  $\mathcal{F}_1$  and  $\mathcal{F}_2$  respectively. Now, since the flux is related to the luminosity distance by eq. (1.50), we can write this equation in a different way with the help of the absolute magnitude  $M$ , which is simply the apparent magnitude of an object observed at a distance of 10 pc, which finally reads

$$m - M = 5 \log_{10} d_L + 25, \quad (1.107)$$

with  $d_L$  measured in pc.

We have then a simple link between cosmology (since  $d_L$  depends on background cosmological quantities) and astrophysical observations. This was the basis of the method used by Riess *et al.* [High-redshift Supoernovae Search Team (HSST) [49] and Perlmutter *et al.* [Supernova Cosmology Project (SCP)] [48], who measuring the luminosities of supernovae, and taking into account the cosmology behind  $d_L$ , independently confirmed the late-time accelerated expansion of the Universe. High amount of data however is crucial to conclude that the Universe is accelerating, since observations are subject to statistical and systematic errors. In fig. 1.4 we shown the distance modulus as a function of  $z$  for a recent collection of supernovae compilations, known as Union 2.1 [3].

From these observations is also possible to put bounds on the cosmological parameters. In fig. 1.4 we also display the confidence region in the  $(\Omega_m, \Omega_\Lambda)$  plane, which is in favor of a model with  $(\Omega_m, \Omega_\Lambda) \sim (0.3, 0.7)$  using the Union 2.1 compilation, which simply rules out the Einstein-de Sitter prediction  $(\Omega_m, \Omega_\Lambda) \sim (1, 0)$ . Similar constraints were found also in 1998 by the HSST and SCP groups, consistent also with this conclusion. This is then the beginning of the *dark energy era*.

## 1.4.2 Large-scale Structure

We will now consider one of the most important probes for the existence of dark energy, and also a basic pillar for our further analysis. As we mentioned in [Subsection 1.3.2](#), the matter power spectrum could give all the information about statistical properties of structures at large scales. Unfortunately, when using real galaxy surveys, we truly measure the *galaxy* density contrast  $\delta_{\text{gal}}$ , which, of course, is different from the matter density contrast  $\delta_{\text{m}}$ . A possible way to overcome this is to consider that both densities are related by a bias factor  $b$ , which in general could depend on time and scale  $b = b(k, z)$ :

$$\delta_{\text{gal}} = b(k, z)\delta_{\text{m}}. \quad (1.108)$$

Thus, since the power spectrum is defined as the square of the expectation value of the density field, we can write the galaxy power spectrum as:

$$P_{\text{gal}} = b^2(k, z)P_{\text{m}}. \quad (1.109)$$

In addition to this, there is an effect coming from the fact that when measuring redshifts, these include a systematic error due by peculiar velocities of galaxies [16]. This effect is called Redshift Space Distortion (RSD), and was first derived by Kaiser in 1987 [80]. In the most simplest form, we can relate the redshift-space galaxy power spectrum, denoted as  $\delta_s(k, z, \mu)$ , with the galaxy power spectrum (in real space) by

$$\delta_s(k, z, \mu) = \delta_r(k, z)(1 + \beta\mu^2), \quad (1.110)$$

being  $\mu = (\mathbf{k} \cdot \mathbf{r})/kr$  the cosine of the angle between the wavevector  $\mathbf{k}$  and the line of sight  $\mathbf{r}$ ,  $\beta$  is the linear RSD parameter:

$$\beta = \frac{f}{b}, \quad (1.111)$$

being  $f$  the *growth rate*:

$$f = \frac{d \ln \delta_{\text{m}}}{d \ln a} = \Omega_{\text{m}}^{\gamma}. \quad (1.112)$$

In the last part of eq. (1.112) an approximation has been used [81], being  $\gamma$  the *growth index* which in the case of the  $\Lambda$ CDM model is roughly 6/11. Modified gravity models predict different values for  $\gamma$ , making RSD a powerful tool to study dark energy cosmologies. We will rewrite now the galaxy power spectrum (corrected with the RSD term), still using the subscript  $_{\text{gal}}$ , as

$$\delta_{\text{gal}}(k, z, \mu) = Gb\sigma_8 \left(1 + \frac{f}{b}\mu^2\right) \delta_{\text{t},0}(k), \quad (1.113)$$

where  $\delta_{t,0} = \delta_{m,0}/\sigma_8$  being  $\sigma_8$  the root-mean-square of density fluctuations (or the normalization of the power spectrum) inside a sphere of radius  $8 h^{-1}$  Mpc [16]:

$$\sigma_8^2 = \frac{1}{2\pi^2} \int P_{m0} W_{R_8}^2(k) dk, \quad (1.114)$$

with  $W_R$  a spherical window function,  $W_R(k) = 3j_1(kR)/(kR)$ , being  $j_\ell(x)$  the spherical Bessel function of the first kind. Also we have for the growth function

$$G(z) = \frac{\delta_m(z)}{\delta_m(0)}. \quad (1.115)$$

Let us finally define the standard form of the galaxy power spectrum in redshift-space that we will use for further calculations [16, 82]:

$$P_{r,\text{obs}}(k_r, \mu_r; z) = \frac{H(z)d_r^2(z)}{H_r(z)d^2(z)} G^2(z) b^2(z) (1 + \beta(z)\mu^2)^2 P_0(k), \quad (1.116)$$

with  $P_0(k) \equiv \delta_{t,0}^2 \sigma_8^2$ . This power spectrum includes also a geometrical correction known as the *Alcock-Paczynski effect* [83]

$$F_{\text{AP}} = \frac{H(z)d_A(z)|_r}{H(z)d_A(z)}, \quad (1.117)$$

which essentially measures the deviation on isotropy in the power spectrum of a cosmological model, w.r.t a reference fiducial (denoted with the subscript  $r$ ).

As a final remark, some recent works showed that a formal treatment of galaxy surveys should take into account corrections due to the finite size of the volume, which add additional terms into the total density fluctuation [84–91]. In a galaxy survey, we count the number of galaxies in the direction  $\mathbf{n}$  at redshift  $z$ , and then we find the redshift density perturbation  $\delta_z(\mathbf{n}, z)$ . However, the volume is also a perturbed quantity, since the solid angle and the redshift bin are distorted between the source and the observer. Thus, the truly observed quantity is the perturbation in the number density of galaxies [84]:

$$\Delta(\mathbf{n}, z) \equiv \delta_z(\mathbf{n}, z) + \frac{\delta V(\mathbf{n}, z)}{V(z)}, \quad (1.118)$$

which indeed is a gauge invariant quantity. Even if the additional corrections are suppressed at large scales, they offer an alternative approach to disentangle the effect of modified gravity in galaxy clustering measurements.

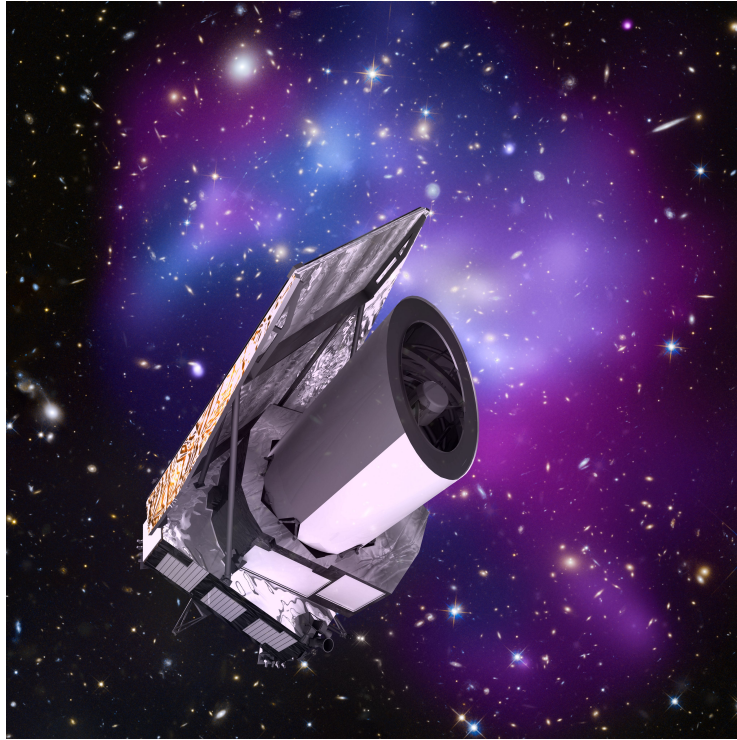


**Figure 1.5:** An artist view of the Euclid Satellite. Credit ESA, Image obtained from the [Euclid Consortium webpage](#).

### 1.4.3 Future Observations: The Euclid Survey

So far we discussed the current observations on dark energy which mainly includes large scale surveys, measuring the power spectrum in galaxy clusters. Of course, as every experiment in physics the purpose, besides theoretical developments, is focussed on the improvement of observational techniques, increase the amount of data, and reduce systematic errors. What is the future concerning our current picture of the universe?. The answer, nor surprisingly should be “*something that can disentangle the nature of the actual expansion of the universe*”. Euclid might be the guy with the ultimate truth. We will here give a short description following the Euclid red book study report [12] and also information from the Euclid Consortium Team <sup>9</sup> webpage.

Euclid is an ESA (European Space Agency) medium class space mission approved in October 2011, and will be launched to the L2 Sun-Earth Lagrange point in 2020, for a mission of 6 years. In addition to the main goal (answer the dark energy issue, i.e. the actual cosmic speed-up), Euclid will also try to find if dark energy is dynamical (looking for time

---

<sup>9</sup><http://www.euclid-ec.org>

variation in the e.o.s  $w$ ), put constraints in the neutrino mass, and find possible modifications of GR. To accomplish this task, Euclid will use two main probes, weak lensing and galaxy clustering (with BAO and RSD), measuring about 10 billion sources, from which around 1 billion will be used for weak lensing, and tens of million redshifts will be used for galaxy clustering. Giving some technical data: It will use a 1.2 m mirror telescope operating in both visible and infrared wavelengths, which will cover an area of about 15000  $\text{deg}^2$  in the redshift range  $0.5 < z < 2.0$ , when the cosmic speed-up its supposed to start.

Euclid seems promising, and a big scientific effort has been made until now (and for sure in the forthcoming years) to improve the theoretical predictions, and also statistical analysis, that would be an enjoyable task of cleaning several Petabytes of data. Being optimistic, around 2025 we may have first releases and also an excellent opportunity to rule out dark energy models, and see if, wether or not,  $\Lambda$  wins his *dark race*. In the next chapter we will meet the contenders of the cosmological constant, based on modifications on the gravity sector.



## DARK ENERGY COSMOLOGIES

*“The next case in simplicity includes those manifoldnesses in which the line-element may be expressed as the fourth-root of a quartic differential expression”*  
*Bernard Riemann, 1854*

The cosmological setup of the previous chapter show us that the standard description of our Universe should be reformulated; the main issue:  $\Lambda$ . This offers however an exciting approach considering that GR can be revisited to take into account the actual accelerated expansion of the Universe, without using the cosmological constant. Since, as we anticipated, GR has successfully satisfied solar system constraints, the possibility is that at large scales (cosmological), Einstein’s theory could be modified. Modifications of GR are not particularly new, since just from the genesis of GR, alternative approaches to describe the gravitational interaction have been born, also attempting to unify geometry with the quantum description. However, when modifying gravity the price you pay is high; instabilities due to the new degrees of freedom, incompatibility with local constraints, and issues of renormalization at quantum level arise. In this chapter we will briefly review the main elements of modified gravity, with special attention to a sub-class of theories with a single scalar field which preserves second order equations of motion: the Horndeski Lagrangian.

### 2.1 Beyond Einstein - A Journey Through Modified Gravity

We want to start now a short trip through the vast land of possibilities when modifying gravity. Our departure point, as previously anticipated in [Chapter 1](#), is at the action level. GR is based on the Einstein-Hilbert action, in which the Lagrangian density is constructed from the simplest scalar we can obtain in a Riemannian manifold  $(\mathcal{M}, g)$ , i.e.,

the Ricci scalar. By 1919, Weyl and Eddington [92] proposed theories built by quadratic Lagrangians (proportional to  $R^2$ ) and particular solutions (Schwarzschild-like describing the space-time outside a spherical and static massive object) had been studied [93]. The action in this case could be written as [94]

$$S_{R^2} = \int_{\mathcal{V}} d^4x \sqrt{-g} (R + \alpha R^2), \quad (2.1)$$

being  $\alpha$  a constant which gives the proper units in the Lagrangian. This action however leads to fourth order equations of motion (recall that our fundamental dynamical variable here is the metric tensor  $g_{\alpha\beta}$ ), and thus extra degrees of freedom in the theory. Another example, just after the publication of Einstein's legendary paper [23], Kretschmann [95] proposed an action with the scalar  $R_{\alpha\eta\gamma\delta} R^{\alpha\eta\gamma\delta}$  instead of the Ricci scalar which afterwards was called the *Kretschmann scalar*

$$S_K = \int_{\mathcal{V}} d^4x \sqrt{-g} R_{\alpha\eta\gamma\delta} R^{\alpha\eta\gamma\delta}. \quad (2.2)$$

Once again, terms like  $\nabla_{\alpha} \nabla_{\beta} R^{\alpha}_{(\gamma\delta)}$  introduces additional degrees of freedom. There is a way to avoid the appearance of these terms, considering the so-called *Gauss-Bonnet scalar* [96] defined as

$$\mathcal{G} = R^2 - 4R_{\alpha\beta} R^{\alpha\beta} + R_{\alpha\beta\gamma\delta} R^{\alpha\beta\gamma\delta}, \quad (2.3)$$

henceforth we write the action in a  $D$ -dimensional space-time as

$$S_{\mathcal{G}} = \int_{\mathcal{V}} d^Dx \sqrt{-g} \mathcal{G}. \quad (2.4)$$

This scalar has a particular attribute [97]. Due to a topological property on four dimensions, the density  $\sqrt{-g} \mathcal{G}$  could be written as a total derivative, and then when making the variation w.r.t.  $g_{\alpha\beta}$ , this contribution vanished at the boundary  $\partial\mathcal{V}$ . Thus, the scalars  $\mathcal{G}$  and the Ricci scalar  $R$  have an interesting property: in a four-dimensional space-time, they lead to second-order derivative contributions to the field equations. Scalars that satisfy such property are known as *Lovelock scalar invariants* [98]. The theory with the Gauss-Bonnet term has been used recently as a candidate for the dark energy problem [99]. An extension of this action occurs when considering an arbitrary function of the Gauss-Bonnet scalar  $f(\mathcal{G})$ , which however has been highly constrained by cosmological data and despite does not reproduce background evolution [100].

The Weyl tensor  $\mathfrak{C}$ , which measure the deviation of the manifold  $\mathcal{M}$  from conformal flatness [28, 32] offers an interesting alternative, since it is invariant under conformal transformations of the metric. We can construct an invariant as total contraction (similar as the Kretschmann scalar) and thus works with the so-called *conformal gravity theory* [101]. Let us conclude this briefly journey through the huge family of modifications of the action with a trending proposed model.  $f(R)$  gravity is a natural extension of the Einstein-Hilbert

action considering an arbitrary function of the Ricci scalar [16, 97]

$$S_{f(R)} = \frac{1}{2\kappa} \int_{\mathcal{V}} d^4x \sqrt{-g} f(R), \quad (2.5)$$

the equations are again fourth order [102–106], but with a Legendre transformation we can map this into a scalar-tensor theory [16].

In summary, these alternatives to GR, coming from geometric scalars other than simply  $R$ , or powers of it, introduce new degrees of freedom or higher order derivatives. In order to have a more systematic way to describe modified gravity, let us use now two powerful theorems. The first one, *Ostrogradski's Theorem* [107] states that there exist a linear instability in any theory, whose fundamental dynamical variable appears in the action with higher than second order time derivatives. The Hamiltonian that can be constructed from the Lagrangian is in this case unbounded, and then in principle accepts configurations with negative energy, see [108]. Thus, to avoid this is desirable that the equations of motion just contain second-order derivatives. The second one, *Lovelock's theorem* [98, 109] states that:

**Theorem 2.1** (Lovelock's Theorem). *In a four dimensional space-time the only divergence-free symmetric rank-2 tensor constructed solely from the metric  $g_{\alpha\beta}$  and its derivatives up to second differential order, and preserving diffeomorphism invariance, is the Einstein tensor plus a cosmological term:*

$$E^{\alpha\beta} = \alpha \sqrt{-g} \left[ R^{\alpha\beta} - \frac{1}{2} g^{\alpha\beta} R \right] + \lambda \sqrt{-g} g^{\alpha\beta}, \quad (2.6)$$

where  $\alpha$  and  $\lambda$  (cosmological constant) are constants, and  $R_{\alpha\beta}$  and  $R$  are the Ricci tensor and scalar curvature, respectively.

Formally, this theorem does not imply that Einstein-Hilbert action is the only action leading to EFE's. In fact, we can write a general Lagrangian [98]

$$\mathcal{L}_L = \sqrt{-g} \sum_n \frac{1}{2^n} \alpha_n \delta_{\gamma_1 \gamma_2 \dots \gamma_{2n}}^{\beta_1 \beta_2 \dots \beta_{2n}} R_{\gamma_1 \gamma_2}^{\beta_1 \beta_2} \dots R_{\gamma_{2n-1} \gamma_{2n}}^{\beta_{2n-1} \beta_{2n}}, \quad (2.7)$$

being  $\delta_{\gamma_1 \gamma_2 \dots \gamma_{2n}}^{\beta_1 \beta_2 \dots \beta_{2n}}$  a generalized Kronecker delta of order  $2n$ , and  $\alpha_n$  are constants, with  $n$  the dimension. However, when varying this action, some contributions vanishes, and gives a contribution to the boundary  $\partial\mathcal{V}$  in the form of the Gauss-Bonnet scalar  $\mathcal{G}$ . In this way, eq. (2.7) is an equivalent action for GR.

We can thus consider the Lovelock's theorem, and the assumptions behind, as a clever way to construct alternative theories beyond Einstein. Indeed, these assumptions means restrictions, which when avoided, leads to different kinds of modifications. These can be written as [110, 111]:

#### RESTRICTIONS TO LOVELOCK'S THEOREM

- L1.** Consider extra degrees of freedom more than the metric tensor.
- L2.** Work in a space with dimensionality different than four.
- L3.** Accept higher than second order derivatives of the metric in the field equations.
- L4.** Consider non-locality.

A nice representation of this set of possibilities was made in Tessa Baker's thesis [4], a similar one also presented in [112]. In fig. 2.1 we have shown an adaptation (colorful) of it; this can be sketched as kind of *islands* beyond the safe ground of Einstein's gravity. In what follows, and for completeness, we want to land in three of these islands, towards our final destination: the Horndeski Lagrangian. We mainly follow the comprehensive treatments given in [4, 110, 112]. Non-locality theories will be no considered here.

### 2.1.1 Higher Derivatives

In the previous section we worked out some examples of modified actions, which include different scalar than the Ricci, or extensions to it. Most of them conduce to field equations which contains derivatives higher than two. These models are quite dangerous due to the Ostrogradski instability; in this way we also avoid Lovelock's restriction. Let us now discuss some particular examples of these kind of theories.

We already encounter one particular example which is suitable for other kind of violation on Lovelock's restriction (adding new degrees of freedom), and has recently gained impressive attention among cosmology and astrophysical tests for GR:  $f(R)$  gravity. Its main ingredient is the action containing an “*arbitrary*”<sup>1</sup> function of the Ricci scalar. The action is given by eq. (2.5), and after varying this action w.r.t. the metric tensor  $g^{\alpha\beta}$  we find the standard form of the modified field equation [102, 103, 106]:

$$f_R R_{\alpha\beta} - \frac{1}{2} f g_{\alpha\beta} - (\nabla_\alpha \nabla_\beta - g_{\alpha\beta} \square) f_R = \kappa T_{\alpha\beta} , \quad (2.8)$$

<sup>1</sup>From solar system constraints and instabilities the first and second derivatives have to be chosen positives  $f_R > 0$ , and  $f_{RR} > 0$ .

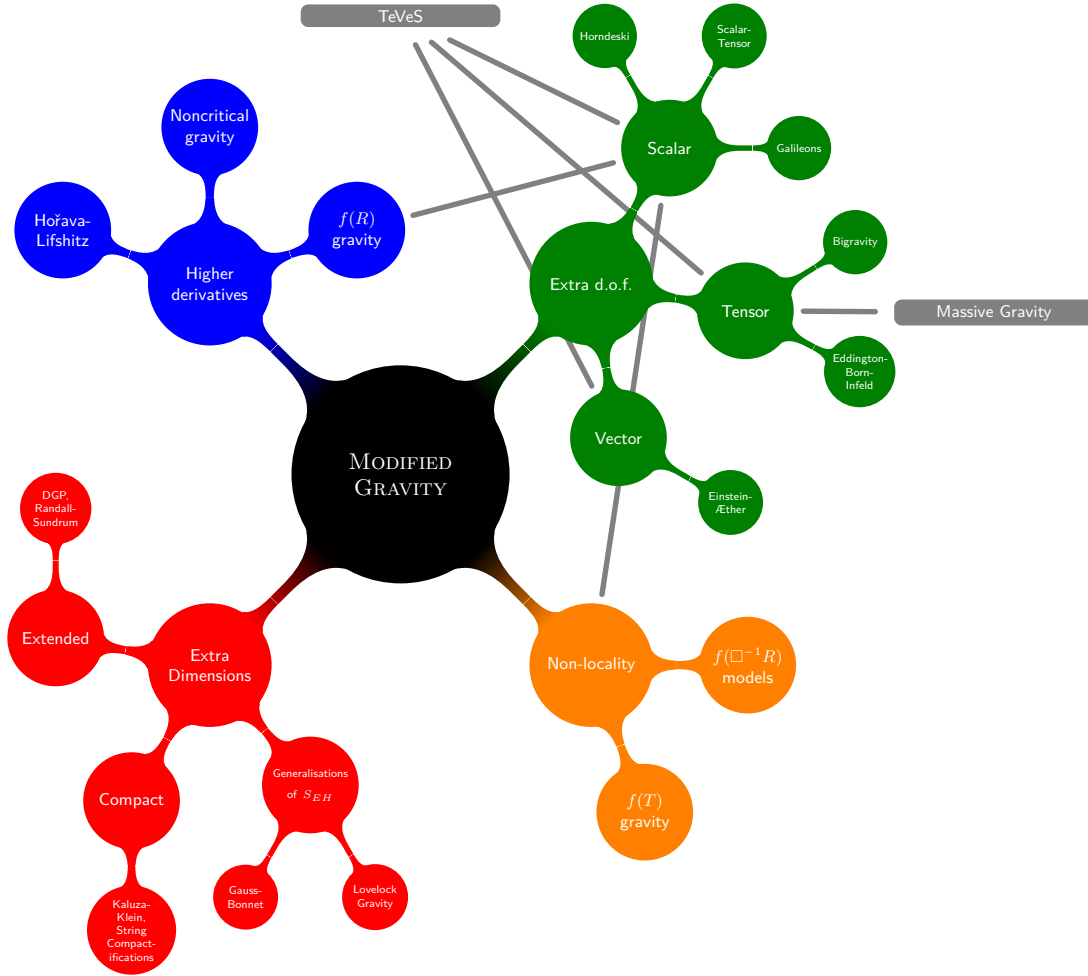


**Figure 2.1:** Islands of modified gravity. Adapted from [4]. Theories are classified according to the way in which they avoid Lovelock’s restrictions.

being  $f_R \equiv \frac{f(R)}{dR}$  and the D’alambertian  $\square \equiv \nabla_\gamma \nabla^\gamma$ . Since the Ricci scalar contains second derivatives of the metric, it is clear that the operator  $\mathcal{D}_{\alpha\beta} \equiv \nabla_\alpha \nabla_\beta - g_{\alpha\beta} \square$  contribute to fourth order derivatives of the metric. This new contributions, besides the cosmological and astrophysical implications, are of particular interest for energy conditions issues [113], and geodesics leading on cosmological distances [114]. However, there is one way to heal this condition, using a Legendre transformation which moves this *metric* representation to a equivalent scalar-tensor one, we will back on this in the next subsection. A complete review on  $f(R)$  gravity could be found in [16, 97].

Additional examples for higher derivatives theories, besides those explained in the previous

section, are constructed with arbitrary functions of the scalars from  $R_{\alpha\beta\gamma\delta}$ ,  $R_{\alpha\beta}$  and  $R$ ; a general form could be written as

$$S = \frac{1}{2\kappa} \int_{\mathcal{V}} d^4x \sqrt{-g} f(R, R_{\alpha\beta} R^{\alpha\beta}, R_{\alpha\beta\gamma\delta} R^{\alpha\beta\gamma\delta}), \quad (2.9)$$

with the explicit form of the Kretschmann scalar  $K$ . Unfortunately, these lagrangian is not conformally related to GR with a scalar field, as the privileged case of  $f(R)$  gravity. In fact, these kinds of theories introduce two gravitons (i.e. additional degrees of freedom), one of which has a negative kinetic operator (a ghost). To avoid that, we can write analogously, an arbitrary function based on the Lovelock invariants  $R$  and  $\mathcal{G}$ , ghost-free, as

$$S = \frac{1}{2\kappa} \int_{\mathcal{V}} d^4x \sqrt{-g} f(R, \mathcal{G}). \quad (2.10)$$

A quite recently proposal, which is an attempt to build a quantum description of gravity, is the so-called Hořava-Lifschitz model [115, 116]. By adding higher order spatial derivatives, without adding higher order time derivatives, the propagator associated to the graviton at the Ultra Violet regime (UV) is modified in a way that the theory becomes renormalizable [110]. To do that, a particular space-time foliation is made introducing a time-dependent lapse function  $N$ , making as expected, vanishing spatial derivatives. In this way, by treating space and time unequally, Hořava's gravity is indeed an example of a *Lorentz violating* theory, since in this case only spatial diffeomorphism is preserved.

### 2.1.2 New Degrees of Freedom

Other example to avoid Lovelock's restrictions, which indeed is very popular nowadays, consist in add new degrees of freedom in the action. The main idea behind is to add scalar, vector or tensor fields (or combinations of them), which couple minimally to the metric. These fields in general add new kinetic terms into the action, which however leads to an inevitable fall into Ortogradski's instability. Among them, the case of non-dynamical fields is interesting. The EFE's, and the Lovelock's theorem assume that  $T_{\alpha\beta}$  is linear into the equations. If we relaxed this condition, is possible to construct theories in which the r.h.s. of EFE's is built with non-linear combinations of  $T_{\alpha\beta}$ , although demanding  $\nabla_{\alpha} T^{\alpha\beta} = 0$ .

A relative of  $f(R)$  gravity, namely the Palatini formulation  $f(\mathcal{R})$  is a good example [117]. In this theory the Ricci scalar  $\mathcal{R} = g^{\alpha\beta} \mathcal{R}_{\alpha\beta}$  is constructed from the connection (not from the metric as usual), and the field equations leads to a similar form of the modified field equations eq. (2.8), without the appearance of terms associated with the operator  $\mathcal{D}_{\alpha\beta}$ . Instead, an auxiliary non-dynamical term appears as kind of metric compatibility

$$\bar{\nabla}_{\gamma} (\sqrt{-h} h^{\alpha\beta}), \quad (2.11)$$

being  $h_{\alpha\beta} = f'(\mathcal{R})g_{\alpha\beta}$  a conformal related metric, and  $\bar{\nabla}_\gamma$  a covariant derivative defined with the independent connection. In comparison to the case of GR in which Palatini and metric version are equivalent, in the case of  $f(R)$  gravity its counterpart produces a very different behavior. Indeed,  $f(\mathcal{R})$  gravity has the same degrees of freedom as GR, in contrast with metric  $f(R)$  which propagates an extra scalar field.

A well-known example of modifications with a single scalar field, are scalar-tensor theories. These theories are used as standard way in which deviations from GR are modeled, due for instance to the simple form of the field equations, allowing exact analytical solutions. The action in this case could be written as

$$S_{S-T} = \frac{1}{2\kappa} \int_{\mathcal{V}} d^4x \sqrt{-g} [f(\phi, R) - K(\phi)\nabla_\gamma\phi\nabla^\gamma\phi - 2V(\phi)] + S_M(\psi, g_{\alpha\beta}), \quad (2.12)$$

being  $V(\phi)$  the potential for the scalar field  $\phi$ , and the functions  $f(\phi)$  and  $K(\phi)$  acts as couplings with gravity and the kinetic term. One particular case of this kind of theories, the so-called Brans-Dicke theories [118], that had been studied to model possible deviations of the Newtonian gravitational constant  $G$ , is obtained if we set  $f(\phi, R) = \phi R$ , and  $K(\phi) = \omega_{BD}/\phi$ , which gives the standard form:

$$S_{BD} = \frac{1}{2\kappa} \int_{\mathcal{V}} d^4x \sqrt{-g} \left[ \phi R - \frac{\omega_{BD}}{\phi} \nabla_\gamma\phi\nabla^\gamma\phi - 2V(\phi) \right] + S_M(\psi, g_{\alpha\beta}). \quad (2.13)$$

Besides the astrophysical and cosmological applications of Brans-Dicke theory, summarized in [110] which unfortunately are beyond our purposes, the form of the action could help us to give an interesting example of a theory who possesses an enviable property among the family of modifications: can be transformed from a higher order theory to a scalar-tensor equivalent, via a Legendre transformation.

We already advertise this is the case of metric  $f(R)$  gravity. The equivalence could be seen considering the following action

$$S = \frac{1}{2\kappa} \int_{\mathcal{V}} d^4x \sqrt{-g} [f(\zeta) + f'(\zeta)(R - \zeta)] + S_M(\psi, g_{\alpha\beta}). \quad (2.14)$$

with prime denoting differentiation w.r.t. the scalar  $\zeta$ . Variation of this action gives  $f''(\zeta)(R - \zeta) = 0$ , thus  $R = \zeta$  for all  $f''(\zeta) \neq 0$ . If we replace  $R = \zeta$  the standard form of the action in metric  $f(R)$  gravity is recovered. If we consider now the transformation  $\phi = f_{,R}$ ,  $V(\phi) = (1/2)[\zeta\phi - f(\zeta)]$ , the action eq. (2.14) is equivalent to eq. (2.13) with  $\omega_{BD} = 0$ .

Another example of extra degrees of freedom, which also can be classified as Lorent-violating approach, is known as *Einstein-Æther* theory. First of all, let us introduce a progenitor theory made by Szekeres in 1955, in which the cosmic time plays the role of a

field variable. The idea behind was to overcome the contradiction between the relativity principle (i.e. the equivalence of *all* reference systems), and the definition of an absolute time in cosmology. For that, a time field  $\phi$  was introduced which then interacts in the action with the metric; all physical implications (vacuum solutions, cosmology, gravitational waves) were also studied in [119]. As an extension to this model, a dynamical unit vector field, the *æther*, was introduced in [120], allowing also the theory to violate Lorentz invariance (via local boost invariance). The action in this case could be written as

$$S_{S-T} = \frac{1}{2\kappa} \int_{\mathcal{V}} d^4x \sqrt{-g} \left[ R + K_{\gamma\sigma}^{\alpha\beta} \nabla_{\alpha} A^{\gamma} \nabla_{\beta} A^{\sigma} + \lambda(A^{\alpha} A_{\alpha} + 1) \right] + S_M(\psi, g_{\alpha\beta}), \quad (2.15)$$

where  $K_{\gamma\sigma}^{\alpha\beta} = c_1 g^{\alpha\beta} g_{\gamma\sigma} + c_2 \delta_{\gamma}^{\alpha} \delta_{\sigma}^{\beta} + c_3 \delta_{\sigma}^{\alpha} \delta_{\gamma}^{\beta}$  for some suitable constants  $c_i$ , and  $\lambda$  is a Lagrange multiplier which constraint the vector field  $A^{\alpha}$  to be time-like. This action includes a kinetic term for the *æther*, coupled to the metric through covariant derivatives. The presence of this Lorentz-violating vector field can affect cosmology. For instance, it can imprint signatures on perturbations at early universe stages [121], and also affect the growth rate of structure [122, 123].

Finally, we will discuss an example of a modified theory based on an additional tensor field. GR is indeed a massless gravity theory. Some attempts to construct theories in which the graviton could have a mass, had been proposed first by Fierz and Pauli in 1939 [124]. They considered a mass term for linear gravitational perturbations, which is uniquely determined by requiring the absence of ghost degrees of freedom. The mass term breaks the gauge invariance of GR, leading to a graviton with five degrees of freedom instead of the usual two of GR. In order to construct a theory which avoids this instability, a new tensor field should be added to the action which interacts with the metric [125]. The *simplest* way is to add a second metric to the action, that can be written as the form of the so-called *bimetric gravity*

$$S_{\mathbf{g},\mathbf{f}} = -\frac{M_g^2}{2} \int_{\mathcal{V}} d^4x \sqrt{-\det g} R_g - \frac{M_f^2}{2} \int_{\mathcal{V}} d^4x \sqrt{-\det f} R_f + m^4 \int_{\mathcal{V}} d^4x \sqrt{-\det g} \sum_{n=0}^4 \beta_n e_n \left( \sqrt{g^{-1}f} \right) + S_M(\psi, g_{\alpha\beta}), \quad (2.16)$$

where  $M_g$  and  $M_f$  are Planck masses and  $R_g$  and  $R_f$  are the Ricci scalars associated with the metrics  $\mathbf{g}$  and  $\mathbf{f}$  respectively. Notice that the action for the matter fields is determined by the metric  $\mathbf{g}$ , and thus matter follow geodesics in the space-time  $g_{\alpha\beta}$ ; there are five interaction terms  $e_n$  and  $\beta_n$  representing arbitrary constants. These theory has recently brought the attention since is cosmologically viable [126–129].

Those few examples were just an appetizer from the vast family of modified theories with extra degrees of freedom. Other possibilities, such as TeVeS [130], which is a mixture of

scalar-tensor (a single scalar field  $\phi$  and Einstein-Æther theories (with a dual vector  $A_\alpha$ ) has also been extensively studied for cosmological purposes [131–133].

### 2.1.3 Extra Dimensions

One of the assumptions when constructing the mathematical space-time in which GR lives, is that it should be 4-dimensional (3 spatial dimensions + 1 temporal). Is plausible thus to consider gravitational theories in more than 4 dimensions. In fact, supergravity (or SUGRA), which is one of the strongest candidates for a quantum description of gravity, is formulated in a space-time of  $D = 11$  dimensions. Most of the approaches consist in extra spatial dimensions, and following [4], can be summarized as:

- (a) Models in which the additional dimensions are *compactified*, that means, those dimensions are “squeezed” to an unnacesible small size, in comparisson with the 3 spatial dimensions. One famous example of this kind, is Kaluza-Klein (KK) theory [134, 135], which is an attempt to construct an unified description of gravity and electromagnetism, with an action written in a  $5D$  space-time. In 5 dimensions, the metric has 15 independent components, 10 of them leads to the standard form of the metric in  $4D$  ( $g_{\alpha\beta}$ ), 4 gives Maxwell equations (via the electromagnetic potential  $A_\alpha$ ), and the additional component is attached to a scalar field  $\phi$  [136]:

$$\hat{g}_{AB} = \begin{pmatrix} g_{\alpha\beta} + \kappa\phi^2 A_\alpha A_\beta & \kappa\phi^2 A_\alpha \\ \kappa\phi^2 A_\alpha & \phi^2 \end{pmatrix}, \quad (2.17)$$

with the indices  $A, B$  running from 0 to 5. An extensive treatment on KK gravity, from spherical solutions, to cosmological applications, could be find in [136]

- (b) Models in which the additional dimensions are large or infinite. In this case, our four-dimensional universe is then referred to as a brane existing in a higher-dimensional bulk spacetime. Among this approach, there exist a well-known case: the Dvali-Gabadadze-Porrati (DGP), a  $5D$  model described by the action [137]:

$$S = \frac{1}{2M_5^3} \int d^4x \sqrt{-^{(5)}g} {}^{(5)}R + \frac{1}{2M_4^2} \int d^4x \sqrt{-g} \left( {}^{(4)}R + \mathcal{L}_m \right), \quad (2.18)$$

being  ${}^{(5)}R$  and  ${}^{(4)}R$  the  $5D$  and  $4D$  Ricci scalars, respectively. In this theory, one define a *crossover scale*  $r_c = M_4^2/2M_5^3$  below which the theory looks 4D, and above which looks like 5D. The Friedmann equation in this model becomes [138]:

$$H^2 = \pm \frac{H}{r_c} = \frac{\kappa}{3}\rho. \quad (2.19)$$

At early times  $H/rc \gg 1$ , and we recover the usual 4D Friedmann equation. For late

times, the Hubble parameter approach to  $H \rightarrow 1/r_c$ , known as the *upper branch*, in which the expansion accelerates, without cosmological constant. On the other hand, the lower branch solution, requires the cosmological constant to realise the accelerated expansion. This theory however is ruled out as candidate for the dark energy problem, since that at linear perturbation level, it suffers a ghost instability [139, 140], additionally, in the linearized case, solar system constraints are not satisfied.

We are now prepared to our landing in a special case of modifications, based on a single scalar field.

## 2.2 The Horndeski Lagrangian

The Lovelock Lagrangian is the most general one, which leads to a second order field equations, with a cosmological constant, i.e. to the EFE's. As first extension one can think in the form of a scalar-tensor like theory, including a single scalar field. This task was made by Horndeski (Lovelock's student) in 1974 [141], theory however forgotten until 2011, when was independently rederived by Deffayet [142]. *Horndeski theory* has been attracted interest recently, since, as we see later, encodes a large family of theories based on a single field [20, 143–147]. The action containing the *Horndeski lagrangian* [141] could be written as:

$$S = \int_{\mathcal{V}} d^4x \sqrt{-g} \left[ \sum_{i=1}^5 \mathcal{L}_i + \mathcal{L}_m[g_{\mu\nu}] \right], \quad (2.20)$$

with the Lagrangians  $\mathcal{L}_i$ :

$$\mathcal{L}_2 = K(\phi, X), \quad (2.21a)$$

$$\mathcal{L}_3 = -G_3(\phi, X) \square \phi, \quad (2.21b)$$

$$\mathcal{L}_4 = G_4(\phi, X) R + G_{4,X} \left[ (\square \phi)^2 - (\nabla_\mu \nabla_\nu \phi)^2 \right], \quad (2.21c)$$

$$\mathcal{L}_5 = G_5(\phi, X) G_{\mu\nu} \nabla^\mu \nabla^\nu \phi - \frac{G_{5,X}}{6} \left[ (\square \phi)^3 - 3(\square \phi) (\nabla_\mu \nabla_\nu \phi)^2 + 2(\nabla_\mu \nabla_\nu \phi)^3 \right]. \quad (2.21d)$$

The functions  $K(\phi, X)$  and  $G_i(\phi, X)$  are arbitrary functions of the scalar field  $\phi$  and its canonical kinetic term  $X = -(\nabla^\mu \phi \nabla_\mu \phi)/2$ . The subscript  $X$  represents derivative w.r.t

$X$ , and subscripts  $\phi$  represent derivatives w.r.t. the scalar field  $\phi$ .

The theories that fit in this description can be obtained via special choices of four arbitrary functions of the scalar field, that appear in the Horndeski Lagrangian. For instance it contains: Brans-Dicke [118] and scalar-tensor gravity,  $f(R)$  gravity (with the scalar-tensor analogue), single-field quintessence and  $K$ -essence theories [148, 149], single-field inflation models, the covariant Galileon, Dirac-Born-Infeld theory, Kinetic Gravity Braiding (KGB) [150, 151], actions involving derivative couplings between a scalar field and the Einstein tensor and  $f(\mathcal{G})$  [152] theories.

In general, the Horndeski Lagrangian could be obtained from an Effective Field Theory (EFT) expansion [153–155]. Specifically, EFT describes the space of scalar field theories, with a Lagrangian written in unitary gauge, that preserves isotropy and homogeneity at background level, assumes the weak equivalence principle, and has only one extra dynamical field. The action in general could be written as [153]:

$$\begin{aligned}
S = \int_{\mathcal{V}} d^4x \sqrt{-g} & \left[ \frac{m_0}{2} [1 + \Omega(\tau)] R + \Lambda(\tau) - a^2 c(\tau) \delta g^{00} + \frac{M_2^2(\tau)}{2} (a^2 \delta g^{00})^2 \right. \\
& - 2\bar{M}_1^3(\tau) a^2 \delta g^{00} \delta K_\mu^\mu - \frac{\bar{M}_2^2(\tau)}{2} (\delta K_\mu^\mu)^2 - \frac{\bar{M}_3^2(\tau)}{2} \delta K_\nu^\mu \delta K_\mu^\nu + \frac{a^2 \hat{M}^2}{2} \delta g^{00} \delta R^{(3)} \\
& \left. + m_2^2(\tau) (g^{\mu\nu} + n^\mu n^\nu) \partial_\mu (a^2 \delta g^{00}) \partial_\nu (a^2 \delta g^{00}) \right] + S_M(\psi, g_{\alpha\beta}), \quad (2.22)
\end{aligned}$$

being  $R$  is the Ricci scalar,  $\delta R^{(3)}$  is its spatial perturbation,  $K_{\mu\nu}$  is the extrinsic curvature, and  $m_0$  is the reduced Planck mass. This action depends on a set of nine time-dependent functions,  $\{\Omega, c, \Lambda, \bar{M}_1^3, \bar{M}_2^4, \bar{M}_3^2, M_2^4, \hat{M}^2, m_2^2\}$ , whose choice specifies the theory. In this way, EFT provides a direct link to any scalar field theory. Based on this EFT scheme, the evolution of perturbations is entirely determined by four independent functions  $\alpha$ 's of time that are related to the functions  $K$  and  $G_i$  of the Horndeski theory, introduced by [156]:

$$M_*^2 \equiv 2(G_4 - 2XG_{4,X} + XG_{5,\phi} - \dot{\phi}HXG_{5,X}), \quad (2.23)$$

$$HM_*^2 \alpha_M \equiv \frac{d}{dt} M_*^2, \quad (2.24)$$

$$\begin{aligned}
HM_*^2\alpha_K &\equiv 2X(K_{,X} + 2XK_{,XX} - 2G_{3,\phi} - 2XG_{3,\phi X}) \\
&+ 12\dot{\phi}XH(G_{3,X} + XG_{3,XX} - 3G_{4,\phi X} - 2XG_{4,\phi XX}) + 12XH^2(G_{4,X} + 8XG_{4,XX} + 4X^2G_{4,XXX}) \\
&- 12XH^2(G_{5,\phi} + 5XG_{5,\phi X} + 2X^2G_{5,\phi XX}) + 4\dot{\phi}XH^3(3G_{5,X} + 7XG_{5,XX} + 2X^2G_{5,XXX})
\end{aligned} \tag{2.25}$$

$$\begin{aligned}
HM_*^2\alpha_B &\equiv 2\dot{\phi}(XG_{3,X} - G_{4,\phi} - 2XG_{4,\phi X}) + 8XH(G_{4,X} + 2XG_{4,XX} - G_{5,\phi} - XG_{5,\phi X}) \\
&+ 2\dot{\phi}XH^2(3G_{5,x} + 2XG_{5,xx})
\end{aligned} \tag{2.26}$$

$$HM_*^2\alpha_T \equiv 2X(2G_{4,X} - 2G_{5,\phi} - (\ddot{\phi} - \dot{\phi}H)G_{5,x}). \tag{2.27}$$

Here,  $M_*$  corresponds to the Planck mass. This formulation indeed represents an important reduction in the number of degrees of freedom: the set of nine parameters of the EFT description has been reduced to a set of four, namely  $\{\alpha_K, \alpha_B, \alpha_M, \alpha_T\}$ . Quoting explicitly [156], the meaning of these four functions could be summarized as follows:

- $\alpha_K$ , *kineticity*: Kinetic energy of scalar perturbations arising from the action. It is the only contribution of perfect-fluid models but is not present at all in archetypal modified gravity models such as  $f(R)$  and  $f(\mathcal{G})$ . Contribution from all of  $K, G_3, G_4, G_5$ .
- $\alpha_B$ , *braiding*: Means braiding or mixing of the kinetic terms of the scalar and the metric. Causes clustering of dark energy. Contributions from  $G_3, G_4, G_5$ .
- $\alpha_M$ , *Planck-mass run rate*: Rate of evolution of the effective Planck mass. Contributions from  $G_4$  and  $G_5$ .
- $\alpha_T$ , *tensor speed excess*: Deviation of the speed of gravitational waves from that of light. This violation of Lorentz-invariance for tensors also changes the response of the Newtonian potential  $\Psi$  to matter sources even in the presence of no scalar perturbations, leading to anisotropic stress. Contributions from  $G_4$  and  $G_5$ .

Let us denote this as the *Bellini-Sawicki parametrization*.

Despite the complicated form of the  $\alpha$ 's, there is a way to put constraints on them, coming from the recent Planck data release. In the particular case of  $\alpha_M = -\alpha_B$ , with  $\alpha_K$  fixed, and setting  $\alpha_T = 0$ , a suitable scaling was made by Ade et al. (Planck collaboration) [5]. In this choice, the only free function is  $\alpha_M$ , which can be written in terms of the parameter  $\Omega$  of the EFT approach as:

$$\alpha_M = \frac{a}{\Omega + 1} \frac{d\Omega}{da}. \tag{2.28}$$

Using the scaling ansatz

$$\alpha_M = \alpha_{M0} a^\beta, \tag{2.29}$$

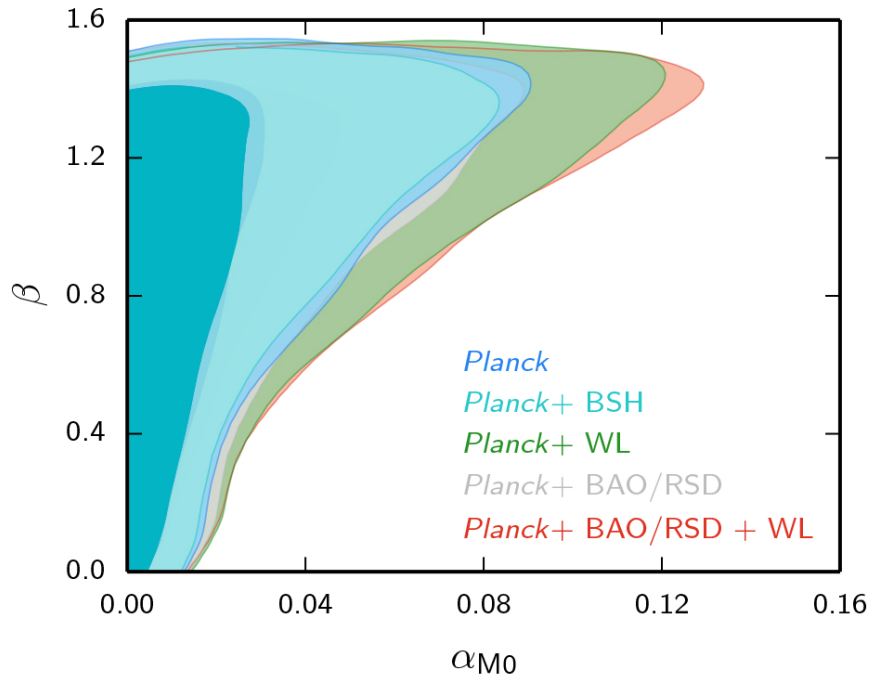


**Figure 2.2:** Marginalized posterior distributions at 68% and 95% confidence level for the two parameters  $\alpha_{M0}$  and  $\beta$  of the exponential evolution,  $\Omega(a) = \exp(\Omega_0 a^\beta) - 1$ .  $\alpha_{M0}$  is defined as  $\Omega_0 \beta$  and the background is fixed to  $\Lambda$ CDM. The value  $\Omega_{M0} = 0$  corresponds to the  $\Lambda$ CDM model also at perturbation level. Figure obtained from [5].

where  $\alpha_{M0}$  is the value of  $\alpha_M$  today, and  $\beta > 0$  which determines how quickly the modification of gravity decreases in the past, eq. (2.28) can be integrated to obtain

$$\Omega(a) = \exp\left(\frac{\alpha_{M0}}{\beta} a^\beta\right) - 1. \quad (2.30)$$

This expression can be evaluated using a EFT version of the Boltzmann code **CAMB**, known as **EFTCAMB** [157]. In fig. 2.2, the marginalized posterior distributions for the two parameters  $\Omega_0 = \alpha_{M0}/\beta$  and  $\beta$ , are plotted. The case  $\alpha_{M0} = 0$  corresponds to the  $\Lambda$ CDM model. Ade et al. used for both, the exponential and the linear model, a flat prior with  $\Omega_0 \in [0, 1]$  and  $\beta \in (0, 3]$ . For  $\beta \rightarrow 0$ , the parameter  $\alpha_M$  remains constant and does not go to zero in the early Universe, while for  $\beta = 3$  the scaling would correspond to  $M$  functions in the action eq. (2.22), which are of the same order as the relative energy density between dark energy and the dark matter at background level.

As final remark, extended theories which contain Horndeski as a particular case have been built [108, 158–163]. They include extra terms in the Lagrangian that can lead to higher

order terms in the field equations, which however does not imply the presence of extra degrees of freedom. These theories are known as *beyond Horndeski theories*.

## 2.3 Modifying Linear Perturbation Equations

Here we want to find the final ingredient towards the model-independent description of dark energy cosmologies. In [Section 1.3](#) we briefly summarized the main elements of cosmological perturbation theory, focusing on scalar perturbations. The metric perturbations in the Newtonian gauge eq. (1.62) are determined by the potentials  $\Phi$  and  $\Psi$ , so we can expect to model relevant degrees of freedom by these potential as functions of scale and time. For instance, the anisotropic stress  $\eta$ , which is defined as the ratio (negative) between the two gravitational potentials  $\eta = -\Phi/\Psi$ , is a signature of modifications of GR [[62](#), [164](#)]. Some of the most popular parametrizations can be summarized as follows

### MODIFIED GRAVITY PARAMETERS

1.  $Q(a, k)$ , which modifies the Poisson equation through extra DE clustering according to

$$k^2\Phi \equiv -4\pi G a^2 Q(a, k) \rho_m \Delta_m, \quad (2.31)$$

being  $\Delta_m$  the comoving density perturbation

2.  $Y(a, k)$ , the clustering of dark energy (or effective gravitational constant also called  $\mu(k, k)$ ), which modifies the equivalent equation for  $\Psi$  rather than  $\Phi$

$$k^2\Psi \equiv -4\pi G a^2 Y(a, k) \rho_m \Delta_m, \quad (2.32)$$

3.  $\Sigma(a, k)$ , which modifies the *lensing potential*  $\Psi - \Phi$

$$k^2(\Psi - \Phi) \equiv -8\pi G a^2 \Sigma(a, k) \rho_m \Delta_m, \quad (2.33)$$

4.  $\eta(a, k)$ , the anisotropic stress or gravitational slip defined by the ratio

$$\eta(a, k) \equiv -\frac{\Phi}{\Psi}, \quad (2.34)$$

These functions are certainly not independent, it is enough to choose two independent functions of scale and time to describe *all* modifications with respect to GR [[6](#)]. Popular choices are  $\{Y, \eta\}$ , which have a simple functional form in many theories;  $\{Y, \Sigma\}$ , which is more related to what we observe given that CMB lensing measure a projection of the lensing potential  $\Phi_{\text{lens}} = \Psi - \Phi$ . We can simply go from one set of parameters to the

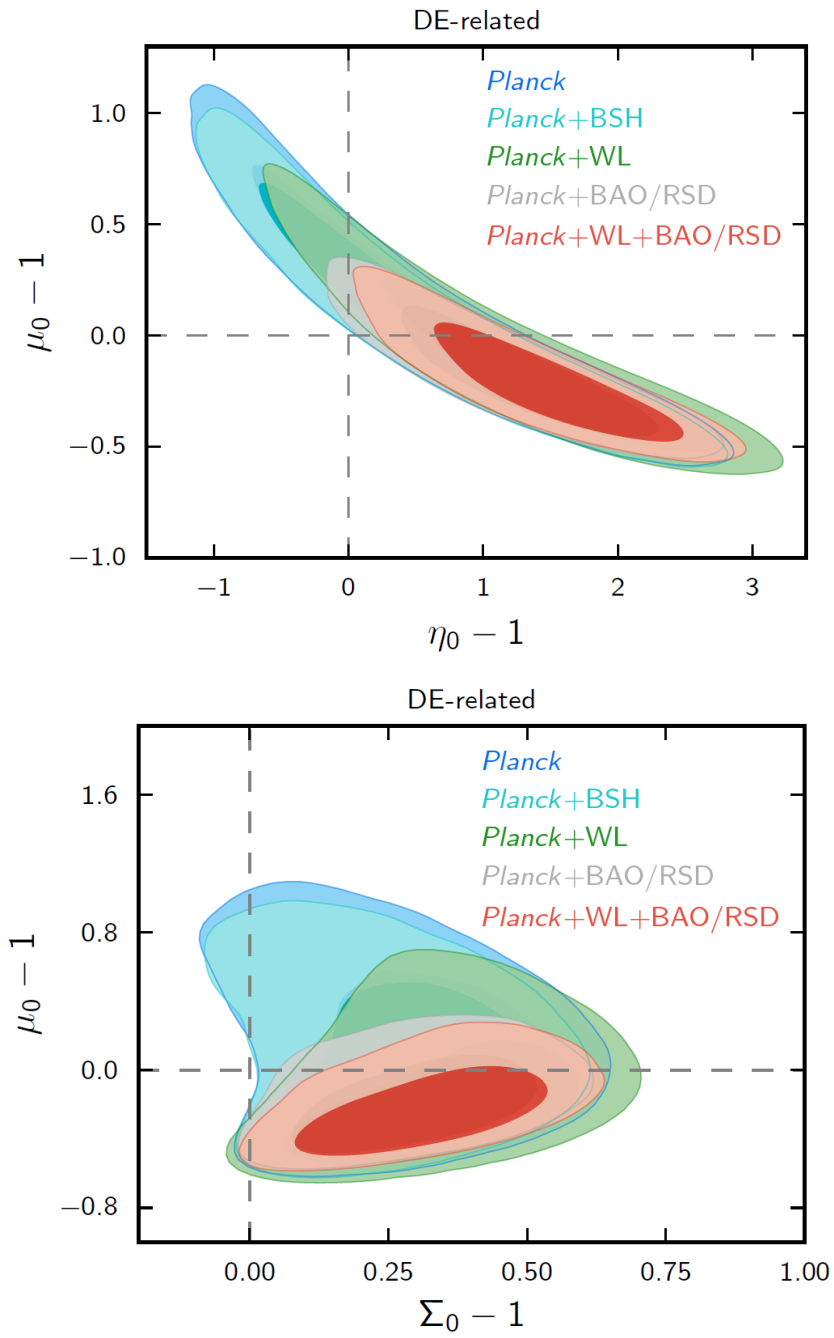


**Figure 2.3:** Planck constraints on modified gravity. 68% and 95% confidence regions for the two parameters  $\Sigma_0$  and  $\mu_0$  ( $Y_0$ ) obtained from Planck CMB measurements in combination with WL, BAO and RSD [5].

another using

$$Y(a, k) \equiv \frac{Q(a, k)}{\eta(a, k)}, \quad (2.35)$$

and

$$\begin{aligned} \Sigma(a, k) &\equiv \frac{1}{2}Q(a, k) \left(1 + \frac{1}{\eta(a, k)}\right), \\ &\equiv \frac{1}{2}Y(a, k) (1 + \eta(a, k)). \end{aligned} \quad (2.36)$$

All these functions are unity in the  $\Lambda$ CDM model:  $Y(a, k) = \eta(a, k) = \Sigma(a, k) = 1$ , thus, if we modify gravity, they deviate from this value. Of great importance is of course to put constraints on these functions, with current observations. Some previous attempts were made on this direction [165–171]. However, given the actual accuracy, is necessary to assume particular time and scale dependence of these functions. One way is to consider these as scale-invariant, and dictate their time dependence by the density parameter associated with  $\Lambda$  [170]:

$$Y(a, k) = Y_0 \Omega_{DE}(a), \quad \Sigma(a, k) = \Sigma_0 \Omega_{DE}(a), \quad (2.37)$$

Simpson et. al. found  $Y_0 - 1 = 0.05 \pm 0.25$  and  $\Sigma_0 - 1 = 0.00 \pm 0.14$  using RSD from the WiggleZ Dark Energy Survey [172] and 6dF Galaxy Survey (6DFGS) [173]. Planck gave constraints on  $Y_0$  and  $\Sigma_0$ <sup>2</sup>, shown in fig. 2.3, combining Planck CMB observations with various external data, as BAO, WL and RSD. The  $\Lambda$ CDM model is in tension with the data at  $3\sigma$  level, if the Planck data is combined with WL and RSD/BAO. This tension is reduced to  $1.7\sigma$  level if we include CMB lensing.

## 2.4 Model-Independent Observables In Dark Energy Cosmologies

In the previous sections we discuss the many ways to modify gravity. In these approaches one fix an action, study its evolution and then compare the effect of the extra degrees of freedom with observations. The case of the extended linear perturbation equations was made to encode somehow the effect of modifications of gravity with a general set of functions, which parametrize large families of theories. But the question arises, which of these set of functions is really *model-independent*? i.e. parametrizations that does not use any particular gravity model? In this subsection we want to summarize the results of Amendola et. al. [20] in which this question was addressed. Their results at the end will establish the basis for the determination of future constraints on model-independent

<sup>2</sup>Notice that the notation in [5] uses  $\mu$  instead of  $Y$ , thus their  $\mu_0$  corresponds to  $Y_0$  in our choice.

observables, the root topic of this thesis.

The main goal of Amendola et. al. was to answer the following questions:

1. In the ideal case of precise cosmological observations (at background and linear perturbation level), which physical properties could in principle be reconstructed if we were to avoid any parameterization of dark energy?
2. Can we use these observable quantities to rule out not just some particular cosmological model, but an entire family of viable single scalar-field models?

Some previous attempts were made to study in a model-independent way, dark energy cosmologies. For instance, at background level a null test to constrain the expansion history was developed in [174, 175], in addition a principle-component analysis of the equation of state for dark energy was made in [176]. For linear perturbations, parametrizations for the growth of structure were studied in [165, 177–180], the so-called Parametrized-Post Friedmann approach which exploits general properties of GR-like theories (as Bianchi identities, energy conservation, and a given background expansion) were discussed in [179, 181–183]. Despite its generality, these models require parametrizations to break degeneracies when contrasted with data, inducing also dependent biases.

The difference of the approach explored in [20] is that, given a minimum set of assumptions, it is possible to elucidate the observables that can be measured without assuming any particular dark energy model. In this way, model-independent observables can provide tests to eliminate or confirm potential candidate models used to explain the current acceleration. Of course, these tests are subject to systematics, and future surveys should be designed to achieve considerable precision in the measurements.

### 2.4.1 Assumptions

The minimum set of assumptions needed to answer those two questions can be listed as:

- (a) The geometry of the Universe is well described by small fluctuations in an FLRW background metric with scale factor  $a(t)$ .
- (b) The matter content is pressureless ( $w = 0$ ) or evolves in a known way.
- (c) The relation between the galaxy distribution and the matter distribution at linear scales can be modeled as  $\delta_{\text{gal}} = b(k, a)\delta_{\text{m}}$ , where  $b(k, a)$ , see [Subsection 1.4.2](#).
- (d) The total action describing the evolution of the Universe reads

$$S = \int_{\mathcal{V}} d^4x \sqrt{-g} \left( \frac{1}{2}R + \mathcal{L}_x + \mathcal{L}_m \right), \quad (2.38)$$

(with  $\kappa = 1$ ) which includes the standard Einstein-Hilbert and the the matter Lagrangian  $\mathcal{L}_m$ . Additional terms thus are described by the dark energy Lagrangian  $\mathcal{L}_x$ .

In order to answer question (1) is quite enough to consider background and linear perturbations equations, that will be matter of next subsection. Question (2) needs an important assumption, regarding the dark energy Lagrangian:

- (e) The Lagrangian  $\mathcal{L}_x$ , which describes dark energy, is any one describing a single scalar field governed by second-order equations of motion, the Horndeski Lagrangian.

### 2.4.2 Background and Linear Perturbation Observables

We will focus now on assumptions (a)-(d). At background level, if we assume that the energy content is composed of matter  $\rho_m$  and density  $\rho_x$  coming from the dark energy Lagrangian  $\mathcal{L}_x$ , we can write the Hubble parameter eq. (1.33) as

$$H^2 - H_0^2 \Omega_{k0} a^{-2} = \frac{1}{3} (\rho_x + \rho_m), \quad (2.39)$$

being again  $H_0$  the present value of the Hubble parameter and  $\Omega_{k0}$  the present curvature density parameter. In addition, since we are assuming pressureless matter,  $\rho_m$  evolves as  $a^{-3}$ . Now, observations of the cosmic expansion are basically estimations of distances  $D(z)$  (encoding this the angular diameter distance  $d_A$  and the luminosity distance  $d_L$ ) or directly  $H(z)$  (for instance with longitudinal baryon acoustic oscillations) assuming the existence of standard candles, rods or clocks. Thus, we can say that background observations can estimate  $D(z)$ , as well as the dimensionless Hubble function  $E(z) \equiv H(z)/H_0$ .

If we combine both, it is possible to estimate the present curvature parameter  $\Omega_{k0}$ . The evolution of the combined matter and dark energy content,  $1 - \Omega_k$ , could be then obtained. In the case of just two components in the fluid, we arrive to the conclusion that the only free parameter is  $\Omega_{m0}$ . In fact, we can write

$$\Omega_x = 1 - \Omega_k - \Omega_m = 1 - \frac{1}{E^2} \left( \Omega_{k0} a^{-2} + \Omega_{m0} a^{-3} \right). \quad (2.40)$$

Summarizing, background observables can reconstruct both  $\Omega_m$  and  $\Omega_x$ , but only up to  $\Omega_{m0}$  [184]. The degeneracy between  $\Omega_x$  and  $\Omega_{m0}$ , could be removed if we assume some parametrized e.o.s. which is usually made in SNIa analysis.

Let us concentrate now on the observables coming from linear perturbations. There are two *sources* that will be considered here and were briefly summarized in the previous chapter, galaxy clustering (large-scale structures) and weak lensing. In the first case we start with the definition of the correlation of galaxy number counts as  $\delta_{\text{gal}}$  which is equivalent

to  $\delta_{\text{gal}} \equiv P_{\text{gal}}^{1/2}(k, z)$  being  $P_{\text{gal}}$  the galaxy power spectrum. The wavenumber  $k$  will be expressed in units of the cosmological horizon,  $k = k_{\text{phys}}/aH$ , and since  $k$  is independent of  $H_0$  if  $k_{\text{phys}}$  is measured in  $h/\text{Mpc}$ , makes  $k$  a time-dependent quantity. As anticipated in [Subsection 1.4.2](#) we truly observe galaxies, not matter perturbations, and thus introduce a bias factor  $b(k, z)$  such that  $\delta_{\text{gal}} = b\delta_{\text{m}}$ . It is useful to define a total density fluctuation  $\delta_{\text{t}} \equiv \Omega_{\text{m}}\delta_{\text{m}} + \Omega_x\delta_x$  built with the contributions from matter and components coming from the dark energy Lagrangian  $\Omega_x\delta_x$ , introducing a similar bias  $B$  we can write

$$\delta_{\text{gal}} = B\delta_{\text{t}} = BZ\Omega_{\text{m}}\delta_{\text{m}}, \quad (2.41)$$

being  $Z(k, a) \equiv 1 + \Omega_x\delta_x/(\Omega_{\text{m}}\delta_{\text{m}})$  a function of space and time depending on the  $x$ -component.

We can define also the initial density fluctuation as  $\delta_{\text{t},\text{in}}^2(k)$  and  $G_{\text{t}}(k, z)$  the scale-dependent growth function of the total perturbation. From the perturbation equations, the velocity field is related to the matter density perturbation as  $\theta_{\text{gal}} = \theta_{\text{m}} = -\delta'_{\text{m}} = -f\delta_{\text{m}}$ , Hence  $\theta_{\text{gal}} = -(f/b)\delta_{\text{gal}}$ , being  $f = G'/G$  the growth rate and  $G(k, z)$  the growth function. Also, this velocity field contributes with RSD, similar to the case of the galaxy clustering power spectrum in redshift space, see eq. (1.110). Thus, the fluctuation in the number counts could be written as [\[80\]](#)

$$\delta_{\text{gal}}(k, z, \mu) = G_{\text{t}}B\sigma_{8,\text{t}} \left(1 + \frac{f}{b}\mu^2\right) \delta_{\text{t},0}(k), \quad (2.42)$$

where  $\sigma_{8,\text{t}}$  is the normalization of the total density spectrum. With  $G_{\text{t}}B = Gb/(Z\Omega_{\text{m}})_0$ , we arrive to the standard expression eq. (1.116)

$$\delta_{\text{gal}}(k, z, \mu) = Gb\sigma_8 \left(1 + \frac{f}{b}\mu^2\right) \delta_{\text{t},0}(k). \quad (2.43)$$

where the normalization  $\sigma_8$  has been written as

$$\sigma_8 = \frac{\sigma_{8,\text{t}}}{(Z\Omega_{\text{m}})_0} = Z_0^{-1} \left( \int Z_0^2 P_{\text{m}0} W^2(k, R_8) dk \right)^{1/2}. \quad (2.44)$$

Now, in [Section 2.3](#) we introduce the parametrizations for modified gravity as extensions of the results from linear perturbations. With a suitable expression for the effective gravitational constant  $Y(k, a)$  the set of parameters  $\{Y, \eta\}$  could be written as [\[147, 180\]](#)

$$Y(k, a) = -\frac{2k^2\Psi}{3\Omega_{\text{m}}\delta_{\text{m}}}, \quad (2.45)$$

$$\eta(k, a) = -\frac{\Phi}{\Psi}. \quad (2.46)$$

We can obtain an expression for the lensing potential in terms of the set  $\{Y, \eta\}$ , also shown in the previous section eq. (2.33)

$$\begin{aligned}
k^2 \Phi_{\text{lens}} &= k^2 (\Psi - \Phi), \\
&= -\frac{3}{2} Y (1 + \eta) \Omega_m \delta_m, \\
&= -\frac{3}{2} Y (1 + \eta) \frac{G_t \sigma_{8,t} \delta_{t,0}}{Z}, \\
&= -\frac{3}{2} \Sigma G \Omega_m \sigma_8 \delta_{t,0},
\end{aligned} \tag{2.47}$$

with<sup>3</sup>  $\Sigma(k, z) \equiv Y(1 + \eta)$ . We can use now another estimator, the ellipticity correlation, which is an integral function of the lensing potential  $\Phi_{\text{lens}}$ , within a window function that depends on the survey geometry. This can be differentiated to obtain:

$$\sigma(k, z) \equiv \frac{2}{3} (k^4 P_{\Phi_{\text{lens}}})^{1/2} = \frac{1}{a^3 E^2} \Omega_{m0} \Sigma G \sigma_8 \delta_{t,0}. \tag{2.48}$$

Thus, we can see that we can measure three quantities: two coming from the galaxy clustering power spectrum  $\delta_{\text{gal}}(k, z, \mu)$  (one related with the amplitude  $A$  and the other one with the RSD contribution  $R$ ), and one from the lensing part  $\sigma(k, z)$ , denoted as  $L$ , and are defined as

$$A = G b \sigma_8 \delta_{t,0}, \tag{2.49a}$$

$$R = G f \sigma_8 \delta_{t,0}, \tag{2.49b}$$

$$L = \Omega_{m0} \Sigma G \sigma_8 \delta_{t,0}. \tag{2.49c}$$

Notice however, that these quantities depends directly on the present power spectrum  $\delta_{t,0}$ , which is unknown without assuming a dark energy model. One simple way to avoid the appearance of this term is to consider ratios of the set of parameters  $A, R, L$ , and derivatives w.r.t. the number of  $e$ -foldings  $N$ . As had been shown in [20] the only independent ratios are

---

<sup>3</sup>Notice that in eq. (2.36) the modified lensing has an additional factor of 1/2, which makes the fiducial unity. In this case, the fiducial value is 2.

$$P_1 \equiv \frac{R}{A} = \frac{f}{b}, \quad (2.50a)$$

$$P_2 \equiv \frac{L}{R} = \frac{\Omega_{m0}\Sigma}{f}, \quad (2.50b)$$

$$P_3 \equiv \frac{R'}{R} = f + \frac{f'}{f}. \quad (2.50c)$$

Additional ratios as  $A/L$  or higher derivatives could be obtained from the previous set. Some of these parameters have been already introduced in the literature, let us summarize them:

- **$P_1$** . This observable was already defined in eq. (1.111) and denoted as  $\beta$  [17]. However, since it depends on the bias  $b$ , which assume an unknown dark energy model, we will not consider it here anymore.
- **$P_2$** . The quantity  $P_2$  has already introduced in [6] denoted as  $E_G$  (up to factor of 2), as a *smoking gun* to test GR. It could be written considering the galaxy-galaxy and galaxy-velocity cross correlations as

$$E_G = \left[ \frac{\nabla^2 \Phi_{\text{lens}}}{3H_0^2 a^{-1} f \delta_m} \right]_{k=\ell/\bar{\chi}, \bar{z}} = \frac{\Omega_{m,0}\Sigma}{2f}, \quad (2.51)$$

being  $\bar{\chi}$  the mean comoving angular diameter distance. From their definition, we see that it does not depend on the bias, neither the initial power spectrum  $\delta_{m,0}$ , but on  $\Omega_{m0}$ , which is not a direct observable.

- **$P_3$** . It contains the quantity  $R$  which as well contains  $Gf\sigma_8$ , also denoted as  $f(z)\sigma_8(z)$  in the literature [185]. It depends on  $\delta_{t,0}$ , and thus is not directly observable. It is important to stress here that in the case of absolute knowledge of  $P_3$ , is not possible to reconstruct  $f$ , since the definition itself contains the derivative  $f'$  unsolved without initial conditions.

We will come back to current observations of these observables, in particular of  $P_2$  and  $P_3$ , in Chapter 3. Henceforth, besides the determination of the Hubble expansion  $E \equiv H/H_0$ , linear observations also can provide the observables  $P_{1-3}$  as functions of time and space. It is mandatory however to use the combination of galaxy clustering and weak lensing information to measure them.

### 2.4.3 The Horndeski Lagrangian: The Quasi-Static Regime

Now we want now to link those model-independent observables with the theory (relying on assumption (e)). As we discussed in Section 2.2, a special case of modifications of

gravity, which includes a single scalar field  $\phi$ , and still gives second-order field equations, is dictated by the Horndeski lagrangian. We want to use now the *quasi-static limit* (hereafter QS) assumed to be valid for the evolution of perturbations. This implies that we are observing scales inside the cosmological horizon,  $k \equiv k_{\text{phys}}/(aH) \gg 1$ , such that terms containing  $k$  dominate over the time-derivative terms. Thus, with this in mind, in the QS limit the expression for the anisotropic stress and the clustering of dark energy could be cast as [147, 186]:

$$\eta = h_2 \left( \frac{1 + k^2 h_4}{1 + k^2 h_5} \right), \quad (2.52)$$

$$Y = h_1 \left( \frac{1 + k^2 h_5}{1 + k^2 h_3} \right). \quad (2.53)$$

being the time-dependent functions  $h_i$  combinations of the proper functions of the Horndeski Lagrangian  $K, G_{3,4,5}$  and derivatives w.r.t. the scalar field  $\phi$  and the kinetic term  $X$ , evaluated at background level. The explicit form of the  $h_i$  functions is presented in the [Appendix B](#) for completeness, since for our further purposes they are not really useful. In the case of the  $\Lambda$ CDM we have  $h_1 = h_2 = 1$  and  $h_3 = h_4 = h_5 = 0$ , thus as we expected  $\eta = Y = 1$ .

We concentrate now on the relation between the perturbation equations and the form of the Horndeski Lagrangian in the QS limit. Some warning before: the perturbation equations listed in [Section 1.3](#) are written in terms of conformal time  $\tau$ , in [20] they used conformal time and the number of e-foldings  $N \equiv \ln a$  as time-variable, in a *interchangeable* way. Here we use also the same notation, keeping in mind that the derivatives may be replaced as

$$\frac{d}{d\tau} \equiv \mathcal{H} \frac{d}{dN}. \quad (2.54)$$

The equation for the matter perturbation can be written as

$$\delta_m'' + \left( 2 + \frac{H'}{H} \right) \delta_m' = -k^2 \Psi = \frac{3}{2} \Omega_m \delta_m h_1 \left( \frac{1 + k^2 h_5}{1 + k^2 h_3} \right), \quad (2.55)$$

if instead we use the growth rate  $f$ , defined in eq. (1.112), which can be written as

$$f = \frac{\delta_m'}{\delta_m}, \quad (2.56)$$

the expression for the matter perturbation eq. (2.55) becomes

$$f' + f^2 + \left(2 + \frac{H'}{H}\right) f = \frac{3}{2} \Omega_m h_1 \left( \frac{1 + k^2 h_5}{1 + k^2 h_3} \right). \quad (2.57)$$

Now, the weak-lensing function  $\Sigma$  introduced eq. (2.36) (again without the additional 1/2 term) reads

$$\Sigma = Y(1 + \eta) = h_6 \left( \frac{1 + k^2 h_7}{1 + k^2 h_3} \right), \quad (2.58)$$

being  $h_6$  and  $h_7$  two new auxiliary functions defined as

$$h_6 = h_1(1 + h_2), \quad (2.59)$$

$$h_7 = \frac{h_5 + h_4 h_2}{1 + h_2}. \quad (2.60)$$

With the observables  $P_i$ ,  $E$  it is possible to write a simple expression for the anisotropic stress  $\eta$ . Notice that from the parameter  $P_2$  we can write the growth as

$$f = \frac{\Omega_{m0}\Sigma}{P_2}, \quad (2.61)$$

and from  $P_3$ :

$$f' = P_3 \frac{\Omega_{m0}\Sigma}{P_2} - \left( \frac{\Omega_{m0}\Sigma}{P_2} \right)^2. \quad (2.62)$$

Inserting this in eq. (2.57), employing eq. (2.58), and doing the algebra explicitly, we have

$$\begin{aligned} P_3 \frac{\Omega_{m0}\Sigma}{P_2} - \left( \frac{\Omega_{m0}\Sigma}{P_2} \right)^2 + \left( \frac{\Omega_{m0}\Sigma}{P_2} \right)^2 + \left( 2 + \frac{H'}{H} \right) \left( \frac{\Omega_{m0}\Sigma}{P_2} \right) &= \frac{3}{2} \Omega_m h_1 \left( \frac{1 + k^2 h_5}{1 + k^2 h_3} \right), \\ P_3 \frac{\Omega_{m0}\Sigma}{P_2} - \left( \frac{\Omega_{m0}\Sigma}{P_2} \right)^2 + \left( \frac{\Omega_{m0}\Sigma}{P_2} \right)^2 + \left( 2 + \frac{H'}{H} \right) \left( \frac{\Omega_{m0}\Sigma}{P_2} \right) &= \frac{3}{2} \Omega_m \frac{\Sigma}{(1 + \eta)}, \\ \frac{\Omega_{m0}\Sigma}{P_2} \left[ P_3 + 2 + \frac{E'}{E} \right] &= \frac{3 \Omega_{m0} (1 + z)^3}{2 E^2} \frac{\Sigma}{(1 + \eta)}, \end{aligned}$$

where we have used that

$$\Omega_m = \frac{\Omega_{m0}(1 + z)^3}{E^2}, \quad (2.63)$$

and  $\frac{H'}{H} \equiv \frac{E'}{E}$ . Hence, finally we arrive to the *master* equation and one of the most important results of [20]:

$$\frac{3P_2(1+z)^3}{2E^2\left(P_3+2+\frac{E'}{E}\right)} - 1 = \eta = h_2 \left( \frac{1+k^2h_4}{1+k^2h_5} \right). \quad (2.64)$$

Notice that the l.h.s. of eq. (2.64) is a function of the model-independent parameters  $P_2, P_3$  and  $E$ , thus giving a model-independent measurement of the anisotropic stress. The form of the r.h.s is determined by the QS limit of the Horndeski Lagrangian. With the help of this equation we can treat  $\eta$  as a kind of *symbiotic entity*, between observations and theory. The expression is powerful, since it allows to exclude dark energy models described by a single scalar field, showing for instance, that the anisotropic stress measured does not follow the particular  $k^2$ -dependence. In fact, eq. (2.64) must be valid at all times and scales. Based on the previous results, this scale-dependence was studied in [187] making measurements at different scales, but fixed redshift in some particular dark energy models. Besides the approximation of single scalar field dark energy models, recently multi-field scalar-tensor models had been studied with also particular interest in the modified gravity parameters  $\{Y, \eta\}$  [188].

In the previous two chapters we settle the basis for our future calculations. We went from basic cosmology, modified gravity theories, and arrive to a simple link between model-independent quantities and theory based in a single-scalar field models. The *dark recipe* is complete and we can move forward to the constraints that future galaxy surveys can imprint in those observables; this will be the main contribution of this thesis.



Part II

Results

## CURRENT CONSTRAINTS ON THE ANISOTROPIC STRESS

*“Dark energy is incredibly strange, but actually it makes sense to me that it went unnoticed, because dark energy has no effect on daily life, or even inside our solar system”.*

*Adam Riess*

In the previous chapter we briefly summarized the ways to study dark energy cosmologies, the approaches are mainly two: in the first one we fix a Lagrangian and study the dynamics of the additional d.o.f., and after we compared the prediction with data. In the second one we try to find general parametrizations of key variables for the dark sector, which allow us to restrict a larger family of modifications. In this chapter, and using the simple expression for the anisotropic stress given by Amendola et. al. [20], we want to obtain the *current* constraints on  $\eta$  using observations of the growth rate  $f(z)\sigma_8(z)$ , the Hubble rate  $H(z)$ , and the quantity  $P_2$  (also denoted, up to a factor of 2, as  $E_G$  in [6, 7]). It is clear that given the current paucity of data, especially from lensing, we expect very weak constraints; however, we think it is a useful exercise to quantify how weak they really are, to identify the progress that it is still to be made in this direction, and to show that, nevertheless, the current and near future data can indeed provide a model-independent measurement of  $\eta$ .

### 3.1 Initial Setup

For our further purposes (specially when dealing with the constraints coming from the Fisher matrix analysis), is useful to define a new set of parameters  $\{\bar{A}, \bar{R}, \bar{L}\}$ , related to

the set  $\{A, R, L\}$  given in eq. (2.49), as

$$\bar{A} \equiv \frac{A}{\delta_{t,0}} = Gb\sigma_8, \quad (3.1a)$$

$$\bar{R} \equiv \frac{R}{\delta_{t,0}} = Gf\sigma_8, \quad (3.1b)$$

$$\bar{L} \equiv \frac{L}{\delta_{t,0}} = \Omega_{m0}\Sigma G\sigma_8. \quad (3.1c)$$

where we explicitly used  $\delta_{t,0} = \delta_{m,0}/\sigma_8$ . Let us consider once again the expression for  $\eta$  based on model-independent observables

$$\eta = \frac{3P_2(1+z)^3}{2E^2\left(P_3 + 2 + \frac{E'}{E}\right)} - 1. \quad (3.2)$$

Later on, when constraining  $\eta$ , we will use an equivalent quantity which we call  $\bar{\eta}$ , defined as

$$\bar{\eta} \equiv \frac{2}{1+\eta} = \frac{2\Psi}{\Psi - \Phi}. \quad (3.3)$$

The reason is that even for large future surveys the expected error on  $P_3$  is substantial, especially when we want to allow for an unknown redshift and scale dependence. This large error makes the division by  $(P_3 + 2 + E'/E)$  in eq. (3.2) badly behaved. The quantity  $\bar{\eta}$  on the other hand is more stable. Explicitly, we have for  $\bar{\eta}$

$$\bar{\eta} = \frac{4E^2\left(P_3 + 2 + \frac{E'}{E}\right)}{3P_2(1+z)^3}. \quad (3.4)$$

We will use also, as a fiducial, a flat  $\Lambda$ CDM, characterized by the WMAP 7-year values,  $\Omega_{m,0}h^2 = 0.134$ ,  $\Omega_{b,0}h^2 = 0.022$ ,  $n_s = 0.96$ ,  $\tau = 0.085$ ,  $h = 0.694$  and  $\Omega_k = 0$ . The dimensionless expansion rate, eq. (1.45), in the fiducial model is given by

$$E^2(z) = \Omega_{m,0}(1+z)^3 + (1 - \Omega_{m,0}), \quad (3.5)$$

and we will often use the dimensionless angular diameter distance, see [Subsection 1.2.3](#),  $\hat{d}_A(z) = \hat{r}(z)/(1+z)$  and the dimensionless luminosity distance  $\hat{d}_L(z) = \hat{r}(z)(1+z)$ , where

in a flat FLRW Universe

$$\hat{r}(z) = \int_0^z \frac{d\tilde{z}}{E(\tilde{z})}. \quad (3.6)$$

which is nothing but the dimensionless comoving distance  $\chi$ , see eq. (1.44). As expected, the usual distances are related to the dimensionless distances through  $\hat{r} = H_0 r$  and  $\hat{d} = H_0 d$ . All numerical calculations on this thesis are performed using the software **MATHEMATICA 9.0** [189].

## 3.2 Current Constraints on $\eta$

In order to have a current constraint on  $\eta$  we need measurements from the different quantities involved on eq. (3.2):

1. Constraints on  $P_2$ : They come from the measurements of the quantity  $E_G$  defined as the ratio between the lensing potential and RSD measured at  $z = 0.32$  [6, 7].
2. Constraints on  $P_3$ : Measurements of  $f\sigma_8$  from RSD (15 observations in the redshift range 0.067 – 0.8 [1]).
3. Constraints on  $E$ : Current measurements of the Hubble parameter (21 observations in the redshift range 0.090 – 1.750 [8], coming from spectroscopic study of luminous red galaxies (LRGs) [9, 10], and early-type galaxies [11]) and supernovae data (Union 2.1 catalog consisting of 580 observations of modulus distance  $\mu$  in the redshift range 0.015 – 1.414 [3]).

Our calculations are strongly restricted by the measurement of  $E_G$ , which consist of a single datum at  $z = 0.32$ . In the next subsection we are going into the details of each contribution.

### 3.2.1 Constraints on $P_2 = 2E_G$

The quantity  $E_G$ , defined as the ratio of the weak gravitational lensing potential and galaxy flows, has been proposed as direct test for gravity at large scales [6, 7]. It could be written considering the galaxy-galaxy and galaxy-velocity cross correlations as

$$E_G = \left[ \frac{\nabla^2(\Psi - \Phi)}{3H_0^2 a^{-1} f \delta_m} \right]_{k=\ell/\bar{\chi}, \bar{z}} = \frac{\Omega_{m,0} \Sigma}{2f}, \quad (3.7)$$

being  $\bar{\chi}$  the mean comoving angular diameter distance. The parameter  $P_2$  is then related to  $E_G$  by eq. (2.50b)

$$P_2 = 2E_G. \quad (3.8)$$

The advantage for analyzing  $E_G$  resides in its insensitivity to galaxy bias  $b$  and to the initial matter power spectrum  $\delta_{m,0}$  [190], implicit on the definition of  $P_2$ . However,  $E_G$

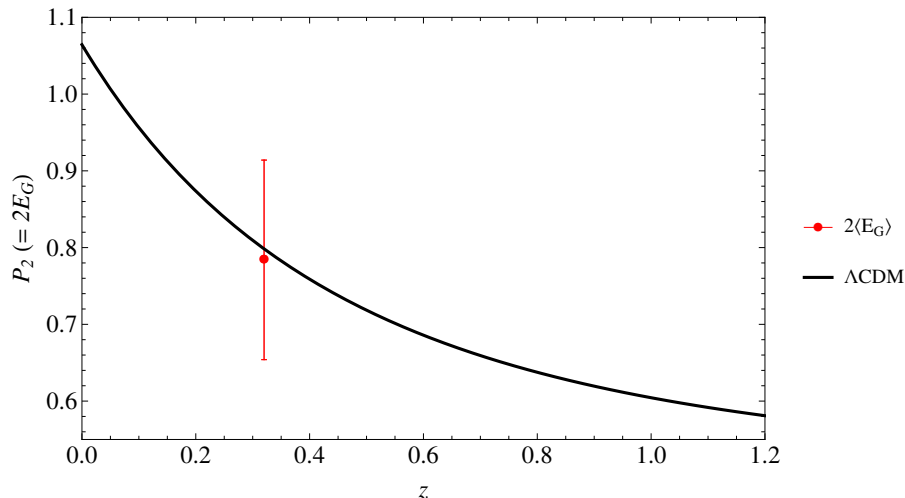


**Figure 3.1:** Constraint on  $P_2 = 2E_G$  at  $z = 0.32$ , from large-scale gravitational lensing, galaxy clustering and structure growth rate [6, 7]. The black line represents the fiducial  $\Lambda$ CDM for  $P_2$ .

alone cannot be employed to test modified gravity (i.e. the functions  $Y, \eta$ ) in a model-independent way, since it depends on the unobservable quantities  $\Omega_{m0}, f$ . It is only in combination with  $P_3$  and  $E$  that a model-independent test of modified gravity becomes possible. Measurements of  $E_G$  comes from large-scale gravitational lensing, galaxy clustering and structure growth rate, specifically, analyzing a sample of 70205 LRGs from the SDSS, giving at  $z = 0.32$  a bound  $\langle E_G \rangle = 0.392 \pm 0.065$ , in agreement with the general relativistic description. Other models, like  $f(R)$  in which  $E_G = \Omega_0 / (1 + f_R) \beta$ , gives a prediction of  $E_G = 0.328 - 0.365$ , and for TeVeS is about  $E_G \simeq 0.22$  [7, 110]. In fig. 3.1 we show the calculated value for  $P_2$  and the  $\Lambda$ CDM prediction.

### 3.2.2 Constraints on $\bar{R} = f\sigma_8$ and $P_3$

Measurements of the growth rate are inferred from peculiar velocities coming from Redshift Space Distortions (RSD). Recent galaxy surveys (WiggleZ, 6dF Galaxy Redshift Survey (6dFGRS), LRG, BOSS and VIPERS) provided constraints on the quantity  $f\sigma_8$  [1], being  $\sigma_8$  the normalization of the power spectrum at scales of  $8h^{-1}$  Mpc.

Furthermore, in order to compare the measurements to predictions from Planck, we have to account for the additional anisotropy introduced by inferring distances from WMAP to Planck parameters. To approximate this Alcock-Paczynski (AP) effect, we thus re-scale

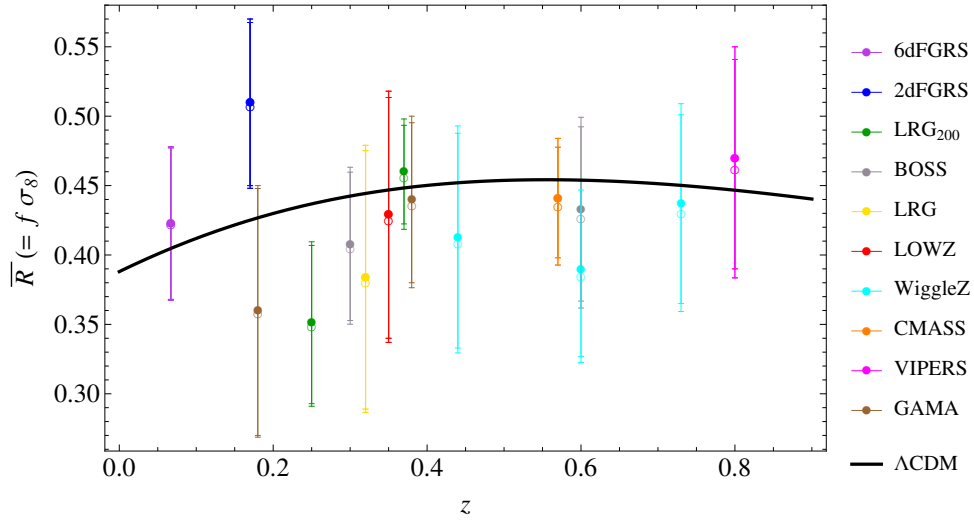


**Figure 3.2:** Observations of  $\bar{R} = f\sigma_8$  from RSD in the redshift range  $0.067 - 0.8$  [1]. The black line represents the fiducial  $\Lambda$ CDM for  $\bar{R}$ . Data with open markers correspond to the original data corrected by the Alcock-Paczynski effect  $F_{\text{AP}}(z)$ .

to growth rate measurements and uncertainties by the ratio

$$F_{\text{AP}}(z) \equiv \frac{H(z)d_A(z)|_{\text{PLANCK}}}{H(z)d_A(z)|_{\text{WMAP}}}, \quad (3.9)$$

being  $d_A$  the angular diametral distance. In fig. 3.2 we show the data from [1] and the fiducial  $\Lambda$ CDM prediction for  $\bar{R}$ .

We define the  $\chi^2$  function as follows:

$$(\chi'_{f\sigma_8})^2 = \sum_{i=1}^{11} \left[ \bar{R}_i - \tilde{R}^{(n)}(z_i) \right] C_{ij}^{-1} \left[ \bar{R}_j - \tilde{R}^{(n)}(z_j) \right], \quad (3.10)$$

being  $\bar{R}_i$  the observational data and  $C_{ij}$  the covariance matrix. The quantity  $\bar{R}$  could be also written as

$$\bar{R}(z) = f(z)G(z)\sigma_8 = \sigma_8 \frac{\delta'}{\delta_0}, \quad (3.11)$$

with  $f(z) = \delta'_m/\delta_m$  the growth rate. We thus will denote the theoretical estimates as  $t_i = \delta'_i/\delta_0$ , and  $\tilde{R}_i = \tilde{R}(z_i) = \sigma_8 t_i$ . Since we do not know the parameter  $\sigma_8$  and cannot use the standard estimates because they have been obtained assuming the standard  $\Lambda$ CDM model, we need to marginalize the likelihood  $L'_{f\sigma_8} = \exp(-(\chi'_{f\sigma_8})^2/2)$  over  $\sigma_8$  between

Survey	$z$	$\bar{R} = f(z)\sigma_8(z)$	Reference
6dFGRS	0.067	$0.423 \pm 0.055$	Beutler et. al. (2012) [173]
2dFGRS	0.17	$0.510 \pm 0.060$	Percival et. a. (2009) [191]
LRG <sub>200</sub>	0.25	$0.351 \pm 0.058$	Samushia et. al. (2012) [192]
	0.37	$0.460 \pm 0.038$	
LRG <sub>60</sub>	0.25	$0.367 \pm 0.060$	Samushia et. al. (2012) [192]
	0.37	$0.403 \pm 0.059$	
BOSS	0.30	$0.408 \pm 0.055$	Tojeiro et al. (2012) [193]
	0.60	$0.433 \pm 0.066$	
WiggleZ	0.44	$0.413 \pm 0.080$	Blake et al. (2012) [172]
	0.60	$0.390 \pm 0.063$	
	0.73	$0.437 \pm 0.072$	
VIPERS	0.8	$0.470 \pm 0.080$	De la Torre et al. (2013) [194]
LRG	0.35	$0.429 \pm 0.089$	Chuang and Wang (2013) [195]
LOWZ	0.32	$0.384 \pm 0.095$	Chuang et al. (2013) [196]
CMASS	0.57	$0.441 \pm 0.043$	Chuang and Wang (2013) [195]
GAMA	0.18	$0.360 \pm 0.090$	Blake et al. (2013) [197]
	0.38	$0.440 \pm 0.060$	

**Table 3.1:** Data for the growth rate  $f\sigma_8$  from RSD [1].

$(0, \infty)$ , such that  $L_{f\sigma_8} = \int d\sigma_8 L'_{f\sigma_8}$ , leading to a new marginalized  $\chi^2$  function:

$$\chi_{\sigma_8}^2 = S_{20} - \frac{S_{11}^2}{S_{02}} + \log S_{02} - 2 \log \left[ 1 + \text{Erf} \left( \frac{S_{11}}{\sqrt{2S_{02}}} \right) \right], \quad (3.12)$$

where the auxiliary quantities  $S_{mn}$  are defined as

$$S_{11} = d_i C_{ij}^{-1} t_j, \quad S_{20} = d_i C_{ij}^{-1} d_j, \quad S_{02} = t_i C_{ij}^{-1} t_j. \quad (3.13)$$

and the standard definition for the ‘‘error function’’

$$\text{Erf}(x) = \frac{2}{\sqrt{\pi}} \int_0^x e^{-t^2} dt. \quad (3.14)$$

In order to derive from the data of  $R$  the derivative  $R'$ , we use a simple polynomial fit for the observational data of  $\bar{R}$ :

$$\tilde{R}^{(n)}(z) \approx \sum_{i=0}^n a_i z^i, \quad (3.15)$$

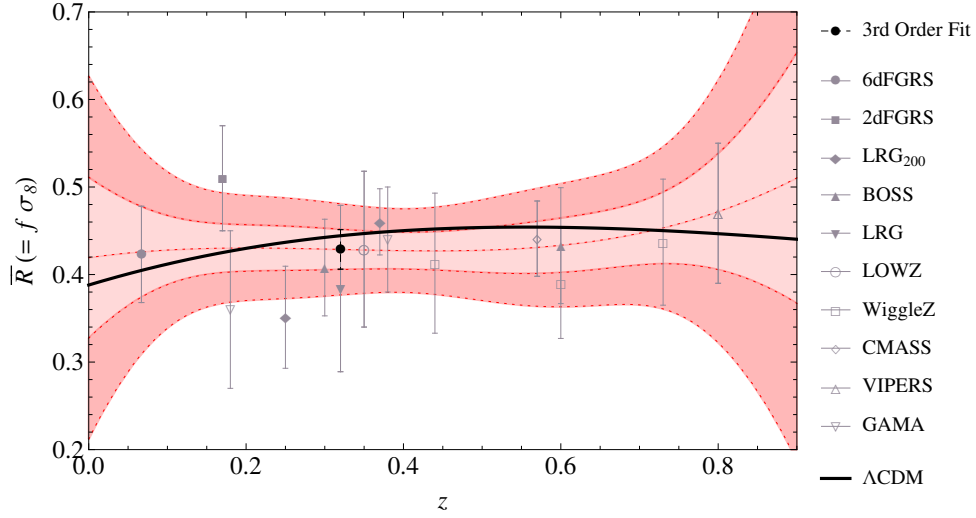


**Figure 3.3:** Third order fit for  $\bar{R}$ ; shadow regions represent the  $1\sigma$  (light) and  $2\sigma$  (dark) level for the fit. The black line represents the fiducial  $\Lambda$ CDM for  $\bar{R}$ .

with the derivative w.r.t. the conformal time given by

$$\bar{R}'^{(n)}(z) = -(1+z) \sum_{i=1}^n a_i (iz^{i-1}), \quad (3.16)$$

The errors in  $\bar{R}$  and  $\bar{R}'$  are obtained from the covariance matrix of the fit parameters  $a_i$  as

$$\sigma_Y^2 = \sum_i \left( \frac{\partial Y}{\partial a_i} \right)^2 \sigma_{a_i}^2 + \sum_{\substack{i,j \\ i \neq j}} \left( \frac{\partial Y}{\partial a_i} \frac{\partial Y}{\partial a_j} \right) \rho_{ij} \sigma_{a_i} \sigma_{a_j}, \quad (3.17)$$

being  $Y = \{\bar{R}, \bar{R}'\}$ ,  $\sigma_{a_i}$  the variances of the parameters and  $\rho_{ij}$  the correlation coefficients between them. In table 3.2 we present the results obtained with a third order fit. This choice is of course arbitrary and the resulting constraint do depend on the order of the polynomial, typically increasing with the order. However, on one side, most cosmological models do have just a few free effective parameters, especially when restricting to a small interval in redshift; on the other, the errors we obtain by using current data are already

$\bar{z}$	$\bar{R}^{(3)}$	$\bar{R}'^{(3)}$
0.32	$0.409 \pm 0.023$	$-0.082 \pm 0.258$

**Table 3.2:** Values of  $\bar{R}$  and  $\bar{R}'$  from  $\chi^2$  minimization with marginalization over  $\sigma_8$ .

very large and there is no point at this stage in making them more robust towards the choice of the underlying model. Finally, we propagate the errors on  $P_3$ , table 3.3.

### 3.2.3 Constraints on $E$ and $E'$

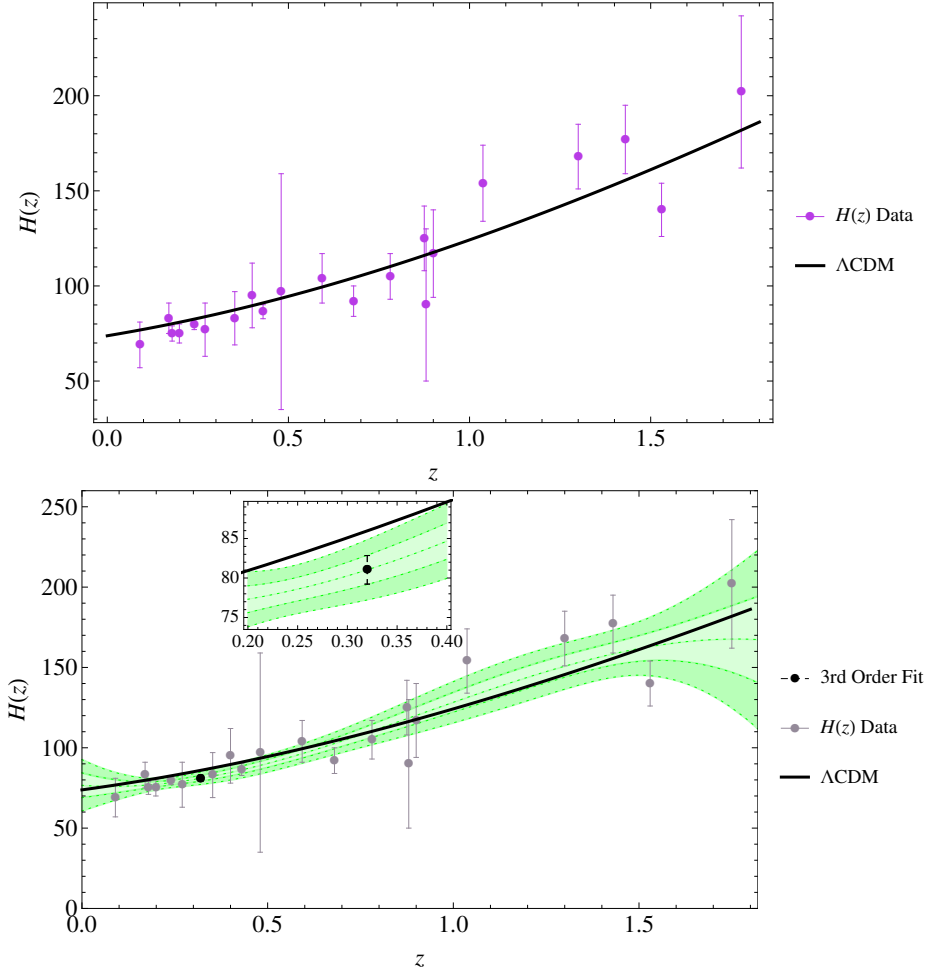


**Figure 3.4:** (Top): Observational data for  $H(z)$  [8], coming from spectroscopic study of luminous red galaxies [9, 10], and early-type galaxies [11], (Bottom): Third order fit to  $H$ , shadow regions represent the  $1\sigma$  (light) and  $2\sigma$  (dark) level for the fit. The black line represent the fiducial  $\Lambda$ CDM for  $H(z)$ .

We can perform a similar analysis as in section 3.2.2 using the compilation of  $H(z)$  data from [8]. As before, we use a simple polynomial fit for the data

$$\tilde{H}^{(n)}(z) \approx \sum_{i=0}^n b_i z^i. \quad (3.18)$$

The derivative w.r.t. the conformal time is given by

$$\bar{H}'^{(n)}(z) = -(1+z) \sum_{i=1}^n b_i (iz^{i-1}), \quad (3.19)$$

and is evaluated at  $z = 0.32$ . The errors in  $\bar{H}$  and  $\bar{H}'$  are obtained from the covariance matrix of the fit parameters  $b_i$  as in eq. (3.17)

$$\sigma_Z^2 = \sum_i \left( \frac{\partial Z}{\partial b_i} \right)^2 \sigma_{b_i}^2 + \sum_{\substack{i,j \\ i \neq j}} \left( \frac{\partial Z}{\partial b_i} \frac{\partial Z}{\partial b_j} \right) \rho_{ij} \sigma_{b_i} \sigma_{b_j}, \quad (3.20)$$

being  $Z = \{\tilde{H}, \tilde{H}'\}$ ,  $\sigma_{b_i}$  the variances of the parameters and  $\rho_{ij}$  the correlation coefficients. In fig. 3.4 we present the results for a third-order fit. Since we actually need  $E$ , not  $H$ , the value of  $H_0$  is immaterial.

We can also obtain constraints on  $E(z)$  by using Union 2.1 SN Ia data. We start considering the likelihood function for the supernovae after marginalization of the offset [16]

$$\mathcal{L} = -\log L = \frac{1}{2} \left( S_2 - \frac{S_1^2}{S_0} \right), \quad (3.21)$$

where

$$S_n = \sum_i \frac{X_i^n}{\sigma_i^2}, \quad (3.22)$$

with  $X_i = m_i - \mu_i$ ,  $\mu_i = 5 \log \hat{d}_L$ , being where  $\hat{d}_L$  is the dimensionless luminosity distance, see Eq. (3.6). We use again a polynomial fit (third order) for the Hubble expansion Eq. (3.18), which allows to write the theoretical form for the distance modulus as

$$\mu_i = 5 \log \left[ \int_0^z \frac{dz'}{\tilde{H}^{(n)}(z')} \right] + 25, \quad (3.23)$$

Thus, we perform a minimization of the likelihood Eq. (3.21) to obtain the set of parameters  $b_i$  that makes the best fit to the observational data of the modulus distance  $\mu_i$ . The results obtained for the ratio  $E'/E$  are presented in table 3.3, which shows a better agreement of the predicted  $\Lambda$ CDM value ( $E'/E = -0.678$ ) with the fit of the  $H(z)$  data. However, due to large data points at low redshift, the error obtained from the SN data are slightly smaller.

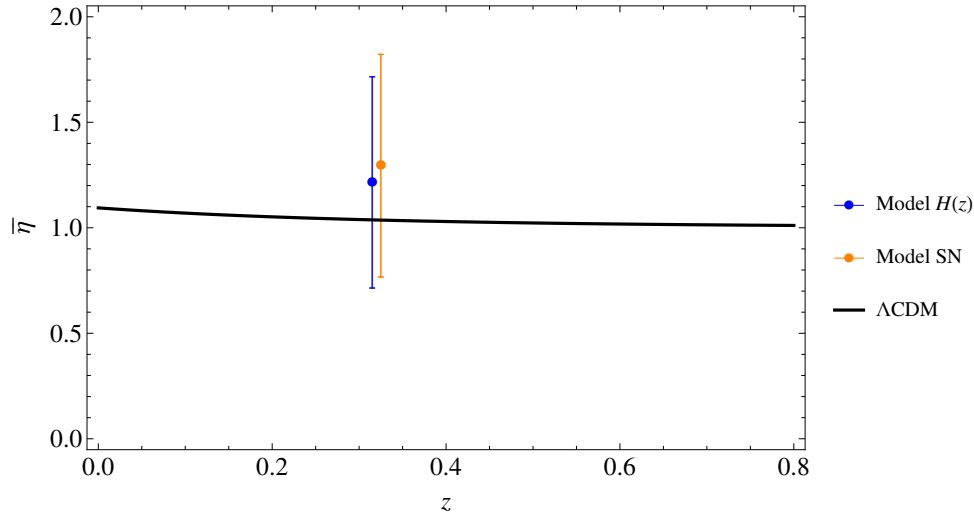


**Figure 3.5:** Observational constraints on  $\bar{\eta}$ . For visualization, we slightly shift the values around  $z = 0.32$ .

### 3.2.4 Constraints on $\eta$

Here we just assume that  $\eta$  and its error could be obtained with error propagation from  $P_2, P_3, E'$ , and  $E$  assuming the data are uncorrelated,

$$\sigma_\eta^2 = \sum_i \left( \frac{\partial \eta}{\partial q_i} \right)^2 \sigma_{q_i}^2, \quad (3.24)$$

with  $q_i = \{P_2, P_3, E, E'\}$ . In table 3.3 we present the estimate for  $\eta$  and its error. In fig. 3.5 we find the respective errors coming from the approaches for calculating the constraints on  $E'/E$ .

Due to the lack of observational data, as we expect, the error on the measure for  $\bar{\eta}$  is quite large (about 60% for  $\bar{\eta}$ ), nevertheless, the mean values are close to unity ( $\Lambda\text{CDM}$  prediction). More observational data, for instance of the parameter  $E_G$  and the growth rate  $f\sigma_8$ , are required to put tight constraints on the scale-independent form of  $\eta$ .

As matter of exercise, we can try to visualize the bounds on  $\eta$  and  $\bar{\eta}$  from the fits, consist

$\bar{z}$	$P_2$	$P_3$	Method	$E'/E$	$\eta$	$\bar{\eta}$
0.32	$0.784 \pm 0.13$	$0.013 \pm 0.470$	Fit on $H(z)$	$-0.651 \pm 0.192$	$0.646 \pm 0.678$	$1.215 \pm 0.500$
			Fit on SN	$-0.724 \pm 0.181$	$0.545 \pm 0.629$	$1.294 \pm 0.527$

**Table 3.3:** Constraints on  $\eta$  and  $\bar{\eta}$ .

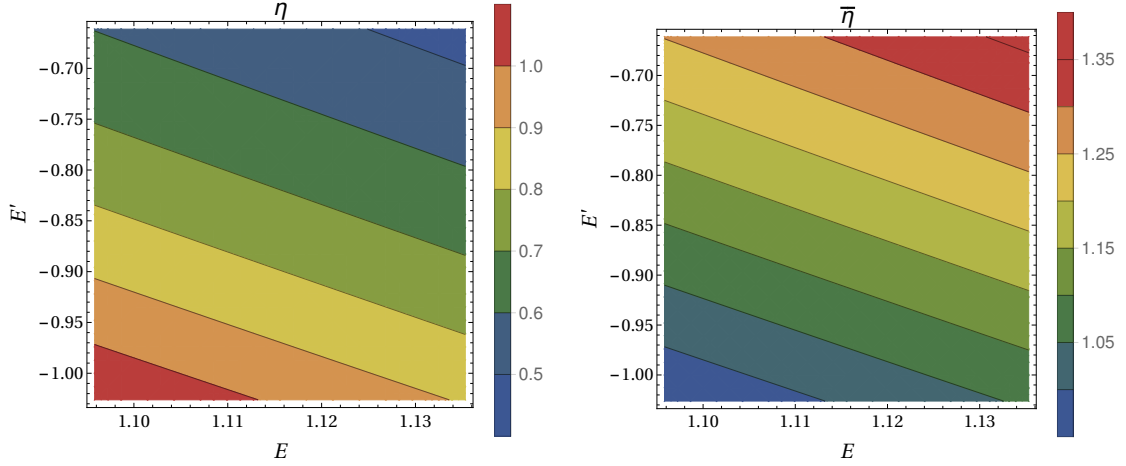


**Figure 3.6:** Contour plots for  $\eta$  and  $\bar{\eta}$  evaluated at the mean of  $P_2$  and  $P_3$  at  $z = 0.32$ .  $E$  and  $E'$  are allowed to vary along their observational bounds (in the case of direct observations of the Hubble expansion  $H(z)$ ). Models like  $f(R)$  gravity who predict an scale-independent value of  $\eta = 1/2$  are inside our constraints.

on fix  $P_2$  and  $P_3$  to the mean values of table 3.3, and allow  $E$  and  $E'$  to vary along their uncertainties, due to the considerable amount of observational data at the moment for the Hubble expansion  $H(z)$  (in comparison of course with the other observables). In fig. 3.6 we shown the contours for  $\eta$  and  $\bar{\eta}$ . Models as  $f(R)$ , which predict a value of  $\eta = 1/2$  ( $k$ -independent) are still inside our current constraints.

### 3.3 Summary and Conclusions

This chapter was devoted to obtain the current observational constraints on the anisotropic stress, based on a model-independent approach. We used observations of the Hubble expansion  $H(z)$ , measurements on  $\bar{R}$  from RSD (which allow us to determine  $P_3$ ), and a single datum of the quantity  $P_2$ , which at the end restrict our calculations to a particular redshift value of  $z = 0.32$ . Even with large uncertainties arising from the lack of observational data, and also for the arbitrary choice in the order of the fits, the values computed for  $\eta$  and the related quantity  $\bar{\eta}$ , are in agreement with the prediction of the  $\Lambda$ CDM model.

We hope that with surveys as the Large Sky Area Multi-Object Fibre Spectroscopic Telescope (LAMOST) and the Square Kilometer Array (SKA) [198], tight constraints on  $E_G$ , and consequently on  $P_2$  will com in the near future. However, is important to emphasize here that by *first* time we are putting constraints on the anisotropic stress in a totally model-independent way, without assuming a particular underlying dark energy model.

---

The next chapter is devoted to alleviate somehow the lack of data on scales, performing a Fisher matrix analysis, and using a key ingredient on our description, relying in the QS form of the Horndeski Lagrangian.



## FUTURE CONSTRAINTS ON THE ANISOTROPIC STRESS

*“Nothing is impossible, not if you can imagine it.  
That’s what being a scientist is all about.”  
Prof. Hubert J. Farnsworth - Futurama*

The current constraints on  $\eta$  obtained in the previous chapter were restricted to a single value at  $z = 0.32$ . Besides the low statistics due to large errors in the model-independent observables, our results agree with the predictions from the  $\Lambda$ CDM model, and also open the possibility to study different approaches, like  $f(R)$  gravity in a scale-independent regime. For this reason, lack of observational data in scales, we want to perform a Fisher matrix analysis to find the constraints that future galaxy surveys (in particular Euclid), will put on our parametrization. In addition, with the expression for the Horndeski Lagrangian in the QS regime, we will be able to alleviate somehow the deficit in  $k$ -dependent current observations. The results of this chapter are based on the joint publication [199].

### 4.1 Fisher Forecast for the Anisotropic Stress

As anticipated, we will use the Fisher matrix formalism in this chapter to forecast the expected precision on  $\bar{A}$ ,  $\bar{R}$  and  $\bar{L}$ , which afterwards will be projected onto the accuracy with which we can obtain  $P_1$ ,  $P_2$  and  $P_3$ , and finally on  $\bar{\eta}$ , based on the expected performance of future large-scale galaxy and weak lensing surveys. In addition, we will also include a supernova survey to improve the constraints on the background expansion rate  $E(z)$ , although we find that its impact on the final constraints on  $\eta$  is rather modest. For the final projection on the anisotropic stress, we will assume four models:

1. First, we assume that  $\eta$  is constant at all scales and at all redshifts. This occurs for instance in  $\Lambda$ CDM and in all models in which dark energy does not cluster and is decoupled from gravity.
2. Second, we assume that  $\eta$  is constant in space but varies in redshift ( $z$ -varying case). In other words, we assume that  $\eta$  has a different arbitrary value for each redshift bin.
3. Third, we assume  $\eta$  varies in both redshift and space ( $z, k$ -varying case).
4. Fourth, we take for  $\eta$  the qQS Horndeski result [20], see [Subsection 2.4.3](#):

$$\eta = h_2 \left( \frac{1 + k^2 h_4}{1 + k^2 h_5} \right). \quad (4.1)$$

(Here we assume  $k$  to be measured in units of  $0.1 h/\text{Mpc}$ , so the  $h_i$  functions are dimensionless). We denote this model as the Horndeski case.

As in the previous chapter, in all cases the fiducial model will be chosen to be flat  $\Lambda$ CDM, for which  $\eta = \bar{\eta} = 1$ . For the first two cases we need only a binning in redshift, while for the third and fourth case we will bin both in redshift and in  $k$ -space. The fiducial values in the first Horndeski case are  $h_2 = 1$ ,  $h_4 = h_5 = 0$ .

In [Subsection 4.1.1](#), [Subsection 4.1.2](#) and [Subsection 4.1.3](#) we set up the Fisher matrix formalism for the galaxy clustering (GC), weak lensing (WL), and SN-Ia observations (SN), respectively. As already mentioned above, we will see that we need to combine the different probes to obtain constraints on  $\eta$ , and we discuss the combination of the Fisher matrices in [Subsection 4.1.4](#)

The initial setup is the same as the used in the previous chapter: a flat  $\Lambda$ CDM characterized by the WMAP 7-year values,  $\Omega_{\text{m},0} h^2 = 0.134$ ,  $\Omega_{\text{b},0} h^2 = 0.022$ ,  $n_s = 0.96$ ,  $\tau = 0.085$ ,  $h = 0.694$  and  $\Omega_k = 0$ . The new WMAP 9-year and Planck results are not very different so the results are not significantly affected by our choice. In the fiducial model, both  $G$  and  $f$  only depend on the scale factor, not on  $k$ . We will combine in the following the Fisher matrices for future galaxy clustering, weak lensing and supernovae surveys. More specifically, we will take for galaxy clustering (GC) and weak lensing (WL) a stage IV kind of survey [200] like Euclid<sup>1</sup> [12]. For supernovae (SN) we assume a survey of  $10^5$  sources with magnitude errors similar to the currently achievable uncertainties, as expected in the LSST survey [201].

---

<sup>1</sup><http://www.euclid-ec.org/>

### 4.1.1 Galaxy Clustering

In this section we deal with the observables  $\bar{A}$  and  $\bar{R}$  coming from galaxy clustering. Using the expression for the galaxy power spectrum eq. (1.116), we can write it using our quantities  $\bar{A}$ ,  $\bar{R}$ , see eq. (3.1), and  $H$ :

$$P(k, \mu) = G^2(z)b^2(z)P_0(k) \left(1 + \beta(z)\mu^2\right)^2 e^{-k^2\mu^2\sigma_r^2}, \quad (4.2)$$

$$\begin{aligned} &= \left(G(z)b(z)\delta_{m,0} + G(z)b(z)\delta_{m,0}\beta(z)\mu^2\right)^2 e^{-k^2\mu^2\sigma_r^2}, \\ &= (A + R\mu^2)^2 e^{-k^2\mu^2\sigma_r^2}, \\ &= (\bar{A} + \bar{R}\mu^2)^2 \delta_{t,0}^2(k) e^{-k^2\mu^2\sigma_r^2}, \end{aligned} \quad (4.3)$$

where in addition we introduced an exponential factor  $\sigma_r = \delta z/H(z)$ ,  $\delta z$  being the absolute error on redshift measurement, and we explicitly use  $P_0^{1/2}(k) = \delta_{m,0} = \sigma_8 \delta_{t,0}$ .

As already emphasized, we will ignore in the following the information contained in  $\delta_{t,0}^2(k)$ , since this depends on initial conditions that are in general not known. This of course will reduce the amount of information available, and increases the error bars.

The dependence on  $E$  is implicitly contained in  $\mu$  and  $k$  through the Alcock-Paczynski effect [83]. However, we can only take into account the  $\mu$  dependence, since the  $k$  dependence occurs through the unknown function  $\delta_{m,0}$ . The Fisher matrix for the parameter vector  $p_\alpha$  is in general [82] (see also Appendix A)

$$F_{\alpha\beta} = \frac{1}{8\pi^2} \int_{-1}^{+1} d\mu \int_{k_{\min}}^{k_{\max}} k^2 \frac{\partial \ln P(k, \mu)}{\partial p_\alpha} \frac{\partial \ln P(k, \mu)}{\partial p_\beta} V_{\text{eff}} dk, \quad (4.4)$$

with

$$V_{\text{eff}} = \left[ \frac{\bar{n}P(k, \mu)}{\bar{n}P(k, \mu) + 1} \right]^2 V_{\text{survey}}, \quad (4.5)$$

is the effective volume of the survey, with  $\bar{n}$  the galaxy number density in each bin. The Fisher matrix is evaluated at the fiducial model. We will use a subscript <sup>GC</sup> to differentiate it from the other contributions, hence we rewrite the Fisher matrix as:

$$F_{\alpha\beta}^{\text{GC}} = \frac{1}{8\pi^2} \int_{-1}^1 d\mu \int_{k_{\min}}^{k_{\max}} k^2 V_{\text{eff}} D_\alpha D_\beta dk, \quad (4.6)$$

where

$$D_\alpha \equiv \left. \frac{d \log P}{dp_\alpha} \right|_r \quad (4.7)$$

is the parameter derivative evaluated on the fiducial values (designated by the subscript ‘ $r$ ’).

For this evaluation we will assume that the bias in  $\Lambda$ CDM is scale independent, and equal to unity, which implies that the barred variables  $\bar{A}$  and  $\bar{R}$  also do not depend on  $k$  in the fiducial model (although of course in general they will be scale dependent).

Our parameters are therefore  $p_\alpha^{\text{GC}} = \{\bar{A}(\bar{z}_1), \bar{R}(\bar{z}_1), E(\bar{z}_1), \bar{A}(\bar{z}_2), \bar{R}(\bar{z}_2), E(\bar{z}_2), \dots\}$ , where the subscripts run over the  $z$  bins. Indices  $\alpha$  or  $\beta$  always label the parameters in the Fisher matrix. From the definition of the galaxy clustering power spectrum, eq. (4.2), we find that<sup>2</sup>

$$D_{\bar{A}} = \frac{2}{\bar{A} + \bar{R}\mu^2}, \quad (4.8)$$

$$D_{\bar{R}} = \frac{2\mu^2}{\bar{A} + \bar{R}\mu^2}, \quad (4.9)$$

and using [16, p. 393]

$$\mu = \frac{H\mu_r}{H_r Q}, \quad (4.10)$$

where

$$Q = \frac{\sqrt{E^2 \hat{d}_A^2 \mu_r^2 - E_r^2 \hat{d}_{Ar}^2 (\mu_r^2 - 1)}}{E_r \hat{d}_A}, \quad (4.11)$$

we get for the derivative with respect to the parameter  $E$

$$D_E = \frac{4\bar{R}\mu^2(1 - \mu^2)}{(\bar{A} + \bar{R}\mu^2)} \left( \frac{1}{E_r} + \frac{1}{\hat{d}_{Ar}} \frac{\partial \hat{d}_A}{\partial E} \right). \quad (4.12)$$

Here we explicitly consider the dependence of the dimensionless angular diameter distance  $\hat{d}_A$  on  $E$  via eq. (3.6).

#### 4.1.1.1 $z$ binning

We consider an Euclid-like survey [12] from  $z = 0.5 - 1.5$  divided in equally spaced bins of width  $\Delta z = 0.2$ , and, in order to prevent accidental degeneracies due to low statistics, a single larger redshift bin between  $z = 1.5 - 2.1$  (thus the number of bins is  $n_B = 6$ ). The

<sup>2</sup>The simplicity of the angular dependence of these expressions and the relative insensitivity of the effective volume, eq. (4.5) to  $\mu$ , mean that the Fisher matrix (4.6) leads to a generic prediction for galaxy clustering surveys. We discuss the results of the generic degeneracy between  $\bar{A}$  and  $\bar{R}$  on Appendix C [202].

lower boundaries of the  $z$ -bins are labeled as  $z_a$  while the center of the bins are labeled as  $\bar{z}_a$  (latin indices  $a, b, \dots$  label the  $z$ -bins). The galaxy number densities in each bin are shown in table 4.1; for the bin between 1.5 and 2.1 we use an average number of  $0.33 \times 10^{-3} (h/\text{Mpc})^3$  [203]. The error on the measured redshift is assumed to be spectroscopic:  $\delta z = 0.001(1+z)$ . The transfer function in the present matter power spectrum ( $\delta_{t,0}^2$ ) is calculated using the Boltzmann code CAMB [77] for the  $\Lambda\text{CDM}$  cosmology. The limits on the integration over  $k$  are taken as  $k_{\min} = 0.007 h/\text{Mpc}$  (but the results are very weakly dependent on this value) and the values of  $k_{\max}$  are chosen to be well below the scale of non-linearity at the redshift of the bin<sup>3</sup>, see table 4.2.

Since the angular diameter distance can be approximated by the expression

$$\hat{d}_A(\bar{z}_a) = \frac{1}{(1+\bar{z}_a)} \sum_{b=0}^{b=a} \frac{\Delta z_b}{E(\bar{z}_b)}, \quad (4.13)$$

we have for the term  $\frac{\partial \hat{d}_A}{\partial E}$  in equation (4.12)

$$\frac{\partial \hat{d}_A(\bar{z}_a)}{\partial E(\bar{z}_b)} = -\frac{\Delta z_b}{(1+\bar{z}_a)E_b^2} \delta_{ab}, \quad (4.14)$$

where  $\delta_{ab}$  is a Kronecker delta symbol. Then we calculate the Fisher matrix block-wise with independent submatrices  $F_{\alpha\beta}^{\text{GC}}$  for each bin.

The errors in the set of parameters  $p_\alpha^{\text{GC}}$  are taken from the square root of the diagonal elements of the inverted Fisher matrix, as explained in Appendix A. In table 4.1 we present the fiducial values for  $\bar{A}$ ,  $\bar{R}$  and  $E$  evaluated at the center of the bins ( $\bar{z}_a$ ), and the respective errors, and in 4.1 we plot their fiducial values and errors.

If we use a redshift dependent bias  $b(z)$  (for instance taking the values from the Euclid specifications, see [12, 13], see fig. 4.2), we get only slight deviations from the errors found for the previous case, as we can see in table 4.1. Thus, our choice of a bias equal to unity does not impact the Fisher errors significantly.

#### 4.1.1.2 $k$ binning

For the third and fourth model we also need a binning in  $k$ -space. Since ultimately we would like to obtain error estimates on three functions,  $h_2, h_4, h_5$ , we will need a minimum of three  $k$ -bins. We denote with latin indices  $a, b, c, \dots$  the  $z$  bins and with indices  $i, j, k, \dots$  the  $k$  bins. So for the first  $z$ -bin we have as parameters  $s_1 = \{\bar{A}_{11}, \bar{R}_{12}, E_1\}$ , for the second  $s_2 = \{\bar{A}_{21}, \bar{R}_{22}, E_2\}$ , and so forth, with  $\bar{A}_{ai} = \bar{A}(\bar{z}_a, \bar{k}_i)$ ,  $\bar{R}_{ai} = \bar{R}(\bar{z}_a, \bar{k}_i)$ , and  $E_a = E(\bar{z}_a)$ , where  $\bar{k}_i$  denote the centers of the  $k$ -bins. The set of parameters is therefore

<sup>3</sup>The values of  $k_{\max}$  are calculated imposing  $\sigma^2(R) = 0.35$ , at the corresponding  $R = \pi/2k$  for each redshift, being  $R$  the radius of spherical cells, see [82], and Subsection 1.3.1.

$\bar{z}$	$\bar{n}(\bar{z}) \times 10^{-3}$	$\bar{A}$	$\Delta\bar{A}$	$\Delta\bar{A}(\%)$	$\bar{R}$	$\Delta\bar{R}$	$\Delta\bar{R}(\%)$	$E$	$\Delta E$	$\Delta E(\%)$
0.6	3.56	0.612	0.0022	0.37	0.469	0.0092	2.0	1.37	0.12	8.5
0.8	2.42	0.558	0.0017	0.3	0.457	0.0068	1.5	1.53	0.073	4.8
1.0	1.81	0.511	0.0015	0.29	0.438	0.0056	1.3	1.72	0.058	3.4
1.2	1.44	0.47	0.0014	0.29	0.417	0.0049	1.2	1.92	0.05	2.6
1.4	0.99	0.434	0.0015	0.35	0.396	0.0047	1.2	2.14	0.051	2.4
1.8	0.33	0.377	0.0018	0.47	0.354	0.0039	1.1	2.62	0.061	2.3

(a)

$\bar{z}$	$\bar{A}$	$\Delta\bar{A}$	$\Delta\bar{A}(\%)$	$\bar{R}$	$\Delta\bar{R}$	$\Delta\bar{R}(\%)$	$E$	$\Delta E$	$\Delta E(\%)$
0.6	0.645	0.0023	0.36	0.469	0.0094	2.	1.37	0.12	8.8
0.8	0.628	0.0018	0.28	0.457	0.0072	1.6	1.53	0.078	5.1
1.0	0.575	0.0015	0.26	0.438	0.0059	1.3	1.72	0.06	3.5
1.2	0.584	0.0014	0.24	0.417	0.0052	1.2	1.92	0.053	2.7
1.4	0.561	0.0015	0.27	0.396	0.005	1.3	2.14	0.053	2.5
1.8	0.561	0.0015	0.26	0.354	0.0038	1.1	2.62	0.056	2.1

(b)

**Table 4.1:** (a) Fiducial values and errors for  $\bar{A}$ ,  $\bar{R}$  and  $E$  using six redshift bins. Units of galaxy number densities are  $(h/\text{Mpc})^3$ . (b) Fiducial values and errors for  $\bar{A}$ ,  $\bar{R}$  and  $E$  using six bins, considering a redshift dependent bias.

$\bar{z}$	$k_{\min}$	$k_1$	$k_2$	$k_{\max}$
0.6	0.007	0.022	0.063	0.180
0.8	0.007	0.023	0.071	0.215
1.0	0.007	0.024	0.078	0.249
1.2	0.007	0.026	0.086	0.287
1.4	0.007	0.027	0.094	0.329
1.8	0.007	0.029	0.112	0.426

**Table 4.2:** Values of  $k_1$ ,  $k_2$  and  $k_{\max}$  for every redshift bin, in units of  $(h/\text{Mpc})$ .

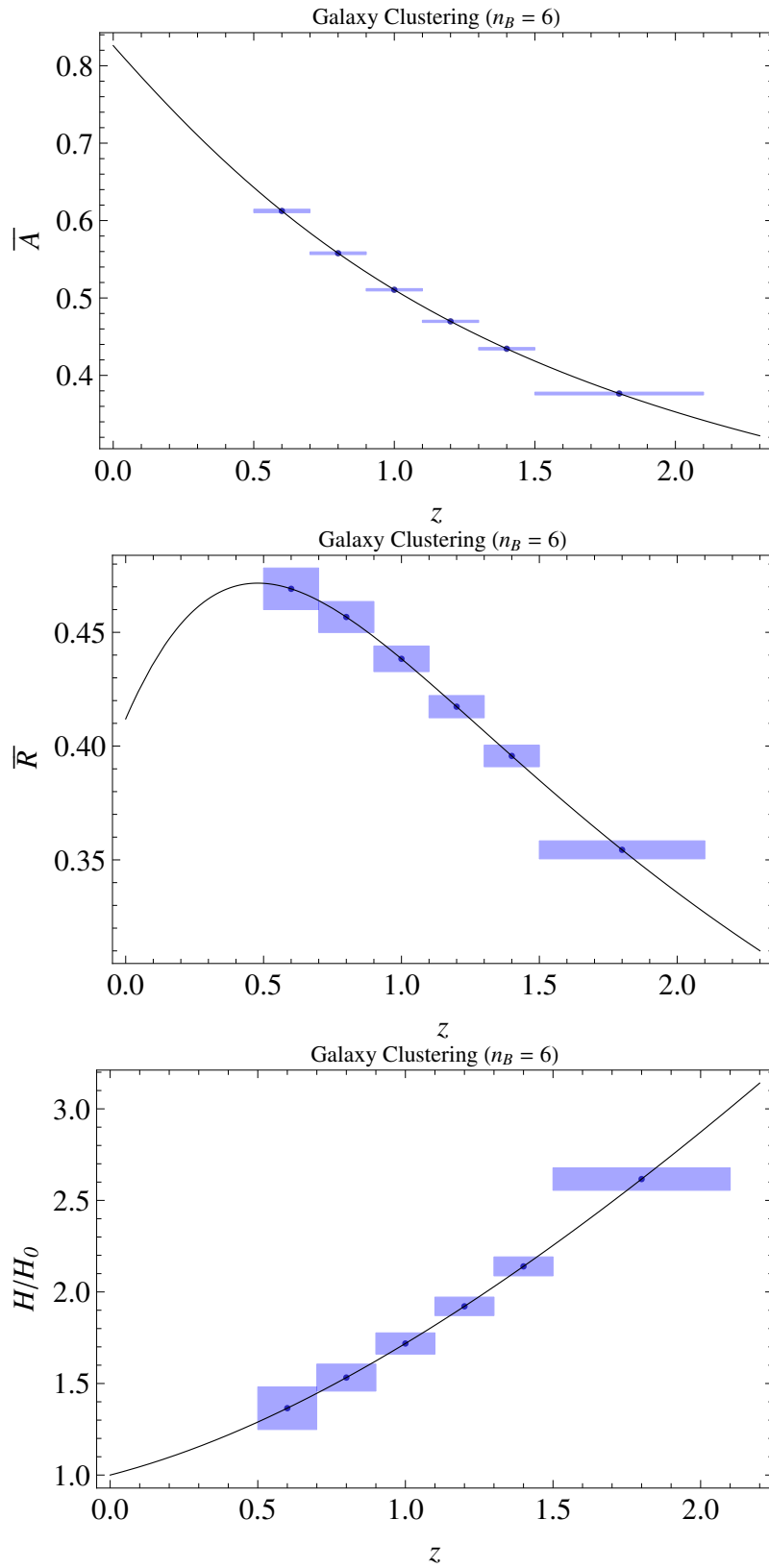


**Figure 4.1:** Errors on  $\bar{A}$ ,  $\bar{R}$  and  $E$  from Galaxy Clustering in the  $z$ -binning case. The black line represents the fiducial  $\Lambda$ CDM model.

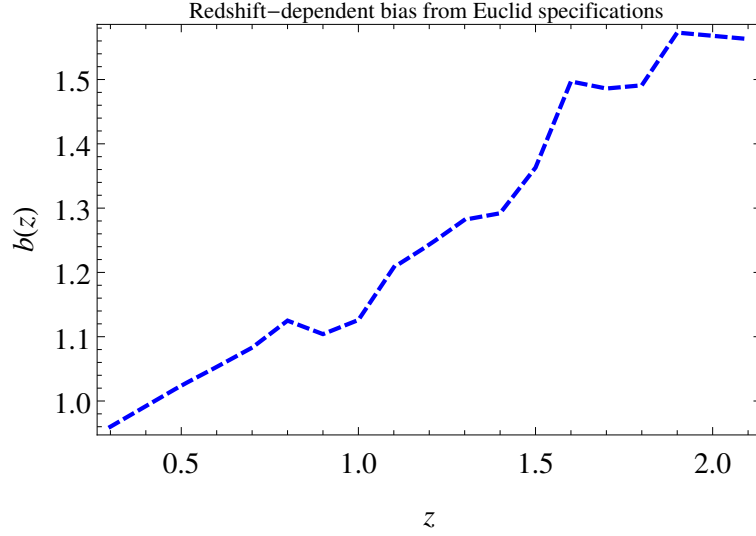


**Figure 4.2:** Redshift-dependent bias  $b(z)$  from Euclid specifications [12, 13].

$p_\alpha^{\text{GC}} = \{s_1, s_2, \dots\}$ . The Fisher matrix integration over  $k$  is split into three  $k$ -ranges between  $k_{\text{max}}$  and  $k_{\text{min}}$  which we choose so that  $\Delta \log k = \text{const.}$  The Fisher matrix becomes

$$F_{\alpha\beta}^{\text{GC}} = \frac{1}{8\pi^2} \int_{-1}^1 d\mu \int_{\Delta k} k^2 V_{\text{eff}} D_\alpha D_\beta dk, \quad (4.15)$$

with  $\Delta k$  representing the respective range of the integration. Denoting the entry  $F_{\bar{A}\bar{R}}$  as  $\bar{A}\bar{R}$ , and so on, we can represent the structure of the matrix for every redshift bin as follows:

$$\begin{pmatrix} \bar{A}_1\bar{A}_1 & \bar{A}_1\bar{R}_1 & 0 & 0 & 0 & 0 & \bar{A}_1E \\ \bar{R}_1\bar{A}_1 & \bar{R}_1\bar{R}_1 & 0 & 0 & 0 & 0 & \bar{R}_1E \\ 0 & 0 & \bar{A}_2\bar{A}_2 & \bar{A}_2\bar{R}_2 & 0 & 0 & \bar{A}_2E \\ 0 & 0 & \bar{R}_2\bar{A}_2 & \bar{R}_2\bar{R}_2 & 0 & 0 & \bar{R}_2E \\ 0 & 0 & 0 & 0 & \bar{A}_3\bar{A}_3 & \bar{A}_3\bar{R}_3 & \bar{A}_3E \\ 0 & 0 & 0 & 0 & \bar{R}_3\bar{A}_3 & \bar{R}_3\bar{R}_3 & \bar{R}_3E \\ E\bar{A}_1 & E\bar{R}_1 & E\bar{A}_2 & E\bar{R}_2 & E\bar{A}_3 & E\bar{R}_3 & EE \end{pmatrix}, \quad (4.16)$$

In table 4.2 we display the values for the integration limits at every redshift (the  $k$ -bins borders), and in table 4.3 we present the errors for all  $(z, k)$ -bins. Notice that the errors on  $E$  are not affected by the  $k$ -binning, as  $E$  does not depend on  $k$ . In fig. 4.3 we shown a representation on the errors for  $\bar{A}$  and  $\bar{R}$ , in the  $(z, k)$ -binning case.

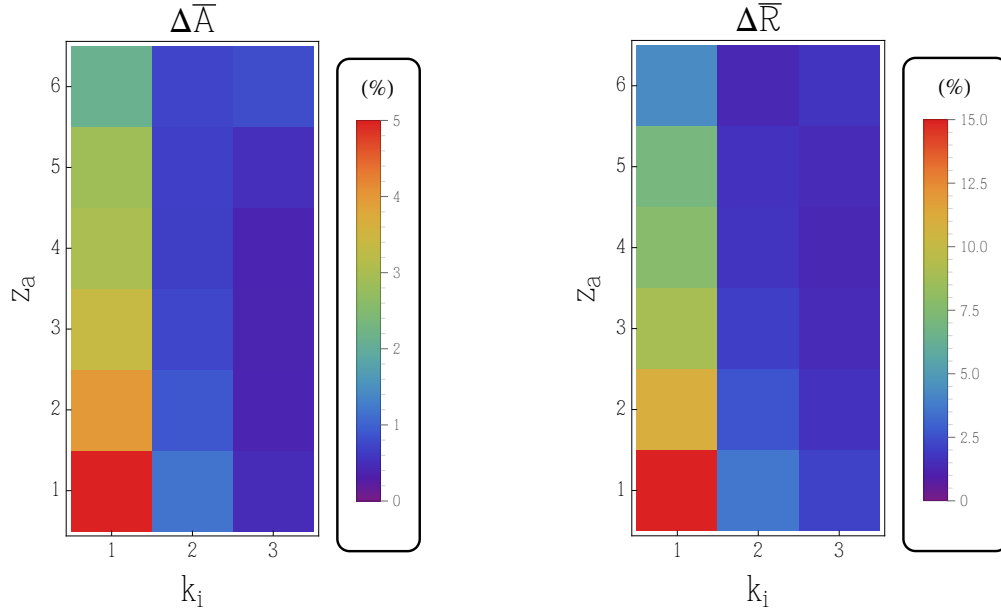


**Figure 4.3:** Graphical representation of the errors on  $\bar{A}$  and  $\bar{R}$  in the  $k$  binning case. The bins are labeled as  $z_a$   $a \in \{1, 6\}$  and  $k_i$  with  $i \in \{1, 3\}$ .

### 4.1.2 Weak Lensing

(This section was made by Adrian Vollmer). Now we consider the Fisher matrix for a future weak lensing survey. We can write lensing convergence power spectrum from a survey divided into several redshift bins (same binning as in [Subsection 4.1.1](#) as [204]

$$P_{ij}(\ell) = H_0 \int_0^\infty p_{ij}(z, \ell) dz \approx H_0 \sum_a \frac{\Delta z_a}{E_a} K_i K_j \bar{L}^2 \delta_{t,0}^2(\bar{z}_a, k(\ell, \bar{z}_a)), \quad (4.17)$$

with the integrand

$$p_{ij}(z, \ell) = \frac{K_i(z) K_j(z)}{E(z)} \bar{L}(z)^2 \delta_{t,0}^2(z, k(\ell, z)), \quad (4.18)$$

where

$$k(\ell, z) = \frac{\ell}{r(z)} \quad \text{and} \quad K_i(z) = \frac{3}{2}(1+z)W_i(z), \quad (4.19)$$

and  $W_i(z)$  is the weak lensing window function for the  $i$ -th bin

$$W_i(z) = H_0 \int_z^\infty \left(1 - \frac{\hat{r}(z)}{\hat{r}(\tilde{z})}\right) n_i(\tilde{z}) d\tilde{z}. \quad (4.20)$$

$\bar{z}$	$i$	$\bar{A}$	$\Delta\bar{A}$	$\Delta\bar{A}(\%)$	$\bar{R}$	$\Delta\bar{R}$	$\Delta\bar{R}(\%)$	$E$	$\Delta E$	$\Delta E(\%)$
0.6	1		0.025	4.		0.07	15.			
	2	0.612	0.0058	0.94	0.469	0.017	3.6	1.37	0.11	8.4
	3		0.0023	0.38		0.0097	2.1			
0.8	1		0.018	3.2		0.05	11			
	2	0.558	0.0039	0.71	0.457	0.012	2.6	1.53	0.074	4.8
	3		0.0018	0.32		0.0074	1.6			
1.0	1		0.014	2.7		0.039	8.9			
	2	0.511	0.003	0.59	0.438	0.0089	2.	1.72	0.058	3.4
	3		0.0016	0.31		0.0062	1.4			
1.2	1		0.011	2.4		0.032	7.7			
	2	0.47	0.0025	0.54	0.417	0.0072	1.7	1.92	0.051	2.6
	3		0.0015	0.32		0.0055	1.3			
1.4	1		0.01	2.3		0.028	7.			
	1	0.434	0.0024	0.55	0.396	0.0065	1.6	2.14	0.052	2.4
	3		0.0018	0.41		0.0057	1.4			
1.8	1		0.0063	1.7		0.015	4.3			
	2	0.377	0.0022	0.58	0.354	0.0047	1.3	2.62	0.059	2.3
	3		0.0024	0.64		0.0061	1.7			

**Table 4.3:** Relative errors for  $\bar{A}$ ,  $\bar{R}$  and  $E$  at every redshift and every  $k$ -bin (labeled with the index  $i$ ). Since fiducial values for  $\bar{A}$ ,  $\bar{R}$  and  $E$  are independent of  $k$ , these are the same for the three  $k$ -bins.

Here,  $n_i(z)$  equals the galaxy density  $n(z)$  if  $z$  lies inside the  $i$ -th redshift bin and zero otherwise. Notice that

$$n_i(z)dz = \frac{n_i(r(z))}{H(z)}dr. \quad (4.21)$$

The overall galaxy density is modeled as

$$n(z) \propto z^a \exp(-(z/z_p)^b). \quad (4.22)$$

We take  $a = 2$ ,  $b = 3/2$  and choose  $z_p$  such that the median of the distribution is at  $z = 0.9$ , i.e.  $z_p = 0.9/1.412 = 0.6374$  [12, 205]. The  $n_i(z)$  (which should not be confused with the  $\bar{n}(z)$  from GC) are then smoothed with a Gaussian, to account for the photometric redshift error (see [205]) and normalized such that  $\int n_i(z)dz = 1$ . Following the Euclid specifications, we set the survey sky fraction  $f_{\text{sky}} = 0.375$  and the photometric redshift error to  $\delta z = 0.05(1 + z)$ .

Including the noise due to intrinsic galaxy ellipticities we have

$$C_{ij} = P_{ij} + \gamma_{\text{int}}^2 \hat{n}_i^{-1} \delta_{ij}, \quad (4.23)$$

with the intrinsic ellipticity  $\gamma_{\text{int}} = 0.22$  and the number of all galaxies per steradian in the

$i$ -th bin,  $\hat{n}_i$ , which can be written as

$$\hat{n}_i = n_\theta \frac{\int_{z_i}^{z_{i+1}} n(z) dz}{\int_0^\infty n(z) dz}, \quad (4.24)$$

where  $n_\theta$  is the areal galaxy density, an important parameter that defines the quality of a weak lensing experiment. We set it to  $n_\theta = 35$  galaxies per square arc minute [12].

For a weak lensing survey that covers a fraction of the sky  $f_{\text{sky}}$ , the Fisher matrix is a sum over  $\ell$  bins of size  $\Delta\ell$  and given by [206]

$$F_{\alpha\beta}^{\text{WL}} = f_{\text{sky}} \sum_{\ell} \Delta\ell \frac{(2\ell + 1)}{2} \frac{\partial P_{ij}}{\partial p_\alpha} C_{jm}^{-1} \frac{\partial P_{mn}}{\partial p_\beta} C_{ni}^{-1}, \quad (4.25)$$

and now the parameters are  $p_\alpha^{\text{GC}} = \{\bar{L}(\bar{z}_1), E(\bar{z}_1), \dots\}$ . Here,  $\ell$  is being summed from 5 to  $\ell_{\text{max}}$  with  $\Delta \log \ell = 0.1$ , where  $\ell_{\text{max}}$  corresponds to the value listed in table 4.4 for the redshift bin  $a$  or  $b$ .

The value  $\ell_{\text{max}}$  is derived as follows. We start with the relationship

$$\frac{\ell}{r(z_{\text{med}}(\ell, a))} = k, \quad (4.26)$$

where  $z_{\text{med}}(\ell, a)$  is the median with respect to  $z$  of  $p_{aa}(z, \ell)$ , which is defined in eq. (4.18). For a given wave number  $k$  and a redshift bin  $a$ , we can solve for  $\ell$ . To find  $\ell_{\text{max}}$  we use the following method:

We begin with  $z_{\text{med}} = 1$ , compute the  $k_{\text{max}}$  for this redshift as before by imposing  $\sigma^2(R) = 0.35$ , solve eq. (4.26) for  $\ell$ , and compute  $z_{\text{med}}(\ell, a)$ . We repeat this step until the value for  $z_{\text{med}}$  converges with an accuracy of approximately 1%. A list of the values for  $\ell_{\text{max}}$  as well as  $z_{\text{med}}$  used in each redshift bin can be found in table 4.4.

To find the derivatives needed in eq. (4.25), we divide the integral in eq. (4.17) into  $n_B$  integrals that each cover one redshift bin. We could assume that  $\bar{L}(z)$  is constant across any redshift bin to get an approximate expression for the integral that depends on  $\bar{L}$  in an analytical way, but the discrepancy between the actual integral and the approximate integral (and consequently the discrepancy of the derivative) can be up to a factor of 2, which may not be sufficient. Assuming that the integrand is linear in  $z$  gives the same result (when using only the center of the bin as the sampling point), so the issue arises when the curvature of the integrand becomes large.

As a solution, we take the actual value of the integral and simply assume that it depends

$\bar{z}$	$\ell_{\max}$	$z_{\text{med}}$	$\bar{L}$	$\Delta\bar{L}$	$\Delta\bar{L}(\%)$	$E$	$\Delta E$	$\Delta E(\%)$
0.6	311	0.26	0.342	0.0044	1.3	1.37	0.0062	0.46
0.8	385	0.31	0.311	0.0044	1.4	1.53	0.0069	0.45
1.0	515	0.40	0.285	0.0059	2.1	1.72	0.017	0.96
1.2	609	0.45	0.262	0.0059	2.3	1.92	0.029	1.5
1.4	760	0.54	0.242	0.014	5.7	2.14	0.029	1.4
1.8	959	0.64	0.210	0.035	16	2.62	0.077	3.0

**Table 4.4:** Errors on  $E$  and  $\bar{L}$  from weak lensing only (with six redshift bins) and a list of the value  $\ell_{\max}$  used at each redshift together with the corresponding  $z_{\text{med}}$  value.

$\bar{z}$	$\ell_0$	$\ell_1$	$\ell_2$	$\ell_3$
0.6	6.3	39	120	410
0.8	7.9	45	190	610
1.0	9.4	66	240	880
1.2	11	83	320	1200
1.4	12	97	390	1500
1.8	14	120	550	2200

**Table 4.5:** Borders of the  $\ell$ -bins for each redshift bin converted from the  $k$ -bins according to (4.26).

quadratically on  $\bar{L}(\bar{z}_a)$ , such that the derivative can be written as

$$\frac{\partial P_{ij}(\ell)}{\partial \bar{L}(\bar{z}_a)} = \frac{2}{\bar{L}(\bar{z}_a)} \int_{z_a}^{z_a+1} p_{ij}(z, \ell) dz. \quad (4.27)$$

Since  $E$  appears in the comoving distance, it is more complicated for the derivatives of  $P_{ij}$  with respect to  $E(\bar{z}_a)$ . We substitute the regular definition of  $E$  by an interpolating function that goes smoothly through all points  $(\bar{z}_a, E(\bar{z}_a))$  and  $(0, 1)$ . Instead of depending on  $\Omega_m$  it now depends on the values of all  $E(\bar{z}_a)$ , and so do all functions that depend on  $E$ , in particular the comoving distance and consequently the window functions  $K_i(z)$ . The derivatives are then obtained by varying the fiducial values of  $E(\bar{z}_a)$  while keeping  $L = \bar{L}\delta_{t,0}$  fixed so that we again do not include the derivative of  $\delta_{t,0}^2$  with respect to  $k$ .

The resulting uncertainties on  $E(\bar{z}_a)$  and  $\bar{L}(\bar{z}_a)$  can be found in table 4.4; they are visualized in fig. 4.4.

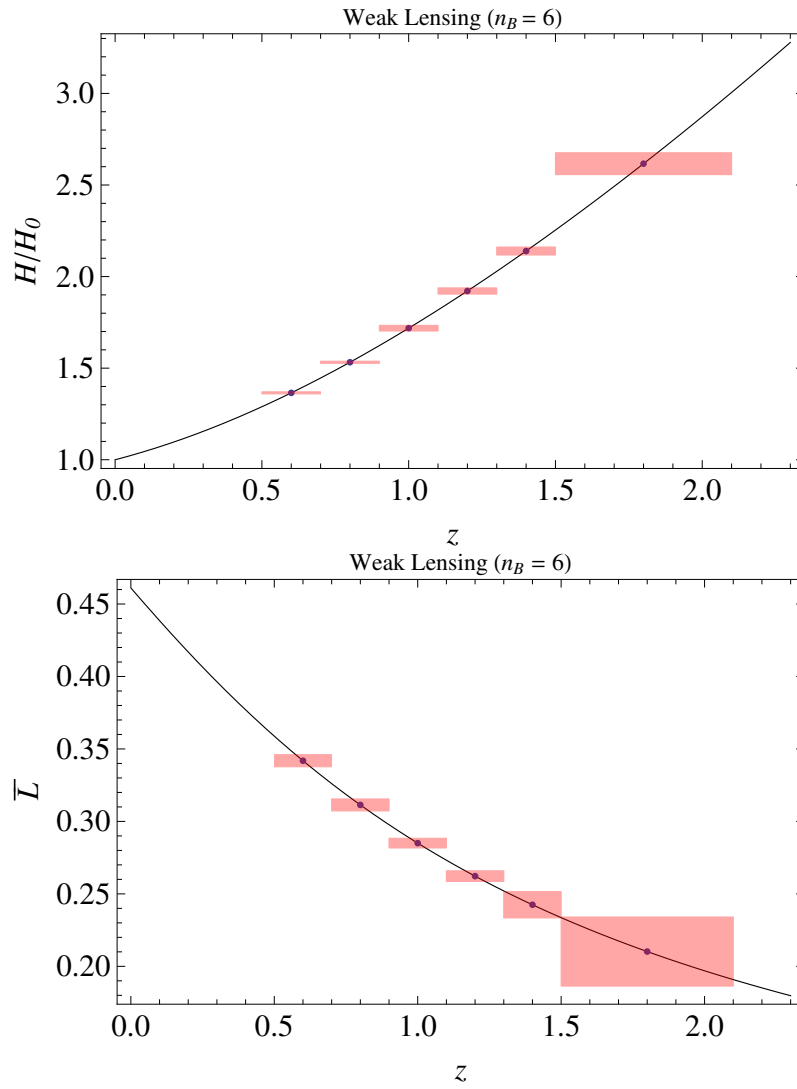


**Figure 4.4:** Errors on  $E(\bar{z}_a)$  and  $\bar{L}(\bar{z}_a)$  from weak lensing. The black line represents the fiducial  $\Lambda$ CDM model. Plots made by Adrian Vollmer.

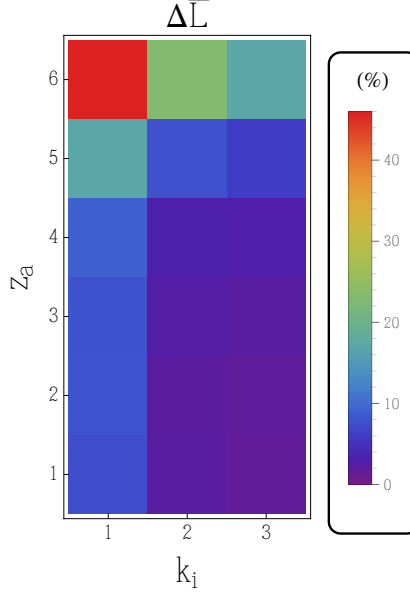


**Figure 4.5:** Graphical representation of the errors on  $\bar{L}$  in the  $k$  binning case, same as fig. 4.5.

#### 4.1.2.1 $k$ binning

As similar as the GC case, we need to consider  $\bar{L}$  as a function of  $k$  (although with the same fiducial value for all  $k$ , as the fiducial model is  $\Lambda$ CDM), and we divide the full  $k$ -range again into the same three bins. The observables are then  $\bar{L}_{an} \equiv \bar{L}(\bar{z}_a, \bar{k}_n)$ , where  $\bar{k}_n$  denote the center of the  $k$ -bins, with  $n = 1, 2, 3$ . They are defined as in [Subsection 4.1.1](#), and are given explicitly in [table 4.2](#). The  $k$ -bins fix the ranges for  $\ell$  via the relation used in [eq. \(4.26\)](#). We label the center of the  $\ell$ -bins accordingly as  $\ell_n$ . See [table 4.5](#) for a list of the  $\ell$ -bins. The derivatives needed for the Fisher matrix will be evaluated at the center of these  $\ell$ -bins.

They can be computed similarly as in [eq. \(4.27\)](#). We find (using Kronecker deltas, no summation):

$$\frac{\partial P_{ij}(\ell)}{\partial \bar{L}(\bar{z}_a, k_n)} = \frac{2\delta_{an}}{\bar{L}(z_a)} \int_{z_a}^{z_{a+1}} p_{ij}(z, \ell) dz \times \begin{cases} 1 & \text{if } \ell_{n-1} < \ell < \ell_n \\ 0 & \text{else.} \end{cases} \quad (4.28)$$

The derivatives with respect to  $E(\bar{z}_a)$  are computed the same way as before. We can then define the parameter vector  $p_\alpha = \{\bar{L}_{11}, E_1, \bar{L}_{12}, E_1, \bar{L}_{13}, E_3, \bar{L}_{21}, E_2, \dots\}$  and evaluate the Fisher matrix formally as before. The structure of the Fisher matrix can be schematically

represented as follows:

$$\begin{pmatrix} \bar{L}_1\bar{L}_1 & 0 & 0 & \bar{L}_1E \\ 0 & \bar{L}_2\bar{L}_2 & 0 & \bar{L}_2E \\ 0 & 0 & \bar{L}_3\bar{L}_3 & \bar{L}_3E \\ \bar{L}_1E & \bar{L}_2E & \bar{L}_3E & EE \end{pmatrix} \quad (4.29)$$

In figure fig. 4.5 we display a graphical representation on the errors for  $\bar{L}$  in the  $k$ -binning case.

### 4.1.3 Supernovae

(This section was made by Simone Fogli). Finally, we consider here the forecasts for a supernovae survey. The likelihood function for the supernovae after marginalization of the offset is [16]

$$\mathcal{L} = -\log L = \frac{1}{2} \left( S_2 - \frac{S_1^2}{S_0} \right), \quad (4.30)$$

where

$$S_n = \sum_i \frac{(m_i - \mu_i)^n}{\sigma_i^2}, \quad (4.31)$$

and  $\mu_i = 5 \log \hat{d}_L$ , where  $\hat{d}_L$  is the dimensionless luminosity distance, see eq. (3.6). This can be written as

$$\mathcal{L} = \frac{1}{2} X_i M_{ij} X_j, \quad (4.32)$$

where  $X_i = m_i - \mu_i$  and

$$M_{ij} = s_i s_j \delta_{ij} - \frac{s_i^2 s_j^2}{S_0}, \quad (4.33)$$

(no sum) where  $s_i = 1/\sigma_i$ . The Fisher matrix can be written as

$$F_{\alpha\beta}^{\text{SN}} = \left\langle \frac{\partial \mathcal{L}}{\partial p_\alpha} \frac{\partial \mathcal{L}}{\partial p_\beta} \right\rangle, \quad (4.34)$$

where now the parameters are  $p_{\alpha_a}^{\text{SN}} = E(\bar{z}_a)$ . Similarly to section Subsection 4.1.1 we can write

$$\hat{d}_L(\bar{z}_a) = (1 + \bar{z}_a) \sum_{b=0}^{b=a} \frac{\Delta z_b}{E(\bar{z}_b)}, \quad (4.35)$$

so that

$$\frac{\partial \hat{d}_L(z_a)}{\partial E(\bar{z}_b)} = -\frac{\Delta z_b}{E_b^2} (1 + z_a) \delta_{ab} \quad (4.36)$$

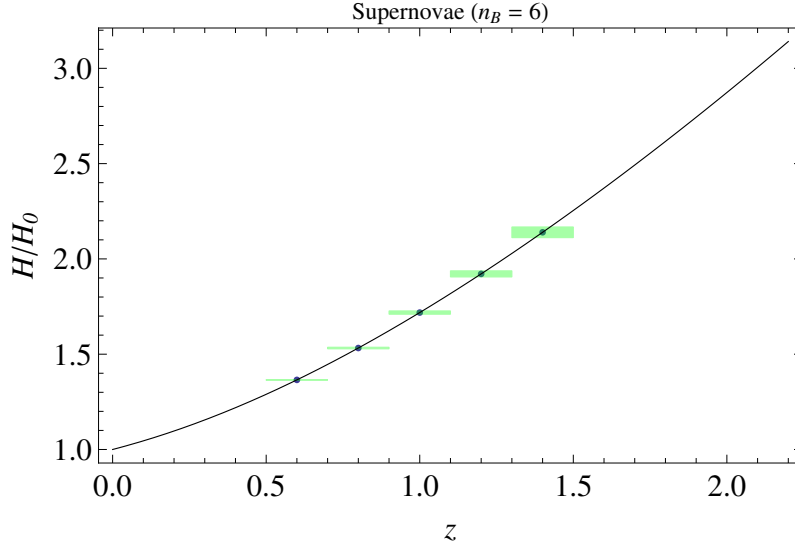


**Figure 4.6:** Errors on  $E$  from Supernovae. The black line represents the fiducial  $\Lambda$ CDM model. Plot made by Simone Fogli.

where  $\delta_{ab}$  is a Kronecker symbol. The Fisher matrix for the parameter vector (which in this case has only one entry) is  $p_\alpha = \{E(z_a)\}$  with  $a$  running over the  $z$ -bins is then

$$F_{\alpha\beta}^{\text{SN}} = \left\langle \left( \frac{\partial \mu_i}{\partial p_{\alpha_a}} M_{ij} X_j \right) \left( \frac{\partial \mu_i}{\partial p_{\beta_b}} M_{ij} X_j \right) \right\rangle = 25 Y_{i\alpha} M_{ij} Y_{j\beta}. \quad (4.37)$$

where

$$Y_{i\alpha} \equiv \frac{\partial \log \hat{d}_L(\bar{z}_i)}{\partial p_\alpha} = \frac{1}{\hat{d}_L(\bar{z}_i)} \frac{\partial \hat{d}_L(\bar{z}_i)}{\partial E(\bar{z}_\alpha)} = -\frac{1}{\hat{d}_L(z_i)} \frac{\Delta \bar{z}_\alpha}{E_\alpha^2} (1 + \bar{z}_i) \delta_{i\alpha}. \quad (4.38)$$

We have to make a choice to define the redshifts  $z_i$  and the uncertainties  $\sigma_i$  for the supernovae of the simulated future experiment. We take the Union 2.1 catalog as a reference (580 SNIa in the range  $0 < z \lesssim 1.5$ ). We assume that the survey will observe supernovae

$\bar{z}$	$\sigma_{\text{data},a}$	$n_a$	$E(\bar{z})$	$\Delta E$	$\Delta E(\%)$
0.6	0.287	46429	1.37	0.0026	0.19
0.8	0.285	25000	1.53	0.0041	0.27
1.0	0.329	16071	1.72	0.0086	0.50
1.2	0.327	7143	1.92	0.016	0.83
1.4	0.258	5357	2.14	0.028	1.3

**Table 4.6:** Redshift uncertainties, number of supernovae, fiducial value of  $E$  and errors for each bin.

$\bar{z}$	$E$	WL		GC		SN		WL+GC		WL+GC+SN	
		$\Delta E$	$\Delta E(\%)$								
0.6	1.37	0.0062	0.46	0.12	8.5	0.0026	0.19	0.0062	0.45	0.0023	0.16
0.8	1.53	0.0069	0.45	0.073	4.8	0.0041	0.27	0.0068	0.44	0.0029	0.19
1.0	1.72	0.017	0.96	0.058	3.4	0.0086	0.50	0.016	0.91	0.0067	0.39
1.2	1.92	0.029	1.5	0.050	2.6	0.016	0.83	0.024	1.2	0.012	0.65
1.4	2.14	0.029	1.4	0.051	2.4	0.028	1.3	0.022	1.0	0.017	0.78
1.8	2.62	0.077	3.0	0.061	2.3	-	-	0.046	1.8	0.043	1.7

**Table 4.7:** Errors on  $E$  from the three probes.

in the redshift range  $0.5 < z < 1.5$ , and divide that interval in bins of fixed width  $\Delta z = 0.2$  just like in Sec. 4.1.1, in order to combine the SN Fisher matrix with the galaxy clustering and the weak lensing ones.

We assume the total number of observed SN to be about  $n_{\text{SN}} = 100000$  in that range, as expected for the LSST survey [201]. We further assume that the supernovae of the future survey will be distributed uniformly in each bin, respecting the proportions of the data of the catalog Union 2.1 and with the same average magnitude error. The values of  $\sigma_{\text{data},a}$  and  $n_a$  for the bins centered in  $\bar{z}_a$  are summarized in table 4.6.

Finally, the corresponding errors on  $E$  from supernovae are shown in fig. 4.6 and in table 4.6. In table 4.7 we compare the errors on  $E$  from the three different probes with each other. We notice that the supernova constraints are the most stringent ones among the three probes and improve the WL+GC constraints by almost a factor of two. All this of course assumes that systematic errors can be kept below statistical errors.

#### 4.1.4 Combining the Matrices

Once we have the three Fisher matrices for galaxy clustering, weak lensing and supernovae, we insert them block-wise into a  $(4n_B) \times (4n_B)$  matrix for the full parameter vector

$$p_\alpha = \{\bar{A}, \bar{R}, \bar{L}, E\} \times n_B, \quad (4.39)$$

Notice that we need also

$$\begin{aligned} \bar{R}' &= -(1+z) \frac{\bar{R}(z+\Delta z) - \bar{R}(z)}{\Delta z}, \\ E' &= -(1+z) \frac{E(z+\Delta z) - E(z)}{\Delta z}. \end{aligned} \quad (4.40)$$

The full schematic structure for every bin will be:

$$\begin{pmatrix} \bar{A}\bar{A} & \bar{A}\bar{R} & 0 & \bar{A}E \\ \bar{A}\bar{R} & \bar{R}\bar{R} & 0 & \bar{R}E \\ 0 & 0 & \bar{L}\bar{L} & \bar{L}E \\ \bar{A}E & \bar{R}E & \bar{L}E & (EE)^\Sigma \end{pmatrix}, \quad (4.41)$$

with  $(EE)^\Sigma = (EE)^{\text{GC}} + (EE)^{\text{WL}} + (EE)^{\text{SN}}$ . This matrix must then be projected onto  $\bar{\eta}$ . It is however interesting to produce two intermediate steps, namely the matrix for  $q_\alpha = \{P_1, P_2, P_3, E\}$  where  $P_1 = \bar{R}/\bar{A}$ ,  $P_2 = \bar{L}/\bar{R}$  and  $P_3 = \bar{R}'/\bar{R}$ , as well as the matrix for  $q_\alpha = \{P_1, P_2, P_3, E'/E\}$ . They are given by

$$F_{\alpha\beta}^{(q)} = F_{\gamma\delta}^{(p)} \frac{\partial p_\gamma}{\partial q_\alpha} \frac{\partial p_\delta}{\partial q_\beta}. \quad (4.42)$$

Notice that as discussed in [Appendix A](#), in order to write the Fisher matrix for other set of parameters, is necessary to find the elements of the transformation, i.e., the elements of the Jacobian. In the first step, for the transformation  $p_\alpha \rightarrow q_\alpha$  these elements yields

$$\frac{\partial P_1}{\partial \bar{A}} = -\frac{R}{A^2}, \quad \frac{\partial P_1}{\partial \bar{R}} = \frac{1}{A}, \quad \frac{\partial P_1}{\partial \bar{L}} = 0, \quad (4.43)$$

$$\frac{\partial P_2}{\partial \bar{A}} = 0, \quad \frac{\partial P_2}{\partial \bar{R}} = -\frac{L}{R^2}, \quad \frac{\partial P_2}{\partial \bar{L}} = \frac{1}{R}, \quad (4.44)$$

$$\frac{\partial P_3}{\partial \bar{A}} = 0, \quad \frac{\partial P_3}{\partial \bar{R}} = -\frac{\bar{R}'}{R^2}, \quad \frac{\partial P_3}{\partial \bar{L}} = 0. \quad (4.45)$$

Similarly, the projection  $q_\alpha \rightarrow s_\alpha$ , with  $s_\alpha = \{P_1, P_2, \bar{\eta}, E\}$  involves explicitly the derivatives of  $\bar{\eta}$  w.r.t.  $P_2, P_3$  and  $E$ :

$$\frac{\partial \bar{\eta}}{\partial P_2} = -\frac{4E^2 \left( P_3 + 2 + \frac{E'}{E} \right)}{3P_2^2(1+z)^3}, \quad (4.46)$$

$$\frac{\partial \bar{\eta}}{\partial P_3} = \frac{4E^2}{3P_2(1+z)^3}, \quad (4.47)$$

$$\frac{\partial \bar{\eta}}{\partial E} = \frac{4}{3P_2(1+z)^3} \left[ 2E \left( P_3 + 2 + \frac{E'}{E} \right) - E' \right], \quad (4.48)$$

The elements of the Jacobian are then evaluated at the fiducial, and later projected via

$$F_{\alpha\beta}^{(s)} = F_{\gamma\delta}^{(q)} \frac{\partial q_\gamma}{\partial s_\alpha} \frac{\partial q_\delta}{\partial s_\beta}. \quad (4.49)$$

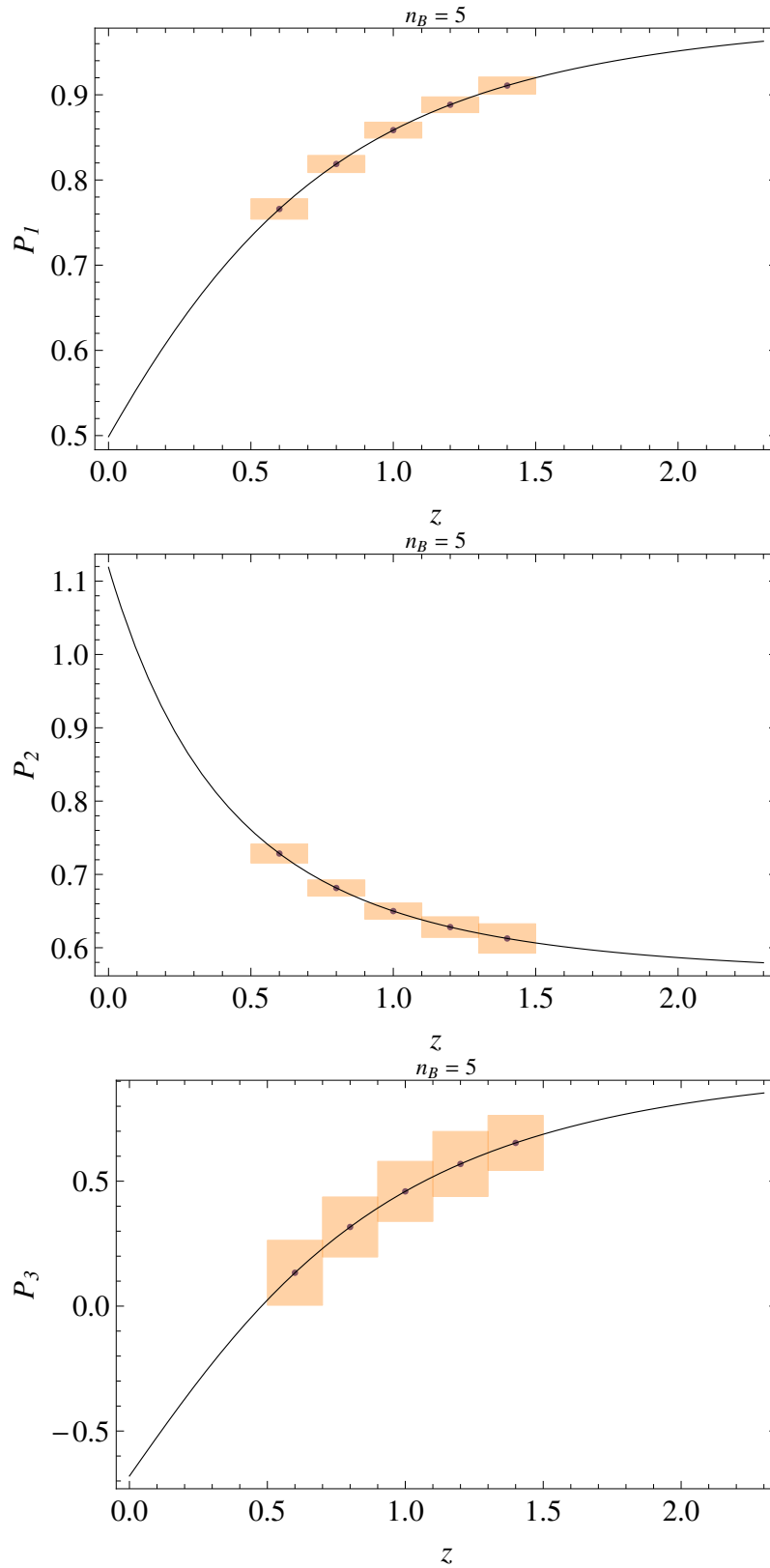


**Figure 4.7:** Errors on  $P_1$ ,  $P_2$  and  $P_3$  in the  $z$ -varying case. The black line represents the fiducial  $\Lambda$ CDM model.

$\bar{z}$	$P_1$	$\Delta P_1$	$\Delta P_1(\%)$	$P_2$	$\Delta P_2$	$\Delta P_2(\%)$	$P_3$	$\Delta P_3$	$\Delta P_3(\%)$	$(E'/E)$	$\Delta E'/E$	$\Delta E'/E(\%)$	$\bar{\eta}$	$\Delta \bar{\eta}$	$\Delta \bar{\eta}(\%)$
0.6	0.766	0.012	1.6	0.729	0.013	1.8	0.134	0.13	99	-0.920	0.022	2.4	1	0.11	11
0.8	0.819	0.010	1.2	0.682	0.011	1.6	0.317	0.12	38	-1.04	0.046	4.4	1	0.091	9.1
1.0	0.859	0.0093	1.1	0.650	0.011	1.7	0.460	0.12	26	-1.13	0.099	8.7	1	0.090	9.0
1.2	0.888	0.0092	1.0	0.628	0.014	2.3	0.569	0.13	23	-1.21	0.12	10	1	0.097	9.7
1.4	0.911	0.010	1.1	0.613	0.020	3.3	0.654	0.11	16	-1.26	0.09	7.1	1	0.073	7.3

**Table 4.8:** Fiducial values and errors for the parameters  $P_1$ ,  $P_2$ ,  $P_3$ ,  $E'/E$  and  $\bar{\eta}$  for every bin. The last bin has been omitted since  $R'$  is not defined there.

$\bar{z}$	$P_1$	$\Delta P_1$	$\Delta P_1(\%)$	$P_2$	$\Delta P_2$	$\Delta P_2(\%)$	$P_3$	$\Delta P_3$	$\Delta P_3(\%)$	$(E'/E)$	$\Delta E'/E$	$\Delta E'/E(\%)$	$\bar{\eta}$	$\Delta \bar{\eta}$	$\Delta \bar{\eta}(\%)$
0.7	0.794	0.0079	0.99	0.703	0.0074	1.0	0.231	0.042	18	-0.983	0.023	2.3	1	0.031	3.1
1.1	0.875	0.0067	0.77	0.638	0.0072	1.1	0.518	0.050	9.7	-1.17	0.044	3.7	1	0.037	3.7
1.5	0.920	0.0099	1.1	0.607	0.010	1.7	0.688	0.048	7.0	-1.29	0.060	4.6	1	0.032	3.2

**Table 4.9:** Same as table 4.8, but with four redshift bins. The last bin has again been omitted.

$\bar{z}$	$P_1$	$\Delta P_1$	$\Delta P_1(\%)$	$P_2$	$\Delta P_2$	$\Delta P_2(\%)$	$P_3$	$\Delta P_3$	$\Delta P_3(\%)$	$\bar{\eta}$	$\Delta \bar{\eta}$	$\Delta \bar{\eta}(\%)$
0.6	0.766	0.14	18	0.729	0.12	17	0.134	1.4	1100	1	1.1	120
		0.032	4.1		0.030	4.1		0.33	240		0.26	26
		0.013	1.7		0.015	2.0		0.15	110		0.12	12
0.8	0.819	0.11	13	0.682	0.092	13	0.317	1.2	380	1	0.93	93
		0.024	2.9		0.021	3.1		0.26	83		0.2	20
		0.011	1.4		0.013	1.9		0.14	43		0.1	10
1.0	0.859	0.093	11	0.65	0.076	12	0.46	1.1	240	1	0.82	82
		0.020	2.3		0.019	2.9		0.23	51		0.17	17
		0.011	1.2		0.012	1.8		0.14	31		0.1	11
1.2	0.888	0.084	9.4	0.628	0.074	12	0.569	1.1	190	1	0.78	78
		0.017	2.0		0.021	3.3		0.23	40		0.16	16
		0.011	1.2		0.017	2.7		0.17	29		0.12	12
1.4	0.911	0.079	8.7	0.613	0.084	14	0.654	0.79	120	1	0.55	55
		0.017	1.9		0.027	4.4		0.17	26		0.12	12
		0.013	1.4		0.023	3.8		0.14	21		0.094	9.4

**Table 4.10:** Here, the errors on  $P_1$ ,  $P_2$ ,  $P_3$  and  $\eta$  are listed for the  $z, k$ -varying case with a similar structure as table 4.3.

In table 4.8 we present the fiducial values for the parameters  $P_1$ ,  $P_2$ ,  $P_3$ ; In fig. 4.7 we plot their fiducial values and errors. Let us call this the basic Fisher matrix.

As we mentioned in the introduction, we decided to consider four models for  $\bar{\eta}$ : constant, variable only in redshift, variable both in space and redshift, and the Horndeski model. For the constant  $\bar{\eta}$  case we project the basic Fisher Matrix for  $P_1, P_2, \bar{\eta}, E$  onto a single constant value for  $\bar{\eta}$ . The resulting uncertainty for  $\bar{\eta}$  is 0.010. For the  $z$ -variable case we project on five  $\bar{\eta}$  parameters, one for each bin. The results are in table 4.8. We see that the error on  $\bar{\eta}$  rises to around 10%. Without the SN data, the final constraints on  $\eta$  would weaken only by roughly 1%. If we collect the data into only three wider  $z$  bins, the error reduces to about 3%.

For the  $z, k$  varying case, we consider the  $k$ -binning of Sec. 4.1.1.2. Now the information is distributed over many more bins, so the errors obviously degrade (see table 4.10). We find errors from 10% to more than 100%.

Finally, for the Horndeski case, table 4.11 gives the absolute errors on  $h_2, h_4$  (measuring  $k$  in units of  $0.1 h/\text{Mpc}$ ). Here we are forced to fix  $h_5$  to its fiducial value (i.e. to zero) due to the degeneracy between  $h_4$  and  $h_4$  when the fiducial model is such that  $h_4 = h_5$ , as in the  $\Lambda\text{CDM}$  case. This means we are only able to measure the difference  $h_4 - h_5$  rather than the two functions separately. The absolute errors on  $h_2, h_4$  are in the range 0.2-0.6. This result implies for instance that, at a scale of  $0.1 h/\text{Mpc}$  and in a redshift bin 0.5-0.7, a Euclid-like mission can detect the presence of a  $k^2$  behavior in  $\eta$  if it is larger than 60% in the  $k$ -independent trend (see fig. 4.8 for a visualization of the constraints on  $\eta$ ).

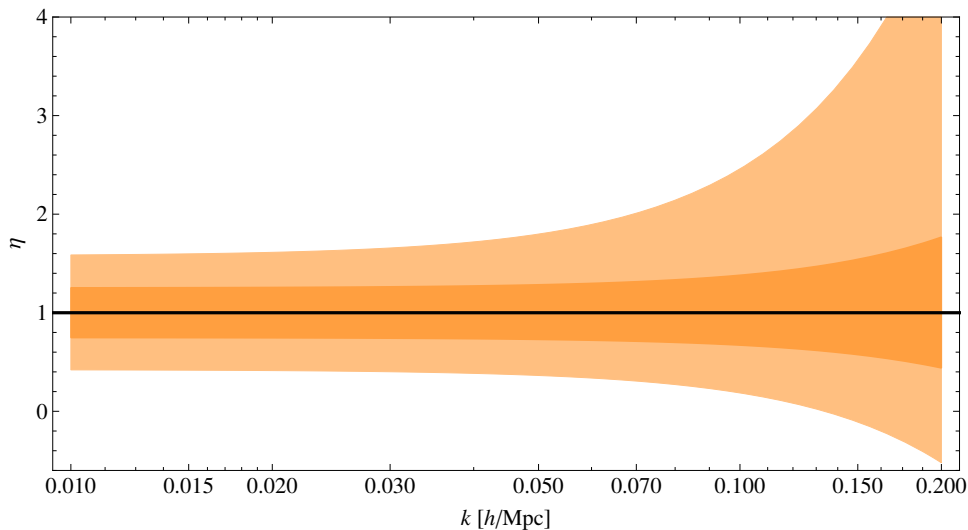


**Figure 4.8:** Constraints on  $\eta(k)$  in the Horndeski case for  $z = 0.6$  (light) and  $z = 1.4$  (dark). The black line represents the fiducial  $\Lambda$ CDM model. Plot made by Adrian Vollmer.

## 4.2 Summary and Conclusions

In this chapter we study the precision in which a future galaxy survey can determine the anisotropic stress in a model-independent way using three probes: galaxy clustering, weak lensing, and supernovae. We found that the expansion rate  $E(z)$  can be determined up to 1% of accuracy in the range  $0.6 \leq z \leq 1.5$ , and up to 4% until a redshift of  $z = 2.0$ . The observables  $P_1$  and  $P_2$  are also constrained with the same precision, until  $z = 1.5$ , in which the errors increase considerable. Due to the appearance of an explicit derivative on  $P_3$  this quantity is less constrained (about 30%). Afterwards we considered four different cases for  $\eta$ . In the first one, in which it is assumed constant, the precision is about 1%. If we assume  $\eta$  varying just in redshift, the errors are around 10% until  $z = 1.5$ .

$\bar{z}$	$\Delta h_2$	$\Delta h_4$
0.6	0.58	0.56
0.8	0.44	0.32
1.	0.37	0.22
1.2	0.35	0.18
1.4	0.25	0.1

**Table 4.11:** Absolute errors on  $h_2$  and  $h_4$ . Because of the degeneracy between  $h_5$  and  $h_4$ ,  $h_5$  has been fixed. The fiducial values are  $h_2 = 1$  and  $h_4 = 0$ .

For the  $(z, k)$ -varying case, the errors can go from 10% until 100%. Finally, in the fourth case, which correspond to the Horndeski, the functions  $h_2$  and  $h_4$  lies in the range 0.2–0.6.

In a posterior work [207], a similar analysis was made using a principal component analysis (PCA), in order also to constraint the set of parameters  $\{Y, \eta\}$  in a general case in which they both varying with scale and redshift. In their parametrizations, the expressions for  $Y$  and  $\eta$  reads:

$$\eta(k, z) = \frac{p_1(z) + p_2(z)k^2}{1 + p_3(z)k^2}, \quad (4.50)$$

$$Y(k, z) = \frac{1 + p_3(a)k^2}{p_4(z) + p_5(a)k^2}, \quad (4.51)$$

thus, in comparison with our parametrization, we have the algebraic relations linking both set of parameters:

$$p_1 \equiv h_2, \quad p_2 \equiv h_2 h_4, \quad p_3 \equiv h_5, \quad h_1 = p_4 \equiv 1, \quad p_5 \equiv h_3. \quad (4.52)$$

Among their results, about 10 eigenmodes coming from the PCA, are constrained with and error smaller than 1%. The degeneracies between the  $p_\alpha$ 's are also presented in their calculations. In our case however, the practical reduction in the number of time-dependent functions made the analysis simpler.



## A COSMOLOGICAL EXCLUSION PLOT

*“You underestimate the power of the Dark Side”  
Darth Vader - Star Wars: Episode VI - Return of the Jedi (1983)*

In this short chapter, we want to show some preliminary results consisting in determine the region of parameter space in  $\eta$ , that can be *excluded* by a future survey, that approximates the performance of the Euclid satellite [12, 203]. This cosmological exclusion plot is an analog of the gravity exclusion plots that can be derived with laboratory experiments, as in e.g. [14, 208]. We will use again the expression coming from the QS regime on the Horndeski Lagrangian

Current data are clearly too limited to give interesting constraints on  $\eta$ . In particular, they give no constraints on its scale dependence, since the data do not retain any scale information. Future data, however, promise to be so rich, in comparison with present ones, that they can be binned both in redshift and in scale. In this way one can put constraints also on the three time-dependent functions  $h_{2,4,5}$  that characterize the Horndeski form eq. (4.1). In the previous chapter the constraints on  $\eta$  were obtained by fixing  $h_5$  to its  $\Lambda$ CDM fiducial value, i.e. zero. It is not possible in fact to obtain meaningful constraints on all three functions since  $h_4, h_5$  are fully degenerate for large  $k$ . Here we wish to continue that analysis by obtaining an exclusion plot, i.e. the region of parameter space that a future, Euclid-like, survey, can achieve. This is obtained by repeating the procedure of [199] obtaining the errors on  $h_2, h_4$  for every possible  $h_5$ . The region outside the errors is therefore the region that an Euclid-like experiment will be able to rule out. A similar analysis was performed in [209] to obtain a exclusion plot for the clustering of dark energy  $Y$ .

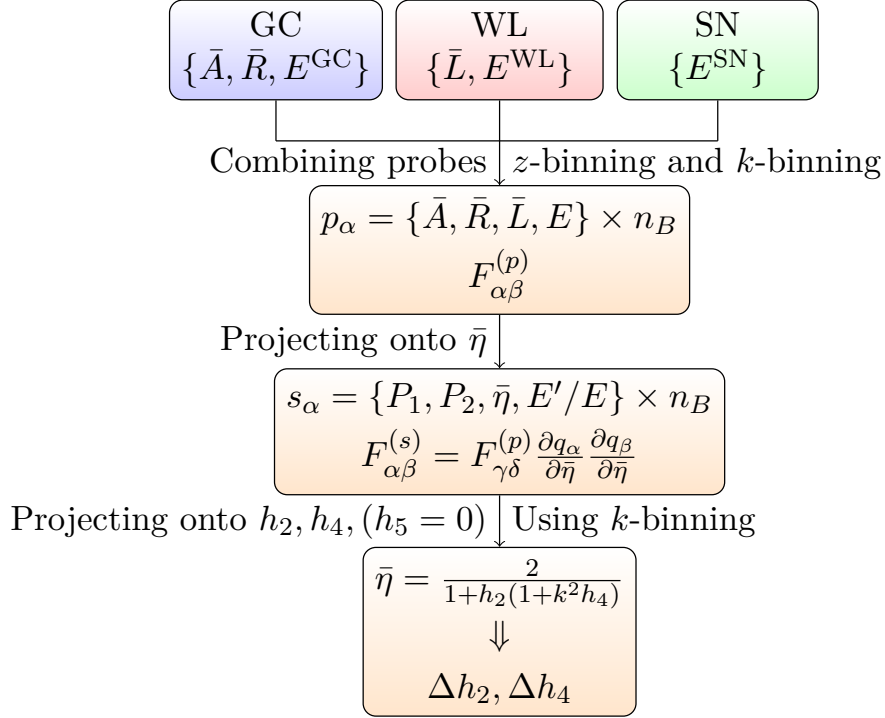


**Figure 5.1:** Fisher analysis scheme for the anisotropic stress.

Additional to the exclusion plot that can be obtained from the errors on  $h_2, h_4$  varying  $h_5$ , we will assume that the anisotropic could represent a Yukawa-like potential. Thus, instead of  $h_{2,4,5}$ , it turns out to be more convenient to use the strength  $Q$  and range  $\lambda$  on a Yukawa term by identifying  $h_4 = (1 + Q)\lambda^2$  and  $h_5 = \lambda^2$  in the term for the gravitational slip in the Horndeski parametrization eq. (4.1). The idea behind is that, at linear level, the Horndeski model induces a Yukawa like-potential which could be written in real space as [16]

$$\Psi(r) = -\frac{GM}{r} \left(1 + Qe^{-r/\lambda}\right), \quad (5.1)$$

representing the correction to the standard Newtonian potential. In Chapter 4 we discuss in detail the Fisher procedure to obtain the constraints in the anisotropic stress  $\eta$ . As matter of visualization, in fig. 5.1 we make a schematic diagram used here to determine the exclusion plot for a Yukawa-like potential, involving the  $h$ 's functions.

## 5.1 Exclusion Plot in the Plane $(\lambda, \Delta Q)$

In order to find the constraints on the strength  $Q$ , we project the Fisher matrix for  $\bar{\eta}(k, z)$  onto the parameter space spanned by  $h_2$  and  $Q$  while fixing  $\lambda$  to a specific value, assuming

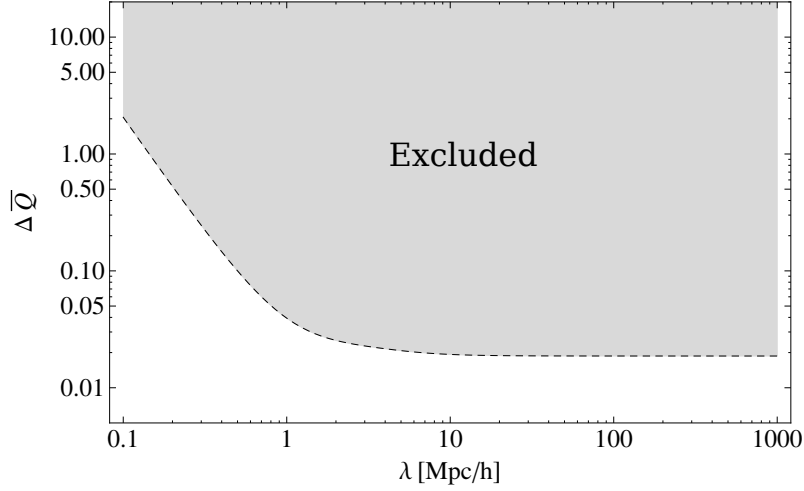


**Figure 5.2:**  $\Delta \bar{Q}$  as a function of  $\lambda$ . The colored region can be excluded by a Euclid-like survey at the  $1\sigma$  level. The curve approaches  $\Delta \bar{Q} \approx 0.021$  for large  $\lambda$ . Plot made by Adrian Vollmer.

that  $\bar{\eta}$  does not depend on  $z$ . This way, we can obtain the uncertainty on  $Q$ , which we call  $\Delta Q$ , as a function of  $\lambda$ . However, in the limit  $\lambda \rightarrow \infty$ , the expression for  $\eta$  becomes

$$\eta = h_2(1 + Q), \quad (5.2)$$

which is degenerate in  $h_2$  and  $Q$ , which means that the uncertainty on  $Q$  diverges for large  $\lambda$ . Thus, we switch from  $Q$  to a slightly different parameter,

$$\bar{Q} \equiv h_2(1 + Q). \quad (5.3)$$

This enables us to plot the region in the  $\bar{Q}$ - $\lambda$  parameter space which can be excluded by a survey like Euclid (see fig. 5.2). The derivatives needed for the projection read

$$\frac{\partial \bar{\eta}}{\partial h_2} = - \frac{2}{(k^2 \lambda^2 + 1) \left( \frac{h_2 + k^2 \lambda^2 \bar{Q}}{k^2 \lambda^2 + 1} + 1 \right)^2}, \quad (5.4)$$

$$\frac{\partial \bar{\eta}}{\partial \bar{Q}} = - \frac{2k^2 \lambda^2}{(k^2 \lambda^2 + 1) \left( \frac{h_2 + k^2 \lambda^2 \bar{Q}}{k^2 \lambda^2 + 1} + 1 \right)^2}. \quad (5.5)$$

They are evaluated at the center of all three  $k$ -bins for each of the five  $z$ -bins and arranged in a  $2 \times 15$  transformation matrix to obtain the Fisher matrix for  $h_2$  and  $\bar{Q}$ .

As matter of comparison, in fig. 5.3 we display a exclusion plot obtained with the aim to test the validity of the equivalence principle. For that purpose, as similar to the approach of [209], the Yukawa interaction had been determined.

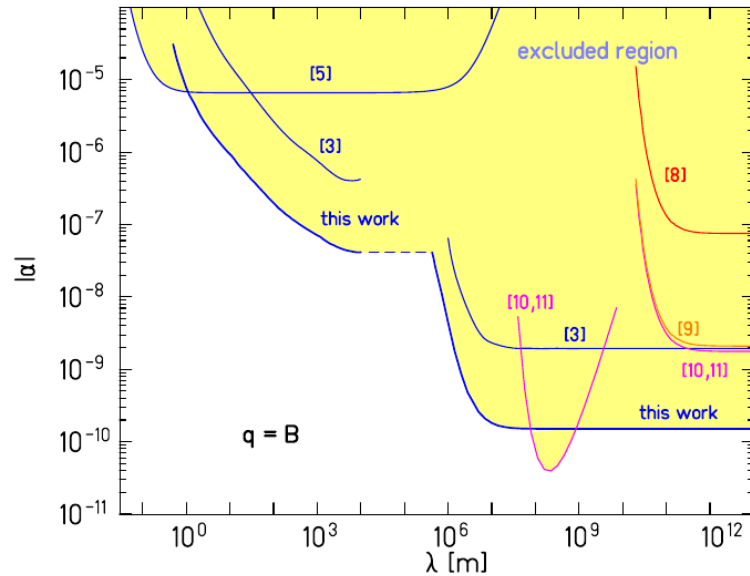


**Figure 5.3:** Testing the equivalence principle with a torsion balance. The plot shows the upper limits for the Yukawa interactions coupled to baryon number with 95% confidence. The shaded region is experimentally excluded. Figure taken from [14]

## 5.2 Exclusion Plot in the Planes $(h_4, h_2)$ and $(h_5, h_2)$

We can obtain two exclusion plots starting from the Fisher matrix for  $\bar{\eta}$ . The first one consist in fix the value of  $h_4$ , and then find the corresponding errors on  $h_2$  (since in the fiducial  $h_2 = 0$ , we still denote the error as  $h_2$ ) for every possible value of  $h_5$ . The second one, in a similar way, could be constructed fixing  $h_5$  and find  $h_2$  as function of  $h_4$ . The results are shown in fig. 5.4.

These plots allow us to rule-out modified gravity models by following the evolution of the time-dependent functions  $h_2$ ,  $h_5$  and  $h_6$ . This could be done using the expressions for the  $\alpha$  functions listed in table 1 of ref. [156]. This work is still in progress [210]; in addition, for the specific case of  $f(R)$  gravity, with an explicit evolution of perturbations equations, we plan to construct exclusion plots with the aim to constraint particular choices of the function  $f(R)$ .

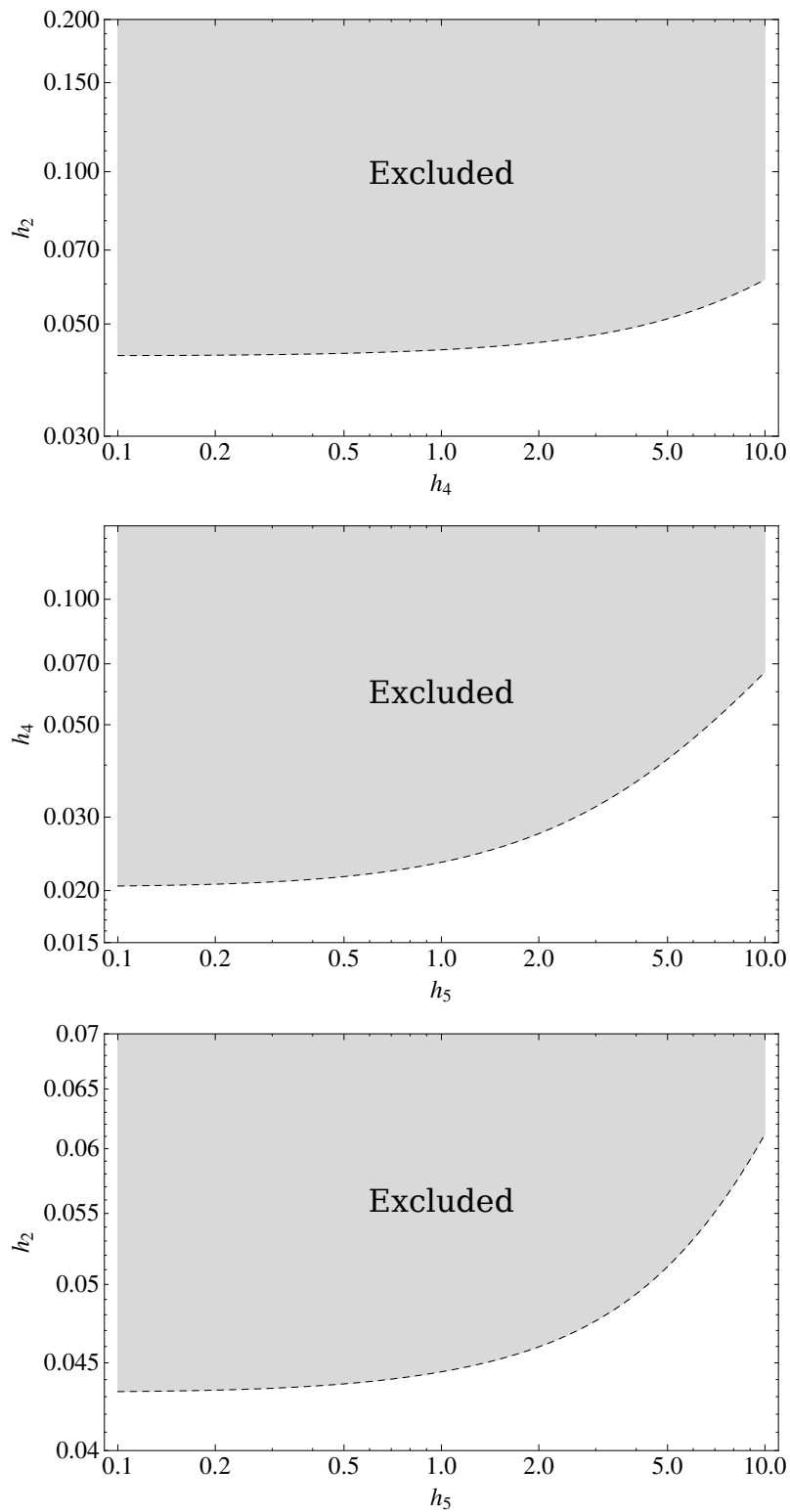


**Figure 5.4:** Exclusion plots for the set of functions  $\{h_2, h_4, h_5\}$ .  $h_2$  as a function of  $h_4$  (top),  $h_4$  as a function of  $h_5$  (mid), and  $h_2$  as a function of  $h_5$  (bottom). The colored region can be excluded by a Euclid-like survey at the  $1\sigma$  level. Plots made by Adrian Vollmer.



## CONCLUSIONS AND OUTLOOK

Dark Energy, the mysterious entity which is responsible for the current acceleration of the Universe is, without a doubt, the most important unsolved problem in physics today. The  $\Lambda$ CDM model, elegantly simple, and supported by various probes, relies, however on the introduction of the cosmological constant, which presents issues when compared to a quantum description of the vacuum energy density. The cosmological model resides in the beautiful mathematical structure of General Relativity (GR), which has been tested with high accuracy (at solar system level), and is among all physical theories the most *perfect*. Nevertheless, its non-renormalizable character suggests that it cannot be valid up to Planck scales; in addition, it becomes unpredictable when singularities such as black holes and the Big Bang arise.

These issues, however, open a window into a fascinating world of alternative approaches: from modifications of GR (including extra degrees of freedom and extra dimensions) to exotic matter contents, these are just a few examples of the vast family of possibilities. Modifying gravity offers an exciting opportunity. Just after the genesis of GR, modifications at the action level, including scalars other than the Ricci scalar, had been considered; at the time, those alternatives arised mainly from the mathematical richness offered by differential geometry, the pilar supporting any gravitational description. After the amazing development of quantum theory, GR acquire a status of non-quantizable theory, this provided an additional plus for those theories. Recently, with the discovery of the cosmic speed-up, modifying gravity seems to be a plausible solution. However, the more you modify, the more you pay: instabilities arising from higher order derivatives, failures to describe Solar system constraints and actual large-scale structure data, makes it *counter-productive* to play with the Lagrangians.

When modeling dark energy cosmologies, it is desirable to have a minimal number of additional free parameters, since this makes a confrontation with observations more suitable.

Popular phenomenological descriptions encoring the effect of modifications of gravity have been proposed. In contrast to the standard procedure of fixing a Lagrangian, studying its dynamics and comparing it with observations, those parametrizations can be tested with minimal assumptions at background and linear perturbation levels. A popular example includes the clustering of dark energy or effective gravitational constant  $Y$ , and the anisotropic stress or gravitational slip  $\eta$ , as core. These quantities provide a powerful tool to constrain deviations from GR. On the other hand, the study of a particular Lagrangian, the so-called Horndeski Lagrangian, had recently attracted considerable attention, since it encodes a large family of modifications with a single scalar field, demanding second-order derivatives in the field equations. In the quasi-static regime, the linear perturbation equations lead to compact expression for  $\{Y, \eta\}$  making explicit the time and scale dependence.

Here, a simple question emerges: are cosmological observables really “observables”? Specifically, having an ideal case of observations at background and perturbation level in a range of redshifts and scales, which quantities are truly independent of the underlying dark energy model? This query was beautifully answered by [20], showing that the only model-independent observable is the anisotropic stress  $\eta$ . Furthermore, an easy expression which links theory (the Horndeski lagrangian) with model-independent quantities, was obtained.

This thesis was devoted to obtaining the future and current constraints on the cosmological anisotropic stress, using a model-independent approach. Coming from this angle, and using current data for the growth rate  $f\sigma_8$  taken from Redshift Space Distortion (RSD) measurements, observations of the Hubble expansion  $H(z)$ , and a constraint for the quantity  $P_2$  defined as the expectation value of the ratio between galaxy-galaxy and galaxy-velocity cross correlations, we found a value at  $z = 0.32$  of  $\eta = 0.646 \pm 0.678$ , in agreement with the predicted value for the  $\Lambda$ CDM model, see Chapter 3. Despite the low statistics and large dispersions in the measurements, dark energy scenarios can be tested, demanding however independence of scale. Is important to stress here that for *first time* we obtained a model-independent measurement, without assuming any underlying dark energy model.

We also studied the precision with which a future large survey of galaxy clustering and weak lensing, such as Euclid, can determine the anisotropic stress of the dark sector with the help of the model-independent cosmological observables, when augmented with a supernovae survey. This alleviates the current lack information of scales. We found that galaxy clustering and weak lensing will achieve precise measurements of the expansion rate  $E(z) = H(z)/H_0$ , with errors of less than a percent, in redshift bins of  $\Delta z = 0.2$  out to  $z = 1.5$ , and with less than 4% out to  $z = 2$ , see table 4.7. They will also be able to measure  $P_1 = f/b$  and  $P_2 = \Omega_{m,0}\Sigma/f$ , to about a percent precision over the full redshift range (in the same bins), except at  $z > 1.5$ , where the errors increase rapidly. The final quantity,  $P_3 = f + f'/f$ , is constrained much less precisely, to only about 30%, because it involves an explicit derivative. The detailed results are given in tables 4.8 and 4.9.

We then considered four different models for  $\eta = -\Phi/\Psi$ :

1. A constant  $\eta$ : In this case we found that we can determine the derived quantity  $\bar{\eta} = 2/(1 + \eta)$  with a precision of about 1%.
2. In the case of a  $z$ -dependent  $\eta$ , we found a precision on  $\bar{\eta}$  of about 10% out to  $z = 1.5$ .
3.  $\bar{\eta}$  varying both in  $z$  and in  $k$ : the errors vary considerably across the  $z, k$  range, from 10% to more than 100%.
4. The Horndeski case: now the absolute errors on  $h_2, h_4$  are in the range 0.2-0.6

We stress again that we used *only* directly observable quantities without any further assumptions about the initial power spectrum, the dark matter, the dark energy model (beyond the behavior of  $\eta$  in the last step) or the bias, as such assumptions may be unwarranted in a general dark energy or modified gravity context. On the other hand, we do assume that a window between non-linear scales and sub-sound-horizon scales exists and is wide enough to cover all the wavelengths we have been employing in our forecasts.

Expectations of the generic degeneracy between the amplitude ( $\bar{A}$ ) and Redshift Space Distortion (RSD) contribution ( $\bar{R}$ ) of the galaxy clustering power spectrum were also obtained, see [Appendix C](#). For instance, galaxy surveys have generically a slightly negative correlation between  $\bar{A}$  and  $\bar{R}$ , and they can always measure  $\bar{R}$  about 3.7 to 4.7 times better than  $\bar{A}$ .

When modeling a future large-scale survey along the lines of the ESA Euclid mission, we produced a cosmological exclusion plot for modified gravity in analogy with the exclusion plots produced in laboratory experiments. Adopting the specific form of  $\eta$  predicted by Horndeski Lagrangian, we discovered how well future clustering and weak lensing surveys can constrain its strength and range; our [fig. 5.2](#) resembles, for instance, a plot for testing the equivalence principle using a torsion balance shown in [fig. 5.3](#). Additional exclusion plots for the  $h$ 's which characterize the time dependence in the quasi-static limit in Horndeski perturbations, have been built. This plots allow us to rule out dark energy cosmologies in a single plot, assuming for instance small deviation at background level when compared with the  $\Lambda$ CDM model. Further results on constraining specific models are still in progress, with special attention to  $f(R)$  gravity models.

Our work could be *easily* extended. One assumption when obtaining the model-independent expression for the anisotropic stress was that matter is pressureless. A further step should thus be to consider non-negligible, sound speed  $c_s$  and equation of state  $w$ , and investigate the impact of these in the cosmological observables. Another possible extension is related to the quasi-static regime, used to construct a simple expression for  $\eta$ , coming from the

Horndeski Lagrangian. Non-linear regimes in the power spectrum could be also implemented, implying however a careful revision of the statistics of the Fisher matrix scheme. The results were obtained following the specifications of a large scale survey like Euclid, which can be easily modified for the radio telescope SKA (Square Kilometer Array) [198]. In the coming years theoretical extensions, new observational techniques, faster and more refined codes will provided greater more opportunities to test the standard cosmological paradigm (and also to increase enormously the zoo of modifications from GR). Despite the long wait for Euclid data, crossed fingers for a *definitive* answer as to the nature of Dark Energy.



## PROPERTIES OF THE FISHER MATRIX

Here we briefly summarize the main elements of the Fisher matrix formalism, following mainly [16, Ch. 13] and [73]. Let us start considering a vector of parameters  $\mathbf{p}$ , and a vector of data  $\mathbf{x}$ , from them we can construct a probability density function  $f(\mathbf{x}, \mathbf{p})$  which basically gives us the probability  $P(\mathbf{x}|\mathbf{p})$  of getting a realization of the data  $\mathbf{x}$  given the theory  $\mathbf{p}$ . However, since is not common a prior knowledge of the exact theory, we can try to draw samples  $\mathbf{x}_i$  of an unknown Probability Density Function (PDF), making experiments in order to infer the estimate on the parameters  $\mathbf{p}$ . Thus, We define the *likelihood function* as

$$\mathcal{L}(\mathbf{p}; \mathbf{x}_i) \equiv \prod_i f(\mathbf{x}_i, \mathbf{p}), \quad (\text{A.1})$$

which is a joint PDF with  $\mathbf{p}$  interpreted as a variable, and  $\mathbf{x}$  a fixed parameter. Cosmology is particular, since we rarely have information on the parameters from observations or theories. For that reason the common approach is to use the *Bayes Theorem*, which states that:

$$P(\mathbf{p}|\mathbf{x}, I) = \frac{P(\mathbf{p}|I)P(\mathbf{x}|\mathbf{p}, I)}{P(\mathbf{x}|I)}, \quad (\text{A.2})$$

being  $I$  the background information. Bayes theorem allow us to invert the situation and ask instead what should be the probability of the theory, given the data. Here the prior is given by  $P(\mathbf{p}|I)$ , and  $P(\mathbf{x}|I)$  is the marginal probability of the data  $\mathbf{x}$ , which usually acts as a normalization factor,  $P(\mathbf{x}|\mathbf{p}, I)$  is identical to the likelihood given by the model. The idea behind the Fisher matrix is quite simple. Let us suppose that we can approximate the posterior with a multivariate Gaussian distribution [16, p. 367]

$$\mathcal{L} \approx N \exp \left[ -\frac{1}{2} (p_\alpha - \hat{p}_\alpha) F_{\alpha\beta} (p_\beta - \hat{p}_\beta) \right], \quad (\text{A.3})$$

where the maximum likelihood estimators  $\hat{p}_\alpha$  are functions of the data, and  $F_{\alpha\beta}$  is the Fisher matrix, also defined as the inverse of the covariance matrix. As a good approximation, (at least near to the peak of the distribution), the posterior can be expanded up to second order in a Taylor series:

$$\ln \mathcal{L}(p_\alpha) \approx \ln \mathcal{L}(\hat{p}_\alpha) + \frac{1}{2} \frac{\partial^2 \ln \mathcal{L}(p_\alpha)}{\partial p_\alpha \partial p_\beta} \Big|_{\text{ML}} (p_\alpha - \hat{p}_\alpha)(p_\beta - \hat{p}_\beta), \quad (\text{A.4})$$

(by definition the first term vanishes since is evaluated at the peak), and then we define the *Fisher matrix* as

$$F_{\alpha\beta} \equiv - \frac{\partial^2 \ln \mathcal{L}(\mathbf{p})}{\partial p_\alpha \partial p_\beta} \Big|_{\text{ML}}, \quad (\text{A.5})$$

Using a more precise explanation, the Fisher matrix is defined as the expected value of the matrix  $-\partial^2 \ln \mathcal{L} / \partial p_\alpha \partial p_\beta$ , to be obtained by averaging the matrix over the data distribution

$$F_{\alpha\beta} \equiv - \left\langle \frac{\partial^2 \ln \mathcal{L}(\mathbf{p})}{\partial p_\alpha \partial p_\beta} \right\rangle = - \int \frac{\partial^2 \mathcal{L}(\mathbf{p})}{\partial p_\alpha \partial p_\beta} \mathcal{L}(\mathbf{x}; \mathbf{p}) d\mathbf{x}, \quad (\text{A.6})$$

Nevertheless, with the approximation of the Gaussian for the likelihood eq. (A.3), both definitions coincide. This definition is not very useful when we need to find the maximum of a multi-dimensional function and then compute the derivatives numerically, however, since in cosmology we use some fiducial model to compute constraints that future galaxy surveys can put on parameters, the Fisher matrix analysis becomes a powerful tool.

## A.1 Properties

There are some interesting properties about the Fisher matrix, here we just summarize them without going deeply into details.

1. **Fixing a parameter.** If we want to know what the Fisher matrix would be given that we knew one particular parameter  $p_\alpha$  precisely, we simply remove the  $\alpha$ -th row and column of the Fisher matrix.
2. **Marginalizing over a parameter.** If we want to eliminate a particular parameter  $p_\alpha$ , we remove the  $\alpha$ -th row and column from the inverse of the Fisher matrix and invert again afterwards. If we are only interested in exactly one parameter  $p_\alpha$ , then

we cross out all other rows and columns until the correlation matrix only has one entry left. That means:

$$\sigma(p_i)^2 = (\mathbf{F}^{-1})_{\alpha\alpha}. \quad (\text{A.7})$$

3. **Combination of Fisher Matrices.** If for instance we include some prior data in our analysis, is straightforward to have the *total* Fisher matrix, which is just the sum of both: add the Fisher matrix:

$$\mathbf{F}^{(\text{Tot})} = \mathbf{F} + \mathbf{F}^{(\text{Prior})}. \quad (\text{A.8})$$

This only holds if both matrices have been calculated with the same fiducial model, i.e. the maximum likelihood is the same. If one matrix covers additional parameters, the other matrix must be extended with rows and columns of zeros accordingly.

4. **Parameter Transformation.** This is a clue property, since we used many times in our forecasts. If we consider an additional set of parameters, saying  $s_\alpha$

$$s_\alpha \equiv s_\alpha(p_\alpha), \quad (\text{A.9})$$

which can occur when combining Fisher matrices from different sources. Then the Fisher matrix transforms like a tensor, that means:

$$\mathbf{F}' = \mathbf{J}^T \mathbf{F} \mathbf{J}, \quad (\text{A.10})$$

being  $\mathbf{J}$  the Jacobian matrix of the transformation, which in components could be written as

$$J_{ij} = \frac{\partial s_i}{\partial p_j}. \quad (\text{A.11})$$

which does not necessarily need to be a square matrix.

5. **Confidence Regions.** In the case we have reduced the Fisher matrix to a  $2 \times 2$  for two parameters  $p_1$  and  $p_2$ , explicitly the covariance matrix becomes ( $\mathbf{C} = \mathbf{F}^{-1}$ )

$$\mathbf{C}_{\alpha\beta} = \begin{pmatrix} \sigma_1^2 & \rho\sigma_1\sigma_2 \\ \rho\sigma_1\sigma_2 & \sigma_2^2 \end{pmatrix}, \quad (\text{A.12})$$

then we can construct confidence regions defined as regions of constant likelihood that contain a determined fraction of the total likelihood. For instance, the semiaxes lengths are equal to the square root of the eigenvalues of the inverse Fisher matrix (the covariance matrix)  $\sqrt{\lambda_i}$ , while the semiaxes are oriented along the corresponding

eigenvectors, they form an angle

$$\tan 2\alpha = \frac{2\rho\sigma_1\sigma_2}{\sigma_1^2 - \sigma_2^2}. \quad (\text{A.13})$$

The area of the ellipse (or volume of an ellipsoid) is proportional to the square root of the determinant of the inverse Fisher matrix.

## A.2 Fisher Matrix for the Power Spectrum

Here we briefly want to derive an expression for the Fisher matrix for an experiment that measures the galaxy power spectrum. The power spectrum, including the Poisson noise could be written as [16, p. 376]

$$\Delta_{\mathbf{k}} \equiv \langle \delta_{\mathbf{k}} \delta_{\mathbf{k}}^* \rangle = \langle \delta_{\mathbf{k}} \delta_{-\mathbf{k}} \rangle = P(\mathbf{k}, z) + \frac{1}{n}, \quad (\text{A.14})$$

being  $n(z)$  the galaxy density. The coefficients  $\delta_{\mathbf{k}}$  are complex variables in which real and imaginary parts obey the same Gaussian statistics. Assuming, again, that the galaxy distribution can be approximated by a Gaussian, the likelihood yields

$$L = \frac{1}{(2\pi)^{m/2} \prod_i \Lambda_i} \exp \left[ -\frac{1}{2} \sum_i^m \frac{\delta_i^2}{\Delta_i^2} \right]. \quad (\text{A.15})$$

In this case  $P(k, z)$  is taken as the theoretical spectrum of the fiducial model described by the parameters  $p_\alpha^{(F)}$ . Thus we have

$$\mathcal{L} = -\ln L = \frac{m}{2} \ln(2\pi) + \sum_i \ln \Delta_i + \sum_i \frac{\delta_i^2}{2\Delta_i^2}. \quad (\text{A.16})$$

Denoting differentiation w.r.t. the  $\alpha$  parameter as  $\Delta_{,\alpha}$ , the Fisher matrix eq. (A.5) becomes

$$F_{\alpha\beta} = \left\langle \frac{\partial^2 \mathcal{L}}{\partial p_\alpha \partial p_\beta} \right\rangle = \sum \left[ \frac{\Delta_{,\alpha\beta}}{\Delta} - \frac{\Delta_{,\alpha} \Delta_{,\beta}}{\Delta^2} - \langle \delta^2 \rangle \left( \frac{\Delta_{,\alpha\beta}}{\Delta^3} - 3 \frac{\Delta_{,\alpha} \Delta_{,\beta}}{\Delta^4} \right) \right], \quad (\text{A.17})$$

$$= \frac{1}{2} \sum_i \frac{\partial \ln P_i}{\partial p_\alpha} \frac{\partial \ln P_i}{\partial p_\beta} \left( \frac{nP}{1+nP_i} \right)^2, \quad (\text{A.18})$$

where  $\langle \delta^2 \rangle = \Delta^2$ . For a more compact expression, we approximate the sum with an integral over  $k$ . Basically, we take into account how many modes lie in the bin defined in the interval  $k, k+dk$  and cosine interval  $d\mu$ , i.e. in the volume  $2\pi K^2 dk d\mu$ . The Fourier space can be discretized into cells of volume  $V_{\text{cell}} = (2\pi)^3 / V_{\text{survey}}$ , so that  $2\pi k^2 dk d\mu / V_{\text{cell}} =$

$(2\pi)^{-2}V_{\text{survey}}k^2dk d\mu$  modes in the survey. Finally, we have [82, 211]

$$F_{\alpha\beta} = \frac{1}{8\pi^2} \int_{-1}^{+1} d\mu \int_{k_{\min}}^{k_{\max}} k^2 \frac{\partial \ln P(k, \mu)}{\partial p_\alpha} \frac{\partial \ln P(k, \mu)}{\partial p_\beta} V_{\text{eff}} dk, \quad (\text{A.19})$$

with

$$V_{\text{eff}} = \left[ \frac{\bar{n}P(k, \mu)}{\bar{n}P(k, \mu) + 1} \right]^2 V_{\text{survey}}, \quad (\text{A.20})$$

which could be seen as an effective survey volume.



## RELATIONS IN THE HORNDESKI LAGRANGIAN

This appendix concerns the properties of the scalar-field theories described by the Horndeski Lagrangian. These results are obtained from [20, App.]. Subscripts here  $, \phi$  and  $, X$ , denote derivation w.r.t. that variable. On a flat FRW background, the energy density and pressure are given by

$$\begin{aligned}
 \rho_x = & 3H^2(1 - w_1) + 2XK_{,X} - K - 2XG_{3,\phi} + & (B.1) \\
 & + 6\dot{\phi}H(XG_{3,X} - G_{4,\phi} - 2XG_{4,\phi X}) + \\
 & + 12H^2(X(G_{4,X} + 2XG_{4,XX}) - G_{5,\phi} - XG_{5,\phi X}) + \\
 & + 4\dot{\phi}XH^3(G_{5,X} + XG_{5,XX}), \\
 P_x = & -\left(3H^2 + 2\dot{H}\right)(1 - w_1) + K - 2XG_{3,\phi} + 4XG_{4,\phi\phi} + \\
 & + 2\dot{\phi}Hw_{1,\phi} - 4X^2H^2G_{5,\phi X} + 2\dot{\phi}XH^3G_{5,X} + \frac{\ddot{\phi}}{\dot{\phi}}(w_2 - 2Hw_1),
 \end{aligned}$$

where, given a slight rearrangement of the results in [147, 186], we define four functions  $w_i$  as

$$\begin{aligned}
w_1 &\equiv 1 + 2 \left( G_4 - 2XG_{4,X} + XG_{5,\phi} - \dot{\phi}XHG_{5,X} \right), \\
w_2 &\equiv -2\dot{\phi}(XG_{3,X} - G_{4,\phi} - 2XG_{4,\phi X}) + \\
&\quad + 2H(w_1 - 4X(G_{4,X} + 2XG_{4,XX} - G_{5,\phi} - XG_{5,\phi X})) - \\
&\quad - 2\dot{\phi}XH^2(3G_{5,X} + 2XG_{5,XX}), \\
w_3 &\equiv 3X(K_{,X} + 2XK_{,XX} - 2G_{3,\phi} - 2XG_{3,\phi X}) + 18\dot{\phi}XH(2G_{3,X} + XG_{3,XX}) - \\
&\quad - 18\dot{\phi}H(G_{4,\phi} + 5XG_{4,\phi X} + 2X^2G_{4,\phi XX}) - \\
&\quad - 18H^2(1 + G_4 - 7XG_{4,X} - 16X^2G_{4,XX} - 4X^3G_{4,XXX}) - \\
&\quad - 18XH^2(6G_{5,\phi} + 9XG_{5,\phi X} + 2X^2G_{5,\phi XX}) + \\
&\quad + 6\dot{\phi}XH^3(15G_{5,X} + 13XG_{5,XX} + 2X^2G_{5,XXX}), \\
w_4 &\equiv 1 + 2 \left( G_4 - XG_{5,\phi} - XG_{5,X}\ddot{\phi} \right).
\end{aligned} \tag{B.2}$$

All of the dynamics of linear perturbations are fully determined by the above four functions. In particular, the speed of propagation of gravitational waves,  $c_T$ , and the normalization of the kinetic term of these tensor perturbations,  $Q_T$ , reads

$$c_T^2 = \frac{w_4}{w_1} > 0, \quad Q_T = \frac{w_1}{4} > 0, \tag{B.3}$$

with positivity required by stability. From the above, it can be seen that  $w_1$  has the meaning of the normalization of the tensor perturbations, i.e. it is the effective Planck mass squared. The corresponding quantities for the scalar degree of freedom, the sound speed of dark energy,  $c_s$ , and the normalization of the kinetic energy for perturbations,  $Q_S$ , in the presence of dust with energy density  $\rho_m$ , are

$$\begin{aligned}
c_s^2 &= \frac{3(2w_1^2w_2H - w_2^2w_4 + 4w_1w_2\dot{w}_1 - 2w_1^2(\dot{w}_2 + \rho_m))}{w_1(4w_1w_3 + 9w_2^2)} > 0, \\
Q_S &= \frac{w_1(4w_1w_3 + 9w_2^2)}{3w_2^2} > 0.
\end{aligned} \tag{B.4}$$

With above definitions in hand, we can define the five scale-independent functions  $h_{1-5}$  which appeared in the result eq. (2.52) and eq. (2.53). All the observables for scalar perturbations in the *quasi-static* regime are determined by these five functions,

$$\begin{aligned}
h_1 &\equiv \frac{w_4}{w_1^2} = \frac{c_T^2}{w_1}, & h_2 &\equiv \frac{w_1}{w_4} = c_T^{-2}, \\
h_3 &\equiv \frac{H^2}{2XM^2} \frac{2w_1^2 w_2 H - w_2^2 w_4 + 4w_1 w_2 \dot{w}_1 - 2w_1^2 (\dot{w}_2 + \rho_m)}{2w_1^2}, \\
h_4 &\equiv \frac{H^2}{2XM^2} \frac{2w_1^2 H^2 - w_2 w_4 H + 2w_1 \dot{w}_1 H + w_2 \dot{w}_1 - w_1 (\dot{w}_2 + \rho_m)}{w_1}, \\
h_5 &\equiv \frac{H^2}{2XM^2} \frac{2w_1^2 H^2 - w_2 w_4 H + 4w_1 \dot{w}_1 H + 2\dot{w}_1^2 - w_4 (\dot{w}_2 + \rho_m)}{w_4},
\end{aligned} \tag{B.5}$$

and where the effective mass squared,  $M^2$ , can be expressed in terms of derivatives of the total pressure and total energy with respect to the scalar as

$$M^2 = \frac{3H (P_{x,\phi} + \rho_{x,\phi}) + \dot{\rho}_{x,\phi}}{\dot{\phi}}. \tag{B.6}$$



## SEMI-ANALYTICAL STUDY ON THE DEGENERACY FOR $\bar{A}$ AND $\bar{R}$

We discuss in [Subsection 4.1.1](#) the Fisher matrix for galaxy clustering, specifically on the measurements of the parameters  $\bar{A}$ ,  $\bar{R}$  and  $H$ . Now we want to obtain some results on the intrinsic degeneracy on galaxy clustering measurements, using just the quantities  $\bar{A}$  and  $\bar{R}$  [\[202\]](#). Let us consider once again the galaxy power spectrum in redshift space

$$P(k, \mu) = (A + R\mu^2)^2 = (\bar{A} + \bar{R}\mu^2)^2 \delta_{t,0}^2(k), \quad (\text{C.1})$$

whit  $\bar{A} = Gb\sigma_8$ ,  $\bar{R} = Gf\sigma_8$ , and we explicitly use  $\delta_{m,0} = \sigma_8\delta_{t,0}$ . The Fisher matrix is in general

$$F_{\alpha\beta} = \frac{1}{8\pi^2} \int_{-1}^1 d\mu \int_{k_{\min}}^{k_{\max}} k^2 V_{\text{eff}} D_\alpha D_\beta dk, \quad (\text{C.2})$$

where  $D_\alpha \equiv \frac{d \log P}{dp_\alpha}$ , and  $V_{\text{eff}}$  is the effective volume of the survey

$$V_{\text{eff}} = \left( \frac{\bar{n}P(k, \mu)}{\bar{n}P(k, \mu) + 1} \right)^2 V_{\text{survey}}, \quad (\text{C.3})$$

being  $\bar{n}$  the galaxy number density in each bin. We want to study the dependence on the angular integration in the Fisher matrix for the set of parameters  $p_\alpha = \{\bar{A}(z_\alpha), \bar{R}(z_\alpha)\}$ . The derivatives of the power spectrum are

$$D_\alpha = \frac{2}{\bar{A} + \bar{R}\mu^2} \{1, \mu^2\}. \quad (\text{C.4})$$

we consider two cases depending on the behavior of  $V_{\text{eff}}$ , equation [\(C.3\)](#):

1. “Enough data”  $\bar{n}P(k, \mu) \gg 1$ , then we have  $V_{\text{eff}} \approx V_{\text{survey}}$  and the Fisher matrix

could be written as

$$F_{\alpha\beta} \approx \frac{1}{2\pi^2} \int_{k_{\min}}^{k_{\max}} k^2 V_{\text{survey}} M_{\alpha\beta} dk, \quad (\text{C.5})$$

where

$$M_{\alpha\beta} = 4 \begin{pmatrix} \frac{\sqrt{\bar{S}} + (\bar{A} + \bar{R}) \tan^{-1} \sqrt{\bar{P}_1}}{\bar{A}^{3/2} \sqrt{\bar{R}} (\bar{A} + \bar{R})} & \frac{-\sqrt{\bar{S}} + (\bar{A} + \bar{R}) \tan^{-1} \sqrt{\bar{P}_1}}{\bar{R}^{3/2} \sqrt{\bar{A}} (\bar{A} + \bar{R})} \\ \frac{-\sqrt{\bar{S}} + (\bar{A} + \bar{R}) \tan^{-1} \sqrt{\bar{P}_1}}{\bar{R}^{3/2} \sqrt{\bar{A}} (\bar{A} + \bar{R})} & \frac{\bar{R}(3\bar{A} + 2\bar{R}) - 3(\bar{A} + \bar{R}) \sqrt{\bar{S}} \tan^{-1} \sqrt{\bar{P}_1}}{\bar{R}^3 (\bar{A} + \bar{R})} \end{pmatrix} \quad (\text{C.6})$$

being  $\bar{S} = \bar{A}\bar{R}$ .

2. Shot-noise dominated  $\bar{n}P(k, \mu) \ll 1$ , and then  $V_{\text{eff}} \approx (\bar{n}P(k, \mu))^2 V_{\text{survey}}$  and since we are interesting only in the  $\mu$  dependence we can write  $V_{\text{eff}} \approx P(k, \mu)^2$ . Then the Fisher matrix becomes

$$F_{\alpha\beta} \approx \frac{1}{2\pi^2} \int_{k_{\min}}^{k_{\max}} k^2 \delta_{t,0}^4(k) N_{\alpha\beta} dk, \quad (\text{C.7})$$

with

$$N_{\alpha\beta} = 8 \begin{pmatrix} \bar{A}^2 + \frac{2\bar{A}\bar{R}}{3} + \frac{\bar{R}^2}{5} & \frac{\bar{A}^2}{3} + \frac{2\bar{A}\bar{R}}{5} + \frac{\bar{R}^2}{7} \\ \frac{\bar{A}^2}{3} + \frac{2\bar{A}\bar{R}}{5} + \frac{\bar{R}^2}{7} & \frac{\bar{A}^2}{5} + \frac{2\bar{A}\bar{R}}{7} + \frac{\bar{R}^2}{9} \end{pmatrix}. \quad (\text{C.8})$$

We notice that in the two limiting cases above, we can move the matrices  $M_{\alpha\beta}$  and  $N_{\alpha\beta}$  outside of the integral, as for the fiducial model  $\bar{A}$  and  $\bar{R}$  do not depend on  $k$ . This means that, although the absolute size of the error ellipse depends on the integral, the relative size and orientation do not. In other words, we can obtain ‘generic expectations’ for the shape of the degeneracy between  $\bar{A}$  and  $\bar{R}$  from galaxy clustering surveys. These results are quite representative for the full range of  $\bar{A}$  and  $\bar{R}$ , i.e. galaxy surveys have generically a slightly negative correlation between  $\bar{A}$  and  $\bar{R}$ , and they can always measure  $\bar{R}$  about 3.7 to 4.7 times better than  $\bar{A}$ , see Figure C.1. In comparison to the results of [212], we remove the dependence on  $\delta_{t,0}$ , (2.49), which is a quantity that depends on inflation or other primordial effects.

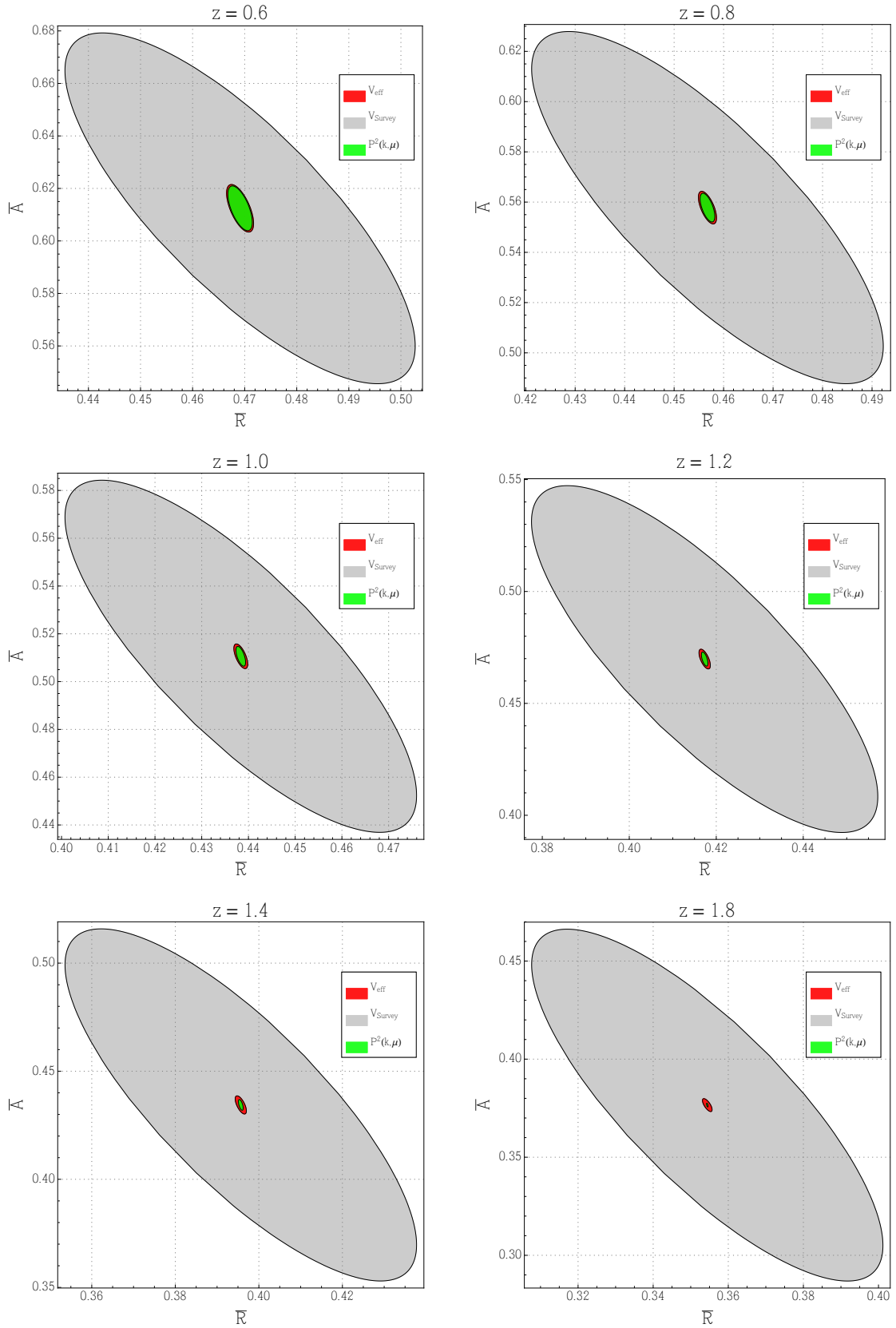


**Figure C.1:** Confidence contours for  $\bar{A}$  and  $\bar{R}$  in the three cases: orange line  $V_{\text{eff}}$ , blue line  $V_{\text{eff}} \approx V_{\text{survey}}$ , and green line  $V_{\text{eff}} \approx P(k, \mu)^2$ .



## BIBLIOGRAPHY

- [1] E. Macaulay, I. K. Wehus, and H. K. Eriksen, “A Lower Growth Rate from Recent Redshift Space Distortions than Expected from Planck,” [arXiv:1303.6583 \[astro-ph.CO\]](#).
- [2] **Planck Collaboration** Collaboration, P. Ade *et al.*, “Planck 2013 results. XVI. Cosmological parameters,” [arXiv:1303.5076 \[astro-ph.CO\]](#).
- [3] N. Suzuki *et al.*, “The Hubble Space Telescope Cluster Supernova Survey. V. Improving the Dark-energy Constraints above  $z > 1$  and Building an Early-type-hosted Supernova Sample,” *Astrophys. J.* **746** no. 1, (2012) 85.
- [4] T. Baker, *Cosmological test of gravity*. PhD thesis, University of Oxford, 2013.
- [5] **Planck Collaboration** Collaboration, P. A. R. Ade *et al.*, “Planck 2015 results. XIV. Dark energy and modified gravity,” [arXiv:1502.01590 \[astro-ph.CO\]](#).
- [6] P. Zhang, M. Liguori, R. Bean, and S. Dodelson, “Probing Gravity at Cosmological Scales by Measurements which Test the Relationship between Gravitational Lensing and Matter Overdensity,” *Phys. Rev. Lett.* **99** (2007) 141302, [arXiv:0704.1932 \[astro-ph\]](#).
- [7] R. Reyes, R. Mandelbaum, U. Seljak, T. Baldauf, J. E. Gunn, L. Lombriser, and R. E. Smith, “Confirmation of general relativity on large scales from weak lensing and galaxy velocities,” *Nature* no. 7286, (2010) 256–258.  
<http://www.nature.com/nature/journal/v464/n7286/full/nature08857.html>.
- [8] O. Farooq, D. Mania, and B. Ratra, “Hubble parameter measurement constraints on dark energy,” *Astrophys. J.* **764** (2013) 138, [arXiv:1211.4253 \[astro-ph.CO\]](#).
- [9] E. Gaztanaga, A. Cabre, and L. Hui, “Clustering of Luminous Red Galaxies IV: Baryon Acoustic Peak in the Line-of-Sight Direction and a Direct Measurement of  $H(z)$ ,” *Mon. Not. Roy. Astron. Soc.* **399** (2009) 1663–1680, [arXiv:0807.3551 \[astro-ph\]](#).
- [10] D. Stern, R. Jimenez, L. Verde, S. A. Stanford, and M. Kamionkowski, “Cosmic Chronometers: Constraining the Equation of State of Dark Energy. II. A Spectroscopic Catalog of Red Galaxies in Galaxy Clusters,” *Astrophys. J. Suppl.* **188** (2010) 280–289, [arXiv:0907.3152 \[astro-ph.CO\]](#).

- [11] M. Moresco, A. Cimatti, R. Jimenez, L. Pozzetti, G. Zamorani, *et al.*, “Improved constraints on the expansion rate of the Universe up to  $z$  1.1 from the spectroscopic evolution of cosmic chronometers,” *JCAP* **1208** (2012) 006, [arXiv:1201.3609 \[astro-ph.CO\]](#).
- [12] R. Laureijs, J. Amiaux, S. Arduini, J. . Auguères, J. Brinchmann, R. Cole, M. Cropper, C. Dabin, L. Duvet, A. Ealet, and *et al.*, “Euclid Definition Study Report,” [arXiv:1110.3193 \[astro-ph.CO\]](#).
- [13] A. Orsi, C. Baugh, C. Lacey, A. Cimatti, Y. Wang, *et al.*, “Probing dark energy with future redshift surveys: A comparison of emission line and broad band selection in the near infrared,” [arXiv:0911.0669 \[astro-ph.CO\]](#).
- [14] S. Schlamminger, K.-Y. Choi, T. Wagner, J. Gundlach, and E. Adelberger, “Test of the equivalence principle using a rotating torsion balance,” *Phys. Rev. Lett.* **100** (2008) 041101, [arXiv:0712.0607 \[gr-qc\]](#).
- [15] **Planck Collaboration** Collaboration, P. Ade *et al.*, “Planck 2013 results. I. Overview of products and scientific results,” [arXiv:1303.5062 \[astro-ph.CO\]](#).
- [16] L. Amendola and S. Tsujikawa, *Dark Energy: Theory and Observations*. Cambridge University Press, 2010.
- [17] S. Dodelson, *Modern Cosmology*. Academic Press, 2003.
- [18] R. Durrer, *The Cosmic Microwave Background*. Cambridge University Press, Cambridge, 2008.
- [19] G. Hinshaw *et al.*, “Nine-year Wilkinson Microwave Anisotropy Probe (WMAP) Observations: Cosmological Parameter Results,” *Astrophys. J.* **208** (Oct., 2013) 19, [arXiv:1212.5226](#).
- [20] L. Amendola, M. Kunz, M. Motta, I. D. Saltas, and I. Sawicki, “Observables and unobservables in dark energy cosmologies,” *Phys. Rev. D* **87** (2013) 023501, [arXiv:1210.0439 \[astro-ph.CO\]](#).
- [21] **SDSS** Collaboration, M. Tegmark *et al.*, “The 3-D power spectrum of galaxies from the SDSS,” *Astrophys. J.* **606** (2004) 702–740, [arXiv:astro-ph/0310725 \[astro-ph\]](#).
- [22] **2DFGRS** Collaboration, M. Colless *et al.*, “The 2dF Galaxy Redshift Survey: Spectra and redshifts,” *Mon. Not. Roy. Astron. Soc.* **328** (2001) 1039, [arXiv:astro-ph/0106498 \[astro-ph\]](#).
- [23] A. Einstein, “Die Grundlage der allgemeinen Relativitätstheorie,” *Annalen der Physik* **354** no. 7, (1916) 769–822. <http://dx.doi.org/10.1002/andp.19163540702>.
- [24] C. M. Will, “The Confrontation between General Relativity and Experiment,” *Living Reviews in Relativity* **9** no. 3, (2006) . <http://www.livingreviews.org/lrr-2006-3>.
- [25] E. Poisson and C. Will, *Gravity: Newtonian, Post-Newtonian, Relativistic*. Cambridge University Press, 2014.
- [26] P. G. Ferreira, *The Perfect Theory: A Century of Geniuses and the Battle Over General Relativity*. Houghton Mifflin Harcourt, 2014.
- [27] C. W. Misner, K. S. Thorne, and J. A. Wheeler, *Gravitation*. W H Freeman and Company, 2 ed., 1973.

- [28] R. M. Wald, *General Relativity*. The University of Chicago Press, 1984.
- [29] S. Carroll, *Spacetime and Geometry: An Introduction to General Relativity*. Benjamin Cummings, 2003.
- [30] S. Hawking and G. Ellis, *The Large Scale Structure of Space-Time*. Cambridge Monographs on Mathematical Physics. Cambridge University Press, 1973.
- [31] B. Schutz, *A First Course in General Relativity*. Series in physics. Cambridge University Press, 1985.
- [32] E. Poisson, *A Relativist's Toolkit: The Mathematics of Black-Hole Mechanics*. Cambridge University Press, 2004.
- [33] M. Nakahara, *Geometry, topology, and physics*. Graduate student series in physics. Institute of Physics Publishing, Bristol, Philadelphia, 2003.
- [34] E. Cartan, "Sur les variétés à connexion affine et la théorie de la relativité généralisée (première partie)," *Ann. Ec. Norm. Super.* **40** (1923) 325.  
[http://archive.numdam.org/article/ASENS\\_1923\\_3\\_40\\_\\_325\\_0.pdf](http://archive.numdam.org/article/ASENS_1923_3_40__325_0.pdf).
- [35] D. W. Sciama, "On the Interpretation of the Einstein-Schrödinger Unified Field Theory," *J. Math. Phys.* **2** no. 4, (1961) 472–477.
- [36] T. W. B. Kibble, "Lorentz Invariance and the Gravitational Field," *J. Math. Phys.* **2** no. 2, (1961) 212–221.
- [37] G. W. Gibbons and S. W. Hawking, "Action integrals and partition functions in quantum gravity," *Phys. Rev. D* **15** (May, 1977) 2752–2756.
- [38] S. W. Hawking and G. T. Horowitz, "The Gravitational Hamiltonian, action, entropy and surface terms," *Class. Quant. Grav.* **13** (1996) 1487–1498, [arXiv:gr-qc/9501014](https://arxiv.org/abs/gr-qc/9501014) [gr-qc].
- [39] A. Palatini, "Deduzione invariante delle equazioni gravitazionali dal principio di Hamilton," *Rendiconti del Circolo Matematico di Palermo (1884-1940)* **43** no. 1, (1919) 203–212.
- [40] S. Weinberg, *Cosmology*. Cosmology. OUP Oxford, 2008.
- [41] E. Harrison, *Cosmology: The Science of the Universe*. Cambridge University Press, 2000.
- [42] A. Einstein, "Kosmologische Betrachtungen zur allgemeinen Relativitätstheorie," *Sitzungsberichte der Königlich Preussischen Akademie der Wissenschaften (Berlin)*, Seite 142-152. (1917) 142–152.
- [43] E. Hubble, "A relation between distance and radial velocity among extra-galactic nebulae," *Proceedings of the National Academy of Sciences* **15** no. 3, (1929) 168–173,  
<http://www.pnas.org/content/15/3/168.full.pdf>.  
<http://www.pnas.org/content/15/3/168.short>.
- [44] A. Einstein, "Zum kosmologischen Problem der allgemeinen Relativitätstheorie," *Sitzungsber. Preuss. Akad. Wiss.* **142** (1931) 235–237. [http://einstein-annalen.mpiwg-berlin.mpg.de/related\\_texts/sitzungsberichte/R583HGCS](http://einstein-annalen.mpiwg-berlin.mpg.de/related_texts/sitzungsberichte/R583HGCS).
- [45] H. Nussbaumer, "Einstein's conversion from his static to an expanding universe," *Eur. Phys. J. H* **39** no. 1, (2014) 37–62.

- [46] G. Gamow, *My world line; an informal autobiography*. Viking Press, 1970.
- [47] S. M. Carroll, “The Cosmological Constant,” *Living Reviews in Relativity* **4** no. 1, (2001) . <http://www.livingreviews.org/lrr-2001-1>.
- [48] S. Perlmutter *et al.*, “Measurements of  $\Omega$  and  $\Lambda$  from 42 High-Redshift Supernovae,” *Astrophys. J.* **517** no. 2, (1999) 565. <http://stacks.iop.org/0004-637X/517/i=2/a=565>.
- [49] A. G. Riess *et al.*, “Observational Evidence from Supernovae for an Accelerating Universe and a Cosmological Constant,” *The Astronomical Journal* **116** no. 3, (1998) 1009. <http://stacks.iop.org/1538-3881/116/i=3/a=1009>.
- [50] I. Etherington, “LX. On the definition of distance in general relativity,” *The London, Edinburgh, and Dublin Philosophical Magazine and Journal of Science* **15** no. 100, (1933) 761–773, <http://dx.doi.org/10.1080/14786443309462220>.
- [51] M. Hobson, G. Efstathiou, and A. Lasenby, *General Relativity: An Introduction for Physicists*. Cambridge University Press, 2006.
- [52] T. Padmanabhan, “Cosmological constant—the weight of the vacuum,” *Phys. Rep.* **380** (2003) 235–320.
- [53] P. J. E. Peebles and B. Ratra, “The cosmological constant and dark energy,” *Rev. Mod. Phys.* **75** (2003) 559–606.
- [54] H. Velten, R. vom Marttens, and W. Zimdahl, “Aspects of the cosmological “coincidence problem”,” *Eur. Phys. J. C* **74** no. 11, (2014) . <http://dx.doi.org/10.1140/epjc/s10052-014-3160-4>.
- [55] L. Amendola, “Coupled quintessence,” *Phys. Rev. D* **62** (Jul, 2000) 043511. <http://link.aps.org/doi/10.1103/PhysRevD.62.043511>.
- [56] I. Zlatev, L. Wang, and P. J. Steinhardt, “Quintessence, Cosmic Coincidence, and the Cosmological Constant,” *Phys. Rev. Lett.* **82** (Feb, 1999) 896–899. <http://link.aps.org/doi/10.1103/PhysRevLett.82.896>.
- [57] A. Vilenkin, “Predictions from Quantum Cosmology,” *Phys. Rev. Lett.* **74** (Feb., 1995) 846–849, [gr-qc/9406010](http://dx.doi.org/10.1103/PhysRevLett.74.846).
- [58] S. Weinberg, “Anthropic bound on the cosmological constant,” *Phys. Rev. Lett.* **59** (Nov., 1987) 2607–2610.
- [59] B. Carter, “Large number coincidences and the anthropic principle in cosmology,” in *Confrontation of Cosmological Theories with Observational Data*, M. S. Longair, ed., vol. 63 of *IAU Symposium*, pp. 291–298. 1974.
- [60] J. M. Bardeen, “Gauge-invariant cosmological perturbations,” *Phys. Rev. D* **22** (Oct, 1980) 1882–1905. <http://link.aps.org/doi/10.1103/PhysRevD.22.1882>.
- [61] R. Durrer, “2 Cosmological Perturbation Theory,” in *The Physics of the Early Universe*, E. Papantonopoulos, ed., vol. 653 of *Lecture Notes in Physics*, pp. 31–69. Springer Berlin Heidelberg, 2005. [http://dx.doi.org/10.1007/978-3-540-31535-3\\_2](http://dx.doi.org/10.1007/978-3-540-31535-3_2).
- [62] V. F. Mukhanov, H. A. Feldman, and R. H. Brandenberger, “Theory of cosmological perturbations,” *Phys. Rept.* **215** (June, 1992) 203–333.

- [63] K. Nakamura, “Gauge Invariant Variables in Two-Parameter Nonlinear Perturbations,” *Prog. Theor. Phys.* **110** no. 4, (2003) 723–755.  
<http://ptp.oxfordjournals.org/content/110/4/723.abstract>.
- [64] K. A. Malik and D. Wands, “Cosmological perturbations,” *Phys. Rept.* **475** no. 1–4, (2009) 1–51.
- [65] K. Nakamura, “Second-order gauge invariant cosmological perturbation theory: Einstein equations in terms of gauge invariant variables,” *Prog. Theor. Phys.* **117** (2007) 17–74, [arXiv:gr-qc/0605108](https://arxiv.org/abs/gr-qc/0605108) [gr-qc].
- [66] H. Kodama and M. Sasaki, “Cosmological Perturbation Theory,” *Progress of Theoretical Physics Supplement* **78** (1984) 1.
- [67] J. M. Stewart and M. Walker, “Perturbations of Space-Times in General Relativity,” *Proceedings of the Royal Society of London A: Mathematical, Physical and Engineering Sciences* **341** no. 1624, (1974) 49–74.
- [68] D. H. Lyth and A. R. Liddle, *The Primordial Density Perturbation*. Cambridge University Press, 2009.
- [69] G. F. R. Ellis and M. Bruni, “Covariant and gauge-invariant approach to cosmological density fluctuations,” *Phys. Rev. D* **40** (Sep, 1989) 1804–1818.  
<http://link.aps.org/doi/10.1103/PhysRevD.40.1804>.
- [70] M. Bruni, S. Matarrese, S. Mollerach, and S. Sonego, “Perturbations of space-time: Gauge transformations and gauge invariance at second order and beyond,” *Class. Quant. Grav.* **14** (1997) 2585–2606, [arXiv:gr-qc/9609040](https://arxiv.org/abs/gr-qc/9609040) [gr-qc].
- [71] K. Nakamura, “Second-order Gauge-Invariant Cosmological Perturbation Theory: Current Status,” *Adv. Astron.* **2010** (2010) 576273, [arXiv:1001.2621](https://arxiv.org/abs/1001.2621) [gr-qc].
- [72] G. Ellis, R. Maartens, and M. MacCallum, *Relativistic Cosmology*. Relativistic Cosmology. Cambridge University Press, 2012.
- [73] A. Vollmer, “Forecasting Constraints on the Evolution of the Hubble Parameter and the Growth Function by Future Weak Lensing Surveys,” [arXiv:1109.5551](https://arxiv.org/abs/1109.5551) [astro-ph.CO].
- [74] A. H. Guth, “Inflationary universe: A possible solution to the horizon and flatness problems,” *Phys. Rev. D* **23** (Jan, 1981) 347–356.  
<http://link.aps.org/doi/10.1103/PhysRevD.23.347>.
- [75] **Planck** Collaboration, P. A. R. Ade *et al.*, “Planck 2015 results. XIII. Cosmological parameters,” [arXiv:1502.01589](https://arxiv.org/abs/1502.01589) [astro-ph.CO].
- [76] J. M. Bardeen, J. Bond, N. Kaiser, and A. Szalay, “The Statistics of Peaks of Gaussian Random Fields,” *Astrophys. J.* **304** (1986) 15–61.
- [77] A. Lewis, A. Challinor, and A. A. Lasenby, “Efficient Computation of CMB anisotropies in closed FRW models,” *Astrophys. J.* **538** (2000) 473–476, [arXiv:9911177](https://arxiv.org/abs/9911177) [astro-ph]. Code available in <http://camb.info/>.
- [78] Y. B. Zel’dovich, “Gravitational instability: An approximate theory for large density perturbations,” *Astron. Astrophys.* **5** (Mar., 1970) 84–89.

- [79] D. Branch and G. A. Tammann, “Type Ia Supernovae as Standard Candles,” *Ann. Rev. Astron. Astrophys.* **30** no. 1, (1992) 359–389, <http://dx.doi.org/10.1146/annurev.aa.30.090192.002043>.
- [80] N. Kaiser, “Clustering in real space and in redshift space,” *Mon. Not. Roy. Astron. Soc.* **227** (1987) 1–27.
- [81] E. V. Linder, “Cosmic growth history and expansion history,” *Phys. Rev. D* **72** (Aug, 2005) 043529. <http://link.aps.org/doi/10.1103/PhysRevD.72.043529>.
- [82] H.-J. J. Seo and D. J. Eisenstein, “Probing dark energy with baryonic acoustic oscillations from future large galaxy redshift surveys,” *Astrophys. J* **598** (2003) 720–740, [arXiv:0307460](http://arxiv.org/abs/0307460) [astro-ph].
- [83] C. Alcock and B. Paczynski, “An evolution free test for non-zero cosmological constant,” *Nature* **281** (Oct., 1979) 358.
- [84] C. Bonvin and R. Durrer, “What galaxy surveys really measure,” *Phys. Rev. D* **84** (Sep, 2011) 063505. <http://link.aps.org/doi/10.1103/PhysRevD.84.063505>.
- [85] A. Challinor and A. Lewis, “Linear power spectrum of observed source number counts,” *Phys. Rev. D* **84** (Aug, 2011) 043516. <http://link.aps.org/doi/10.1103/PhysRevD.84.043516>.
- [86] J. Yoo, A. L. Fitzpatrick, and M. Zaldarriaga, “New perspective on galaxy clustering as a cosmological probe: General relativistic effects,” *Phys. Rev. D* **80** (Oct, 2009) 083514. <http://link.aps.org/doi/10.1103/PhysRevD.80.083514>.
- [87] J. Yoo, “General relativistic description of the observed galaxy power spectrum: Do we understand what we measure?,” *Phys. Rev. D* **82** (Oct, 2010) 083508. <http://link.aps.org/doi/10.1103/PhysRevD.82.083508>.
- [88] M. Bruni, R. Crittenden, K. Koyama, R. Maartens, C. Pitrou, and D. Wands, “Disentangling non-Gaussianity, bias, and general relativistic effects in the galaxy distribution,” *Phys. Rev. D* **85** (Feb, 2012) 041301. <http://link.aps.org/doi/10.1103/PhysRevD.85.041301>.
- [89] D. Jeong, F. Schmidt, and C. M. Hirata, “Large-scale clustering of galaxies in general relativity,” *Phys. Rev. D* **85** (Jan, 2012) 023504. <http://link.aps.org/doi/10.1103/PhysRevD.85.023504>.
- [90] D. Bertacca, R. Maartens, A. Raccanelli, and C. Clarkson, “Beyond the plane-parallel and Newtonian approach: wide-angle redshift distortions and convergence in general relativity,” *Journal of Cosmology and Astroparticle Physics* **2012** no. 10, (2012) 025. <http://stacks.iop.org/1475-7516/2012/i=10/a=025>.
- [91] E. Di Dio, F. Montanari, J. Lesgourgues, and R. Durrer, “The CLASSgal code for Relativistic Cosmological Large Scale Structure,” *JCAP* **1311** (2013) 044, [arXiv:1307.1459](http://arxiv.org/abs/1307.1459) [astro-ph.CO].
- [92] H. Weyl, *Raum, Zeit, Materie*. Springer-Verlag, Berlin, 1921.
- [93] E. Pechlaner and R. Sexl, “On quadratic lagrangians in General Relativity,” *Communications in Mathematical Physics* **2** no. 1, (1966) 165–175. <http://dx.doi.org/10.1007/BF01773351>.

- [94] D. Wands, “Extended gravity theories and the Einstein-Hilbert action,” *Class. Quant. Grav.* **11** (1994) 269–280, [arXiv:gr-qc/9307034](https://arxiv.org/abs/gr-qc/9307034) [gr-qc].
- [95] E. Kretschmann, “Über den physikalischen Sinn der Relativitätspostulate, A. Einsteins neue und seine ursprüngliche Relativitätstheorie,” *Ann. Phys. (Leipzig)* **53** (1917) 575–614.
- [96] K. Stelle, “Classical gravity with higher derivatives,” *Gen. Rel. Grav.* **9** no. 4, (1978) 353–371. <http://dx.doi.org/10.1007/BF00760427>.
- [97] A. D. Felice and S. Tsujikawa, “ $f(R)$  Theories,” *Living Reviews in Relativity* **13** no. 3, (2010) . <http://www.livingreviews.org/lrr-2010-3>.
- [98] D. Lovelock, “The Einstein tensor and its generalizations,” *J. Math. Phys.* **12** (1971) 498–501.
- [99] T. Koivisto and D. F. Mota, “Cosmology and Astrophysical Constraints of Gauss-Bonnet Dark Energy,” *Phys. Lett.* **B644** (2007) 104–108, [arXiv:astro-ph/0606078](https://arxiv.org/abs/astro-ph/0606078) [astro-ph].
- [100] B. Li, J. D. Barrow, and D. F. Mota, “Cosmology of modified Gauss-Bonnet gravity,” *Phys. Rev. D* **76** (Aug, 2007) 044027. <http://link.aps.org/doi/10.1103/PhysRevD.76.044027>.
- [101] R. Bach, “Zur Weylschen Relativitätstheorie und der Weylschen Erweiterung des Krümmungstensorbegriffs,” *Mathematische Zeitschrift* **9** no. 1-2, (1921) 110–135.
- [102] H. A. Buchdahl, “Non-linear Lagrangians and cosmological theory,” *MNRAS* **150** (1970) 1.
- [103] M. S. Madsen and J. D. Barrow, “De Sitter ground states and boundary terms in generalised gravity,” *Nuclear Physics B* **323** no. 1, (1989) 242–252. <http://www.sciencedirect.com/science/article/pii/0550321389905968>.
- [104] N. H. Barth, “The fourth-order gravitational action for manifolds with boundaries,” *Class. Quant. Grav.* **2** no. 4, (1985) 497. <http://stacks.iop.org/0264-9381/2/i=4/a=015>.
- [105] M. Francaviglia and M. Raiteri, “Hamiltonian, energy and entropy in general relativity with nonorthogonal boundaries,” *Class. Quant. Grav.* **19** (2002) 237–258, [arXiv:gr-qc/0107074](https://arxiv.org/abs/gr-qc/0107074) [gr-qc].
- [106] A. Guarnizo, L. Castaneda, and J. M. Tejeiro, “Boundary Term in Metric  $f(R)$  Gravity: Field Equations in the Metric Formalism,” *Gen. Rel. Grav.* **42** (2010) 2713–2728, [arXiv:1002.0617](https://arxiv.org/abs/1002.0617) [gr-qc].
- [107] M. Ortogradski, “Memoires sur les equations differentielles relatives au probleme des isoperimetres,” *Mem. Ac. St. Petersbourg* **VI** **4** (1850) 385.
- [108] T.-j. Chen, M. Fasiello, E. A. Lim, and A. J. Tolley, “Higher derivative theories with constraints: Exorcising Ostrogradski’s Ghost,” *JCAP* **1302** (2013) 042, [arXiv:1209.0583](https://arxiv.org/abs/1209.0583) [hep-th].
- [109] D. Lovelock and H. Rund, *Tensors, Differential forms, and variational principles*. Dover Publications, 1989.
- [110] T. Clifton, P. G. Ferreira, A. Padilla, and C. Skordis, “Modified Gravity and Cosmology,” *Phys. Rept.* **513** (2012) 1–189, [arXiv:1106.2476](https://arxiv.org/abs/1106.2476) [astro-ph.CO].
- [111] K. Koyama, “Cosmological Tests of Gravity,” [arXiv:1504.04623](https://arxiv.org/abs/1504.04623) [astro-ph.CO].

- [112] E. Berti *et al.*, “Testing General Relativity with Present and Future Astrophysical Observations,” [arXiv:1501.07274 \[gr-qc\]](#).
- [113] J. Santos, J. S. Alcaniz, M. J. Rebouças, and F. C. Carvalho, “Energy conditions in  $f(R)$  gravity,” *Phys. Rev. D* **76** (Oct, 2007) 083513.  
<http://link.aps.org/doi/10.1103/PhysRevD.76.083513>.
- [114] A. Guarnizo, L. Castaneda, and J. M. Tejeiro, “Geodesic Deviation Equation in  $f(R)$  Gravity,” *Gen. Rel. Grav.* **43** (2011) 2713–2728, [arXiv:1010.5279 \[gr-qc\]](#).
- [115] P. Hořava, “Membranes at Quantum Criticality,” *JHEP* **03** (2009) 020, [arXiv:0812.4287 \[hep-th\]](#).
- [116] P. Hořava, “Quantum gravity at a Lifshitz point,” *Phys. Rev. D* **79** (Apr, 2009) 084008.  
<http://link.aps.org/doi/10.1103/PhysRevD.79.084008>.
- [117] G. J. Olmo, “Palatini Approach to Modified Gravity:  $f(R)$  Theories and Beyond,” *Int. J. Mod. Phys. D* **20** (2011) 413–462, [arXiv:1101.3864 \[gr-qc\]](#).
- [118] C. Brans and R. H. Dicke, “Mach’s Principle and a Relativistic Theory of Gravitation,” *Phys. Rev.* **124** (Nov, 1961) 925–935.  
<http://link.aps.org/doi/10.1103/PhysRev.124.925>.
- [119] G. Szekeres, “New Formulation of the General Theory of Relativity,” *Phys. Rev.* **97** (Jan, 1955) 212–223. <http://link.aps.org/doi/10.1103/PhysRev.97.212>.
- [120] T. Jacobson and D. Mattingly, “Einstein-Aether waves,” *Phys. Rev. D* **70** (2004) 024003, [arXiv:gr-qc/0402005 \[gr-qc\]](#).
- [121] E. A. Lim, “Can we see Lorentz-violating vector fields in the CMB?,” *Phys. Rev. D* **71** (2005) 063504, [arXiv:astro-ph/0407437 \[astro-ph\]](#).
- [122] T. G. Zlosnik, P. G. Ferreira, and G. D. Starkman, “Growth of structure in theories with a dynamical preferred frame,” *Phys. Rev. D* **77** (Apr, 2008) 084010.  
<http://link.aps.org/doi/10.1103/PhysRevD.77.084010>.
- [123] J. Zuntz, T. G. Zlosnik, F. Bourliot, P. G. Ferreira, and G. D. Starkman, “Vector field models of modified gravity and the dark sector,” *Phys. Rev. D* **81** (May, 2010) 104015.  
<http://link.aps.org/doi/10.1103/PhysRevD.81.104015>.
- [124] M. Fierz and W. Pauli, “On Relativistic Wave Equations for Particles of Arbitrary Spin in an Electromagnetic Field,” *Proceedings of the Royal Society of London A: Mathematical, Physical and Engineering Sciences* **173** no. 953, (1939) 211–232.
- [125] S. F. Hassan and R. A. Rosen, “Confirmation of the Secondary Constraint and Absence of Ghost in Massive Gravity and Bimetric Gravity,” *JHEP* **04** (2012) 123, [arXiv:1111.2070 \[hep-th\]](#).
- [126] F. Könnig, A. Patil, and L. Amendola, “Viable cosmological solutions in massive bimetric gravity,” *JCAP* **1403** (2014) 029, [arXiv:1312.3208 \[astro-ph.CO\]](#).
- [127] F. Könnig and L. Amendola, “Instability in a minimal bimetric gravity model,” *Phys. Rev. D* **90** (2014) 044030, [arXiv:1402.1988 \[astro-ph.CO\]](#).
- [128] A. R. Solomon, J. Enander, Y. Akrami, T. S. Koivisto, F. Könnig, and E. Mörtsell, “Cosmological viability of massive gravity with generalized matter coupling,” *JCAP* **1504** no. 04, (2015) 027, [arXiv:1409.8300 \[astro-ph.CO\]](#).

- [129] M. Lagos and P. G. Ferreira, “Cosmological perturbations in massive bigravity,” *JCAP* **1412** (2014) 026, [arXiv:1410.0207 \[gr-qc\]](#).
- [130] J. D. Bekenstein, “Relativistic gravitation theory for the MOND paradigm,” *Phys. Rev. D* **70** (2004) 083509, [arXiv:astro-ph/0403694 \[astro-ph\]](#). [Erratum: *Phys. Rev. D* **71**, 069901(2005)].
- [131] J. G. Hao and R. Akhoury, “Can relativistic MOND theory resolve both the dark matter and dark energy paradigms?,” *Int. J. Mod. Phys. D* **18** (2009) 1039–1048, [arXiv:astro-ph/0504130 \[astro-ph\]](#).
- [132] C. Skordis, “The tensor-vector-scalar theory and its cosmology,” *Class. Quant. Grav.* **26** no. 14, (2009) 143001. <http://stacks.iop.org/0264-9381/26/i=14/a=143001>.
- [133] C. Skordis, D. F. Mota, P. G. Ferreira, and C. Boehm, “Large Scale Structure in Bekenstein’s theory of relativistic Modified Newtonian Dynamics,” *Phys. Rev. Lett.* **96** (2006) 011301, [arXiv:astro-ph/0505519 \[astro-ph\]](#).
- [134] T. Kaluza, “On the Problem of Unity in Physics,” *Sitzungsber. Preuss. Akad. Wiss. Berlin (Math. Phys.)* **1921** (1921) 966–972.
- [135] O. Klein, “Quantentheorie und fünfdimensionale Relativitätstheorie,” *Zeitschrift für Physik* **37** no. 12, (1926) 895–906.
- [136] J. M. Overduin and P. S. Wesson, “Kaluza-Klein gravity,” *Phys. Rept.* **283** (1997) 303–380, [arXiv:gr-qc/9805018 \[gr-qc\]](#).
- [137] G. R. Dvali, G. Gabadadze, and M. Porrati, “4-D gravity on a brane in 5-D Minkowski space,” *Phys. Lett. B* **485** (2000) 208–214, [arXiv:hep-th/0005016 \[hep-th\]](#).
- [138] C. Deffayet, G. Dvali, and G. Gabadadze, “Accelerated universe from gravity leaking to extra dimensions,” *Phys. Rev. D* **65** (Jan, 2002) 044023. <http://link.aps.org/doi/10.1103/PhysRevD.65.044023>.
- [139] D. Gorbunov, K. Koyama, and S. Sibiryakov, “More on ghosts in DGP model,” *Phys. Rev. D* **73** (2006) 044016, [arXiv:hep-th/0512097 \[hep-th\]](#).
- [140] K. Koyama, “Are there ghosts in the self-accelerating brane universe?,” *Phys. Rev. D* **72** (2005) 123511, [arXiv:hep-th/0503191 \[hep-th\]](#).
- [141] G. W. Horndeski, “Second-order scalar-tensor field equations in a four-dimensional space,” *Int. J. Th. Phys.* **10** (1974) 363–384.
- [142] C. Deffayet, X. Gao, D. Steer, and G. Zahariade, “From k-essence to generalised Galileons,” *Phys. Rev. D.* **84** (2011) 064039, [arXiv:1103.3260 \[hep-th\]](#).
- [143] C. Charmousis, E. J. Copeland, A. Padilla, and P. M. Saffin, “General second order scalar-tensor theory, self tuning, and the Fab Four,” *Phys. Rev. Lett.* **108** (2012) 051101, [arXiv:1106.2000 \[hep-th\]](#).
- [144] C. Deffayet, G. Esposito-Farese, and A. Vikman, “Covariant Galileon,” *Phys. Rev. D.* **79** (2009) 084003, [arXiv:0901.1314 \[hep-th\]](#).
- [145] C. Deffayet, S. Deser, and G. Esposito-Farese, “Generalized Galileons: All scalar models whose curved background extensions maintain second-order field equations and stress-tensors,” *Phys. Rev. D.* **80** (2009) 064015, [arXiv:0906.1967 \[gr-qc\]](#).

- [146] T. Kobayashi, M. Yamaguchi, and J. Yokoyama, “Generalized G-inflation: Inflation with the most general second-order field equations,” *Prog. Theor. Phys.* **126** (2011) 511–529, [arXiv:1105.5723 \[hep-th\]](#).
- [147] A. De Felice, T. Kobayashi, and S. Tsujikawa, “Effective gravitational couplings for cosmological perturbations in the most general scalar-tensor theories with second-order field equations,” *Phys. Lett.* **B706** (2011) 123–133, [arXiv:1108.4242 \[gr-qc\]](#).
- [148] C. Armendariz-Picon, T. Damour, and V. F. Mukhanov, “ $k$  - inflation,” *Phys. Lett.* **B458** (1999) 209–218, [arXiv:hep-th/9904075 \[hep-th\]](#).
- [149] C. Armendariz-Picon, V. F. Mukhanov, and P. J. Steinhardt, “Essentials of  $k$  essence,” *Phys. Rev. D* **63** (2001) 103510, [arXiv:astro-ph/0006373 \[astro-ph\]](#).
- [150] C. Deffayet, O. Pujolas, I. Sawicki, and A. Vikman, “Imperfect Dark Energy from Kinetic Gravity Braiding,” *JCAP* **1010** (2010) 026, [arXiv:1008.0048 \[hep-th\]](#).
- [151] O. Pujolas, I. Sawicki, and A. Vikman, “The Imperfect Fluid behind Kinetic Gravity Braiding,” *JHEP* **11** (2011) 156, [arXiv:1103.5360 \[hep-th\]](#).
- [152] S. M. Carroll, A. De Felice, V. Duvvuri, D. A. Easson, M. Trodden, and M. S. Turner, “The Cosmology of generalized modified gravity models,” *Phys. Rev. D* **71** (2005) 063513, [arXiv:astro-ph/0410031 \[astro-ph\]](#).
- [153] C. Cheung, P. Creminelli, A. L. Fitzpatrick, J. Kaplan, and L. Senatore, “The Effective Field Theory of Inflation,” *JHEP* **03** (2008) 014, [arXiv:0709.0293 \[hep-th\]](#).
- [154] G. Gubitosi, F. Piazza, and F. Vernizzi, “The Effective Field Theory of Dark Energy,” *JCAP* **1302** (2013) 032, [arXiv:1210.0201 \[hep-th\]](#). [JCAP1302,032(2013)].
- [155] J. Bloomfield, É. É. Flanagan, M. Park, and S. Watson, “Dark energy or modified gravity? An effective field theory approach,” *JCAP* **2013** no. 08, (2013) 010. <http://stacks.iop.org/1475-7516/2013/i=08/a=010>.
- [156] E. Bellini and I. Sawicki, “Maximal freedom at minimum cost: linear large-scale structure in general modifications of gravity,” *JCAP* **1407** (2014) 050, [arXiv:1404.3713 \[astro-ph.CO\]](#).
- [157] B. Hu, M. Raveri, A. Silvestri, and N. Frusciante, “Exploring massive neutrinos in dark cosmologies with *EFTCAMB*/ *EFTCosmoMC*,” *Phys. Rev. D* **91** no. 6, (2015) 063524, [arXiv:1410.5807 \[astro-ph.CO\]](#).
- [158] M. Zumalacárregui and J. García-Bellido, “Transforming gravity: From derivative couplings to matter to second-order scalar-tensor theories beyond the Horndeski Lagrangian,” *Phys. Rev. D* **89** (Mar, 2014) 064046. <http://link.aps.org/doi/10.1103/PhysRevD.89.064046>.
- [159] C. Charmousis, “From Lovelock to Horndeski’s Generalized Scalar Tensor Theory,” *Lect. Notes Phys.* **892** (2015) 25–56, [arXiv:1405.1612 \[gr-qc\]](#).
- [160] J. Gleyzes, D. Langlois, F. Piazza, and F. Vernizzi, “Exploring gravitational theories beyond Horndeski,” *JCAP* **1502** (2015) 018, [arXiv:1408.1952 \[astro-ph.CO\]](#).
- [161] C. Lin, S. Mukohyama, R. Namba, and R. Saitou, “Hamiltonian structure of scalar-tensor theories beyond Horndeski,” *JCAP* **1410** no. 10, (2014) 071, [arXiv:1408.0670 \[hep-th\]](#).

- [162] J. Gleyzes, D. Langlois, F. Piazza, and F. Vernizzi, “Healthy theories beyond Horndeski,” *Phys. Rev. Lett.* **114** no. 21, (2015) 211101, [arXiv:1404.6495 \[hep-th\]](#).
- [163] J. B. Jiménez, R. Durrer, L. Heisenberg, and M. Thorsrud, “Stability of Horndeski vector-tensor interactions,” *JCAP* **1310** (2013) 064, [arXiv:1308.1867 \[hep-th\]](#).
- [164] I. D. Saltas, I. Sawicki, L. Amendola, and M. Kunz, “Anisotropic Stress as a Signature of Nonstandard Propagation of Gravitational Waves,” *Phys. Rev. Lett.* **113** no. 19, (2014) 191101, [arXiv:1406.7139 \[astro-ph.CO\]](#).
- [165] R. Bean and M. Tangmatitham, “Current constraints on the cosmic growth history,” *Phys. Rev. D* **81** (2010) 083534, [arXiv:1002.4197 \[astro-ph.CO\]](#).
- [166] Y.-S. Song, G.-B. Zhao, D. Bacon, K. Koyama, R. C. Nichol, and L. Pogosian, “Complementarity of weak lensing and peculiar velocity measurements in testing general relativity,” *Phys. Rev. D* **84** (Oct, 2011) 083523. <http://link.aps.org/doi/10.1103/PhysRevD.84.083523>.
- [167] S. F. Daniel and E. V. Linder, “Confronting general relativity with further cosmological data,” *Phys. Rev. D* **82** (Nov, 2010) 103523. <http://link.aps.org/doi/10.1103/PhysRevD.82.103523>.
- [168] J. N. Dossett, M. Ishak, and J. Moldenhauer, “Testing general relativity at cosmological scales: Implementation and parameter correlations,” *Phys. Rev. D* **84** (Dec, 2011) 123001. <http://link.aps.org/doi/10.1103/PhysRevD.84.123001>.
- [169] S. F. Daniel, E. V. Linder, T. L. Smith, R. R. Caldwell, A. Cooray, A. Leauthaud, and L. Lombriser, “Testing general relativity with current cosmological data,” *Phys. Rev. D* **81** (Jun, 2010) 123508. <http://link.aps.org/doi/10.1103/PhysRevD.81.123508>.
- [170] F. Simpson *et al.*, “CFHTLenS: testing the laws of gravity with tomographic weak lensing and redshift-space distortions,” *Mont. Not. Roy. Astron. Soc.* **429** no. 3, (2013) 2249–2263, <http://mnras.oxfordjournals.org/content/429/3/2249.full.pdf+html>.
- [171] B. Hu, M. Liguori, N. Bartolo, and S. Matarrese, “Parametrized modified gravity constraints after Planck,” *Phys. Rev. D* **88** (Dec, 2013) 123514. <http://link.aps.org/doi/10.1103/PhysRevD.88.123514>.
- [172] C. Blake *et al.*, “The WiggleZ Dark Energy Survey: joint measurements of the expansion and growth history at  $z \approx 1$ ,” *Mont. Not. Roy. Astron. Soc.* **425** (Sept., 2012) 405–414, [arXiv:1204.3674](#).
- [173] F. Beutler *et al.*, “The 6dF Galaxy Survey:  $z \approx 0$  measurements of the growth rate and  $\sigma_8$ ,” *Mont. Not. Roy. Astron. Soc.* **423** (July, 2012) 3430–3444, [arXiv:1204.4725](#).
- [174] A. Shafieloo and C. Clarkson, “Model independent tests of the standard cosmological model,” *Phys. Rev. D.* **81** (2010) 083537, [arXiv:0911.4858 \[astro-ph.CO\]](#).
- [175] A. Shafieloo and E. V. Linder, “Cosmographic Degeneracy,” *Phys. Rev. D.* **84** (2011) 063519, [arXiv:1107.1033 \[astro-ph.CO\]](#).
- [176] D. Huterer and G. Starkman, “Parameterization of dark-energy properties: A Principal-component approach,” *Phys. Rev. Lett.* **90** (2003) 031301, [arXiv:astro-ph/0207517 \[astro-ph\]](#).

- [177] R. R. Caldwell and M. Doran, “Dark-energy evolution across the cosmological-constant boundary,” *Phys. Rev. D.* **72** (2005) 043527, [arXiv:astro-ph/0501104](#) [astro-ph].
- [178] E. V. Linder, “Cosmic growth history and expansion history,” *Phys. Rev. D.* **72** (2005) 043529, [arXiv:astro-ph/0507263](#) [astro-ph].
- [179] W. Hu and I. Sawicki, “A Parameterized Post-Friedmann Framework for Modified Gravity,” *Phys. Rev. D* **76** (2007) 104043, [arXiv:0708.1190](#) [astro-ph].
- [180] L. Amendola, M. Kunz, and D. Sapone, “Measuring the dark side (with weak lensing),” *JCAP* **0804** (2008) 013, [arXiv:0704.2421](#) [astro-ph].
- [181] E. Bertschinger, “On the Growth of Perturbations as a Test of Dark Energy,” *Astrophys. J.* **648** (2006) 797–806, [arXiv:astro-ph/0604485](#) [astro-ph].
- [182] T. Baker, P. G. Ferreira, C. Skordis, and J. Zuntz, “Towards a fully consistent parameterization of modified gravity,” *Phys. Rev. D.* **84** (2011) 124018, [arXiv:1107.0491](#) [astro-ph.CO].
- [183] T. Baker, P. G. Ferreira, and C. Skordis, “The Parameterized Post-Friedmann Framework for Theories of Modified Gravity: Concepts, Formalism and Examples,” [arXiv:1209.2117](#) [astro-ph.CO].
- [184] M. Kunz, “The dark degeneracy: On the number and nature of dark components,” *Phys.Rev.* **D80** (2009) 123001, [arXiv:astro-ph/0702615](#) [astro-ph].
- [185] W. J. Percival and M. White, “Testing cosmological structure formation using redshift-space distortions,” *Mon. Not. Roy. Astron. Soc.* **393** (2009) 297–308, [arXiv:0808.0003](#) [astro-ph].
- [186] A. De Felice and S. Tsujikawa, “Conditions for the cosmological viability of the most general scalar-tensor theories and their applications to extended Galileon dark energy models,” *JCAP* **1202** (2012) 007, [arXiv:1110.3878](#) [gr-qc].
- [187] M. Motta, I. Sawicki, I. D. Saltas, L. Amendola, and M. Kunz, “Probing Dark Energy through Scale Dependence,” *Phys. Rev. D.* **88** no. 12, (2013) 124035, [arXiv:1305.0008](#) [astro-ph.CO].
- [188] V. Vardanyan and L. Amendola, “How can we tell whether dark energy is composed of multiple fields?,” *Phys. Rev.* **D92** no. 2, (2015) 024009, [arXiv:1502.05922](#) [gr-qc].
- [189] W. Research, “Mathematica 9.0,” 2012.
- [190] L. Lombriser, A. Slosar, U. Seljak, and W. Hu, “Constraints on  $f(R)$  gravity from probing the large-scale structure,” *Phys. Rev. D.* **85** (2012) 124038, [arXiv:1003.3009](#) [astro-ph.CO].
- [191] **2dFGRS** Collaboration, W. J. Percival *et al.*, “The 2dF Galaxy Redshift Survey: Spherical harmonics analysis of fluctuations in the final catalogue,” *Mon. Not. Roy. Astron. Soc.* **353** (2004) 1201, [arXiv:astro-ph/0406513](#) [astro-ph].
- [192] L. Samushia, W. J. Percival, and A. Raccanelli, “Interpreting large-scale redshift-space distortion measurements,” *Mon. Non. Roy. Astron. Soc.* **420** (Mar., 2012) 2102–2119, [arXiv:1102.1014](#).

- [193] R. Tojeiro *et al.*, “The clustering of galaxies in the SDSS-III Baryon Oscillation Spectroscopic Survey: measuring structure growth using passive galaxies,” *Mont. Not. Roy. Astron. Soc.* **424** (Aug., 2012) 2339–2344, [arXiv:1203.6565](#).
- [194] S. de la Torre *et al.*, “The VIMOS Public Extragalactic Redshift Survey (VIPERS). Galaxy clustering and redshift-space distortions at  $z = 0.8$  in the first data release,” *Astron. Astrophys.* **557** (2013) A54, [arXiv:1303.2622](#) [[astro-ph.CO](#)].
- [195] C.-H. Chuang and Y. Wang, “Modelling the anisotropic two-point galaxy correlation function on small scales and single-probe measurements of  $H(z)$ ,  $D_A(z)$  and  $f(z)\sigma_8(z)$  from the Sloan Digital Sky Survey DR7 luminous red galaxies,” *Mont. Not. Roy. Astron. Soc.* **435** (Oct., 2013) 255–262, [arXiv:1209.0210](#).
- [196] C.-H. Chuang *et al.*, “The clustering of galaxies in the SDSS-III Baryon Oscillation Spectroscopic Survey: single-probe measurements from CMASS and LOWZ anisotropic galaxy clustering,” [arXiv:1312.4889](#) [[astro-ph.CO](#)].
- [197] C. Blake *et al.*, “Galaxy And Mass Assembly (GAMA): improved cosmic growth measurements using multiple tracers of large-scale structure,” *Mont. Not. Roy. Astron. Soc.* **436** (Dec., 2013) 3089–3105, [arXiv:1309.5556](#).
- [198] **SKA Cosmology SWG** Collaboration, R. Maartens, F. B. Abdalla, M. Jarvis, and M. G. Santos, “Overview of Cosmology with the SKA,” *PoS AASKA14* (2015) 016, [arXiv:1501.04076](#) [[astro-ph.CO](#)].
- [199] L. Amendola, S. Fogli, A. Guarnizo, M. Kunz, and A. Vollmer, “Model-independent constraints on the cosmological anisotropic stress,” *Phys. Rev. D* **89** (2014) 063538, [arXiv:1311.4765](#) [[astro-ph.CO](#)].  
<http://link.aps.org/doi/10.1103/PhysRevD.89.063538>.
- [200] A. Albrecht, G. Bernstein, R. Cahn, W. L. Freedman, J. Hewitt, *et al.*, “Report of the Dark Energy Task Force,” [arXiv:astro-ph/0609591](#) [[astro-ph](#)].
- [201] **LSST Collaboration** Collaboration, J. A. Tyson, “Large synoptic survey telescope: Overview,” *Proc. SPIE Int. Soc. Opt. Eng.* **4836** (2002) 10–20, [arXiv:astro-ph/0302102](#) [[astro-ph](#)].
- [202] A. Guarnizo, L. Amendola, M. Kunz, and A. Vollmer, “Semi-analytical study on the generic degeneracy for galaxy clustering measurements,” in *Statistical Challenges in 21st Century Cosmology*, vol. 10 of *Proceedings of the International Astronomical Union*, pp. 347–350. 5, 2014. [http://journals.cambridge.org/article\\_S1743921314010771](http://journals.cambridge.org/article_S1743921314010771).
- [203] **Euclid Theory Working Group** Collaboration, L. Amendola *et al.*, “Cosmology and fundamental physics with the Euclid satellite,” [arXiv:1206.1225](#) [[astro-ph.CO](#)].
- [204] W. Hu, “Power spectrum tomography with weak lensing,” *Astrophys. J.* **522** (1999) L21–L24, [arXiv:astro-ph/9904153](#) [[astro-ph](#)].
- [205] Z. Ma, W. Hu, and D. Huterer, “Effects of Photometric Redshift Uncertainties on Weak-Lensing Tomography,” *Astrophys. J.* **636** (2006) 21–29, [arXiv:0506614](#) [[astro-ph](#)].
- [206] D. J. Eisenstein, W. Hu, and M. Tegmark, “Cosmic Complementarity: Joint Parameter Estimation from Cosmic Microwave Background Experiments and Redshift Surveys,” *Astrophys. J.* **518** (June, 1999) 2–23, [astro-ph/9807130](#).

- 
- [207] A. Hojjati, L. Pogosian, A. Silvestri, and G.-B. Zhao, “Observable physical modes of modified gravity,” *Phys. Rev. D* **89** (Mar, 2014) 083505.  
<http://link.aps.org/doi/10.1103/PhysRevD.89.083505>.
- [208] T. Jenke *et al.*, “Gravity Resonance Spectroscopy Constrains Dark Energy and Dark Matter Scenarios,” *Phys. Rev. Lett.* **112** (Apr, 2014) 151105.  
<http://link.aps.org/doi/10.1103/PhysRevLett.112.151105>.
- [209] L. Taddei and L. Amendola, “A cosmological exclusion plot: Towards model-independent constraints on modified gravity from current and future growth rate data,” *JCAP* **1502** no. 02, (2015) 001, [arXiv:1408.3520](https://arxiv.org/abs/1408.3520) [[astro-ph.CO](https://arxiv.org/abs/1408.3520)].
- [210] A. Guarnizo, L. Jaime, A. Vollmer, and L. Amendola, “A cosmological exclusion plot for modified gravity,” *In preparation* .
- [211] M. Tegmark, “Measuring cosmological parameters with galaxy surveys,” *Phys. Rev. Lett.* **79** (1997) 3806–3809, [arXiv:astro-ph/9706198](https://arxiv.org/abs/astro-ph/9706198) [[astro-ph](https://arxiv.org/abs/astro-ph/9706198)].
- [212] Y.-S. Song and I. Kayo, “Decomposition of spectra from redshift distortion maps,” *Mon. Not. Roy. Astron. Soc.* **407** (Sept., 2010) 1123–1127, [arXiv:1003.2420](https://arxiv.org/abs/1003.2420).



# A MODEL-INDEPENDENT APPROACH TO DARK ENERGY COSMOLOGIES: CURRENT AND FUTURE CONSTRAINTS

ALEJANDRO GUARNIZO TRILLERAS



*“Doing Our 4th Quarter Income Taxes” (2012) - Gregory Horndeski*

This thesis was typeset using the L<sup>A</sup>T<sub>E</sub>X typesetting system originally developed by Leslie Lamport, based on T<sub>E</sub>X created by Donald Knuth. All numerical calculations were performed using the software **MATHEMATICA 9.0**. Front and back cover were made using TikZ and PGF packages for T<sub>E</sub>X <http://sourceforge.net/projects/pgf/>, with a slight change of the manual cover by Till Tantau. Back image *“Doing Our 4th Quarter Income Taxes”* by Gregory Horndeski, is used here solely for artistic purposes and with his explicit permission.